Spring 5-15-2019

Understanding the Meaning of Microbialites as Geobiological Archives

Scott Randall Beeler
Washington University in St. Louis

WASHINGTON UNIVERSITY IN ST. LOUIS

Department of Earth and Planetary Sciences
Arts and Sciences

Dissertation Examination Committee:
Alexander S. Bradley, Chair
Jeffrey G. Catalano
David A. Fike
Fernando J. Gomez
Bronwen L. Konecky

Understanding the Meaning of Microbialites as Geobiological Archives

by

Scott R. Beeler

A dissertation presented to
The Graduate School
of Washington University in
partial fulfillment of the
requirements for the degree
of Doctor of Philosophy

May 2019
St. Louis, Missouri

Table of Contents

List of Figures

List of Tables

Acknowledgments

The completion of this dissertation would not have been possible without the support and encouragement of many others. First, I would like to acknowledge my academic mentors whose guidance and advice have helped me to develop and grow as a scientist. Thank you to my advisor, Alex Bradley, for providing me with the opportunity and encouragement to pursue my scientific interests. Thanks to Fernando Gomez for serving as an invaluable collaborator and for facilitating the field campaigns necessary for the completion of this research. Thank you to the rest of my committee members David Fike, Jeff Catalano, and Brownen Konecky for sharing your knowledge and expertise. I would also like to thank the many teachers I have had at both Washington University and throughout my academic career all of whom have contributed to this achievement.

Next, I would like to thank my colleagues in the Department and Earth and Planetary Sciences at Washington University who I have had the pleasure to work with over the past five years. Thank you to my fellow graduate students for your friendship during my time in St. Louis. Specifically, I would like to thank my officemates Roger Bryant and Joss Richardson for making it fun to come to work every day and providing a sounding board for ideas. Thanks to the rest of our "first year" crew of Kelsey Prissel, Melody Eimer, Michael Bouchard, and Xiaochen Mao for making the last five years such an amazing experience from day one. Special thanks to the many members of the Bradley and Fike labs both past and present who have provided feedback and advice that has vastly improved the quality of my research. Particularly, I would like to acknowledge the contributions of Melanie Suess, Derek Smith, and Wil Leavitt whose laboratory expertise and assistance were critical to the completion of this work. Thank you to the members

of the office staff for making the bureaucratic aspects of graduate school far less painful. Special thanks to both the McDonnell Center for the Space Sciences and the Department of Earth and Planetary Sciences for providing financial support during my time at Washington University.

I would also like to thank the many other friends and colleagues outside of Washington University who have contributed to the successful completion of this dissertation. Thanks to my fellow classmates and the instructors and staff of the 2016 International Geobiology Course for providing one of the best educational experiences of my life. Thanks to my Argentine colleagues Agustin Mors and Flavia Boidi for your insights and friendship during this research. Thanks to the Old Sharks Hockey Club for giving me a place to take a break from grad school life. Thanks to my lifelong friends Peyton Branch, David Crisler, and Johnathan Jones for your continued friendship over the last five years.

Finally, a huge thanks to my parents and brother, Drew, for a lifetime of encouraging me to pursue my dreams and instilling in me a love of learning and nature both of which have been critical in my development as a geologist. Lastly, to Sarah, thanks so much for your love, support, and scientific insight throughout this entire process. I couldn't have done any of this without you.

Scott Beeler

Washington University in St. Louis

May 2019

ABSTRACT OF THE DISSERTATION

Understanding the meaning of microbialites as geobiological archives

by

Scott Randall Beeler

Doctor of Philosophy in Earth and Planetary Sciences

Washington University in St. Louis, 2019

Associate Professor Alexander S. Bradley, Chair

Microbialites, sedimentary structures formed from the interaction of microorganisms with their environment, provide one of the oldest and most complete records of life on Earth, making them an invaluable tool in the field of geobiology. However, much of the information that could be gained from microbialites remains obscured due to our incomplete understanding of how variability in the microbial, geochemical, and physical processes driving their formation affect their morphological and geochemical characteristics. Modern environments of active microbialite formation provide the opportunity to study the relationship between variability in these environmental processes and the resultant mineral product and can act as an analog for understanding ancient examples. However, compared to the vast number of microbialites preserved in the geologic record, microbialite forming environments are relatively rare on modern Earth generating concerns about the generalizability of the knowledge gained from these environments and highlighting the need for study of additional modern settings. The work presented in this dissertation analyzes the processes controlling the formation, morphogenesis, and geochemical compositions of the microbialites of Laguna Negra, Argentina, a location which had previously been understudied compared to other modern environments.

Specifically, we investigated the processes controlling the megascale distributions of microbialites, the stable isotopic compositions of the carbonate minerals comprising the structures, and the lipid biomarker compositions preserved in the microbialites. Our results showed that each of these characteristics of microbialites reflect to varying degrees the biological, geochemical, and physical processes that control their formation. Overall, this work highlights the importance of a multifaceted approach to the analysis of microbialites integrating multiple lines of evidence in order to understand the processes controlling their formation and growth and provides a stronger framework for interpreting their meaning in the geologic record.

Chapter 1: Introduction

The central goal of geobiology is to understand the interactions between the geosphere and the biosphere and how these systems have co-evolved through Earth's history (Knoll et al., 2012). To achieve this goal, we analyze the rock record for evidence of changes in life and its environment through geologic time preserved in the form of geochemical, fossil, and sedimentological signatures. Among the most recognizable of these signatures are sedimentary structures formed from the interaction of microbial, geochemical, and physical processes known as microbialites (Burne and Moore, 1987). Microbialites are among the oldest evidence of life on Earth and occur throughout its history allowing these structures to provide one of the most complete records of the co-evolution of life and the environment through geologic time (Riding and Liang, 2005; Allwood et al., 2007; Peters et al., 2017). Accordingly, microbialites have been widely utilized to make inferences regarding geobiological processes throughout Earth's history (Awramik, 1992; Riding, 2000). Furthermore, in addition to their use as archives of geobiological information on Earth, microbialites present a compelling target in the search for extraterrestrial life because they provide geological evidence of microbial processes that may be recognized at the macroscale (Cady et al., 2003; Des Marais et al., 2008)

However, despite first being recognized over a century ago, microbialites and the information that may be gained from their study still remain largely enigmatic (Kalkowsky, 1908). Variability in the abundance and characteristics of microbialites are well documented through geologic time and space, however our ability to interpret the meaning of this variability remains incomplete confounding interpretation of their geobiological significance (Grotzinger and Knoll, 1999; Bosak et al., 2013). Furthermore, in some cases even the biogenicity of

structures interpreted as microbialites may be ambiguous, as structures morphologically similar to microbialites have been shown to be capable of being produced through entirely abiotic processes (Grotzinger and Rothman, 1996). This realization is particularly problematic for our ability to use microbialites as evidence for the origin of life on Earth or of life's presence on other planets (Buick et al., 1981; Banfield et al., 2001; Allwood et al., 2018). Geochemical signatures (e.g. stable isotopes, organic molecules, or trace elements) preserved in microbialites may provide a method to establish their biogenicity or reconstruct information about the microorganisms or environmental conditions associated with their formation (Spear and Corsetti, 2013). Yet, the meaning of these signatures may be similarly ambiguous as the meaning of morphological variability. Ultimately, all of these issues result from the lack of a mechanistic understanding of the controls of the formation and morphogenesis of microbialites highlighting the need for further work investigating these processes.

The study of modern environments of microbialite formation can help to resolve these problems by enabling analysis microbialites alongside the environmental processes that control their formation. Unfortunately, modern settings of microbialite formation are relatively rare compared to their near ubiquity for most of Earth's history (Grotzinger and Knoll, 1999). The cause of this scarcity on modern Earth, while still a topic of active debate, is generally attributed to the rise of metazoan life disrupting the substrates on which microbialites form as well as changes in ocean chemistry (Grotzinger, 1990; Riding, 2006; Peters et al., 2017). Regardless of the cause, the limited number of modern microbialite forming environments that have been studied presents concerns about the generalizability of information learned about the processes controlling microbialite formation in these settings to the interpretation of microbialites in the rock record (Bosak et al., 2013). Moreover, most microbialites formed in modern settings

contain microfabrics that differ from those found in examples from the geologic record providing further questions about their applicability as analogs for ancient systems (Frantz et al., 2015). Study of additional modern environments, ideally with microbialites containing microfabrics more comparable to ancient examples, are necessary to resolve these concerns.

1.2 Outline of the Dissertation

To develop a more robust understanding of the controls of microbialite formation and the geochemical signatures they preserve we analyzed the modern microbialites of Laguna Negra, a high altitude evaporative lake located in the Andes Mountains of northwestern Argentina. The microbialites of Laguna Negra were first described in Gomez et al. (2014), and consequently provides a novel setting for understanding the processes controlling microbialite formation. Intriguingly, the microfabrics comprising Laguna Negra's microbialites are comparable to those of Precambrian examples suggesting their potential as a more genuine analog for ancient microbialite formation (Gomez et al., 2014). Additionally, evaporative lake deposits have been found on Mars indicating the utility for Laguna Negra to serve as an analog in the search for extraterrestrial life (Di Achille et al., 2009; Cabrol et al., 2010). The research presented in this dissertation investigates processes controlling the formation and growth of Laguna Negra's microbialites and the geochemical signatures they preserve in order to enhance our ability to interpret the geobiological significance of microbialites in the geologic record of Earth and potentially other planets .

Chapter 2 focuses on understanding the geospatial relationships between carbonate morphology, microbial communities, and geochemical parameters at the macro- to mega- (meters and greater) scale. Previous work at Laguna Negra has primarily focused on how variability in biological, geochemical, and physical processes drive changes in the formation and

characteristics of microbialites and abiogenic carbonates at Laguna Negra at the micro- to meso-scales (microns to centimeters; Gomez et al., 2018, 2014; Mlewski et al., 2018). Expanding our understanding of these relationships to larger spatial scales enables multi-scale perspectives of the influence of changes in environmental processes on microbialite formation and growth. Generally, the characteristics and spatial distribution of microbialites at the macro- to mega-spatial scales have been interpreted to reflect variability in physical processes rather than the microbial processes that are more dominant at smaller spatial scales (Andres and Reid, 2006; Ibarra and Corsetti, 2016). We sought to determine these relationships at Laguna Negra in order to generate a better understanding of the processes controlling microbialite formation at the lake and enable better interpretation of the meaning of geospatial variability in microbialite distributions and characteristics in the rock record.

To achieve this task, we collected high resolution aerial imagery, field geochemical measurements, and ground truth observations and integrated these datasets into a geographic information system (GIS) database. This GIS database was utilized to map and statistically interrogate the geospatial relationships between carbonate morphology, microbial mat distributions, and geochemistry at Laguna Negra. Our results indicated that carbonate morphologies were variably distributed across the zone of carbonate formation at the lake, and that this variability was associated with statistically significant changes in the types of sedimentary matrices with which they were associated (i.e. microbial mats, carbonate muds, salt deposits, and grass). Specifically, carbonate morphologies interpreted as microbialitic based on microscale analyses were more commonly associated with microbial mats than those interpreted as forming abiogenically. These results suggest that the macroscale distribution of microbialites are driven by the distributions of microbial mats, in contrast to other systems where mats are

ubiquitous and microbialite distributions are dominantly controlled by physical processes (i.e. wave action, sedimentation, or tectonic processes). Additionally, this work indicates the utility of approaches employing geospatial statistics to better understand the processes controlling microbialite formation at these scales.

Chapter 3 investigates the processes controlling the formation of highly enriched carbon and oxygen isotopic compositions in microbialites and abiogenic carbonate structures at Laguna Negra. The stable isotopic compositions of carbonate minerals preserve information regarding the environmental conditions associated with their formation and thus provide a potentially valuable tool in understanding the processes associated with microbialite formation (Zeebe and Wolf-Gladrow, 2001). In particular, stable carbon isotopic enrichments may arise as a result of microbial action and could potentially serve as evidence of biogenicity or even specific microbial communities associated with microbialite formation (Andres et al., 2006; Birgel et al., 2015). However, isotopic signatures for a particular process may be non-unique highlighting a need for a better understanding of the manner in which isotopic signatures in microbialites are generated in order to better interpret their meaning.

We analyzed the spatial variability in the isotopic compositions of Laguna Negra's waters to determine the processes driving their evolution in order to better understand the isotopic signatures preserved in the carbonates. We found that highly enriched isotopic compositions preserved in the microbialites and abiogenic carbonates of Laguna Negra can be explained by a combination of the abiotic processes of evaporation, degassing, and carbonate precipitation despite their presence within structures of a biogenic origin. More generally, these results suggest that similar processes could locally generate or enhance carbon isotopic excursions in the rock record, such as the Lomagundi Isotopic Excursion, which are commonly interpreted as

global in origin (Kump and Arthur, 1999; Bekker, 2014). This work highlights the importance of investigating lateral scale variability in isotopic compositions of microbialites and carbonates in addition to stratigraphic variability in order to better interpret the meaning of isotopic enrichments preserved in microbialites.

Chapter 4 explores the capacity of lacustrine microbialites to serve as archives of terrestrial paleoenvironmental information by investigating the processes controlling the trends in stable oxygen isotopic of carbonate minerals ($\delta^{18}O_{carb}$) preserved across sequential laminae in individual microbialites. Microbialites in modern settings and Cenozoic sedimentary deposits have begun to receive attention as potential reservoirs of paleoclimate information through geochemical proxy data preserved in the carbonate minerals of which they are comprised (Solari et al., 2010; Frantz et al., 2014; Petryshyn et al., 2016). In order to confidently utilize lacustrine microbialites as tools in paleoclimate reconstructions a better understanding of the fidelity with which they record paleoclimate variability is required. Laguna Negra provides an ideal setting for this purpose because regional climate data has previously been independently established enabling comparison of trends preserved in microbialites to these regional records (Valero-Garces et al., 1996; Grosjean et al., 1997; Grosjean et al., 1998). Previous work at Laguna Negra found a general decreasing trend in $\delta^{18}O_{carb}$ through time preserved within individual microbialites, which was interpreted to result from a decrease in water oxygen isotopic compositions ($\delta^{18}O_{H2O}$) due to increased water balance at the lake through time (Buongiorno et al., 2018). Yet, variability in temperature may also affect $\delta^{18}O_{carb}$ and could potentially be overprinting or enhancing changes in $\delta^{18}O_{H2O}$ leading to improper interpretation of the meaning of these trends (Kim and O'Neil, 1997).

To resolve this problem, we utilized clumped isotope thermometry to reconstruct the relative importance of changes in temperature versus changes in $\delta^{18}O_{H2O}$ on the $\delta^{18}O_{carb}$ trends preserved in Laguna Negra's microbialites (Ghosh et al., 2006; Affek, 2012). Our results show that temperatures at which carbonates precipitated at Laguna Negra are relatively consistent compared to the high seasonal and daily temperature variability at the lake, and that shifts in $\delta^{18}O_{carb}$ are correlated with changes in $\delta^{18}O_{H2O}$ but not temperature. These results support previous interpretations that the oxygen isotopic compositions preserved in Laguna Negra provide evidence of increasing water balance at the lake through time consistent with regional climate trends (Buongiorno et al., 2018). Together these results provide further validation for the use of lacustrine microbialites as archives of paleoclimate information.

Chapter 5 examines the ability of the lipid biomarkers preserved in microbialites to provide information regarding the structure and function of microbial communities associated with their formation. The structural diversity and compound specific carbon isotopic compositions of lipids found can provide information regarding the organisms responsible for their formation, and because lipids are recalcitrant over geologic time scales they may provide a link between modern genomic studies of the processes governing microbialite formation and the study of ancient microbialites where genomic material is no longer present (Peters et al., 2005; Summons and Lincoln, 2012; Spear and Corsetti, 2013). However, the lipids preserved in microbialites may not necessarily be representative of the organisms associated with their formation due to diagenetic alternations or the influence of allochtonously derived organic compounds, which complicates our ability to interpret their meaning in the geologic record. Developing a better understanding of the relationship between the lipid compositions of

microbial mats associated with microbialite formation and the lipid compositions that are preserved in the microbialites is necessary to more confidently interpret their meaning

We analyzed the fatty acid and sterol profiles and the compound specific carbon isotopic compositions of fatty acids preserved within microbialites and abiogenic carbonates at Laguna Negra and compared them to those from the extant microbial communities with which they are currently associated. We found that the structural and isotopic compositions of the lipids from the modern microbial communities were consistent with previous microscopic and genomic observations of an ecosystem with primary productivity dominated by diatoms and the presence of a diverse bacterial community. However, the lipid profiles preserved within the microbialites differed from those of extant microbial communities and more closely resembled a bacterially dominated community due to the preferential loss of unsaturated compound during early diagenesis. These results suggest that the lipid biomarkers preserved within microbialites may not necessarily be representative of the microbial communities associated with their formation and highlights the importance of the consideration of diagenetic processes when interpreting their meaning in the geologic record.

1.3 References

Di Achille G., Hynek B. M. and Searls M. L. (2009) Positive identification of lake Strandlines in Shalbatana Vallis, Mars. *Geophysical Research Letters* **36**, L14201.

Affek H. P. (2012) Clumped Isotope Paleothermometry: Principles, Applications, and Challenges. *The Paleontological Society Papers* **18**, 101–114.

Allwood A. C., Rosing M. T., Flannery D. T., Hurowitz J. A. and Heirwegh C. M. (2018) Reassessing evidence of life in 3,700-million-year-old rocks of Greenland. *Nature* **563**, 241–244.

Allwood A. C., Walter M. R., Burch I. W. and Kamber B. S. (2007) 3.43 billion-year-old stromatolite reef from the Pilbara Craton of Western Australia: ecosystem-scale insights to early life on Earth. *Precambrian Research* **158**, 198–227.

Andres M. S. and Reid R. P. (2006) Growth morphologies of modern marine stromatolites: A case study from Highborne Cay, Bahamas. *Sedimentary Geology* **185**, 319–328.

Andres M. S., Sumner D. Y., Reid R. P. and Swart P. K. (2006) Isotopic fingerprints of microbial respiration in aragonite from Bahamian stromatolites. *Geology* **34**, 973–976.

Awramik S. M. (1992) The History and Significance of Stromatolites. In *Early Organic Evolution* Springer Berlin Heidelberg, Berlin, Heidelberg. pp. 435–449.

Banfield J. F., Moreau J. W., Chan C. S., Welch S. A. and Little B. (2001) Mineralogical Biosignatures and the Search for Life on Mars. *Astrobiology* **1**, 447–465.

Bekker A. (2014) Lomagundi Carbon Isotope Excursion. In *Encylopedia of Astrobiology* pp. 1–6.

Birgel D., Meister P., Lundberg R., Horath T. D., Bontognali T. R. R., Bahniuk A. M., Rezende C. E., Vásconcelos C. and McKenzie J. A. (2015) Methanogenesis produces strong 13C enrichment in stromatolites of Lagoa Salgada, Brazil: a modern analogue for Palaeo-/Neoproterozoic stromatolites? *Geobiology* **13**, 245–266.

Bosak T., Knoll A. H. and Petroff A. P. (2013) The Meaning of Stromatolites. *Annual Review of Earth and Planetary Sciences* **41**, 21–44.

Buick R., Dunlop J. S. R. and Groves D. I. (1981) Stromatolite recognition in ancient rocks: an appraisal of irregularly laminated structures in an Early Archaean chert-barite unit from North Pole, Western Australia. *Alcheringa: An Australasian Journal of Palaeontology* **5**, 161–181.

Buongiorno J., Gomez F. J., Fike D. A. and Kah L. C. (2018) Mineralized microbialites as archives of environmental evolution, Laguna Negra, Catamarca Province, Argentina. *Geobiology*.

Burne R. V and Moore L. S. (1987) Microbialites: organosedimentary deposits of benthic microbial communities. *Palaios* **2**, 241–254.

Cabrol N. A., Grin E. A., Achille G. di and Hynek B. M. (2010) *Lakes on Mars*., Elsevier.

Cady S. L., Farmer J. D., Grotzinger J. P., Schopf J. W. and Steele A. (2003) Morphological biosignatures and the search for life on Mars. *Astrobiology* **3**, 351–368.

Frantz C. M., Petryshyn V. A. and Corsetti F. A. (2015) Grain trapping by filamentous cyanobacterial and algal mats: Implications for stromatolite microfabrics through time. *Geobiology* **13**, 409–423.

Frantz C., Petryshyn V. and Marenco P. (2014) Dramatic local environmental change during the Early Eocene Climatic Optimum detected using high resolution chemical analyses of Green River Formation. *Palaeogeography, Palaeoclimatology, Palaeoecology* **405**, 1–15.

Ghosh P., Adkins J., Affek H., Balta B., Guo W., Schauble E. A., Schrag D. and Eiler J. M. (2006) 13C–18O bonds in carbonate minerals: A new kind of paleothermometer. *Geochimica et Cosmochimica Acta* **70**, 1439–1456.

Gomez F. J., Kah L. C., Bartley J. K. and Astini R. A. (2014) Microbialites in a high-altitude Andean lake: multiple controls on carbonate precipitation and lamina accretion. *Palaios* **29**, 233–249.

Gomez F. J., Mlewski C., Boidi F. J., Farías M. E. and Gérard E. (2018) Calcium Carbonate Precipitation in Diatom-rich Microbial Mats: The Laguna Negra Hypersaline Lake, Catamarca, Argentina. *Journal of Sedimentary Research* **88**, 727–742.

Grosjean M., Geyh M. A., Messerli B., Schreier H. and Veit H. (1998) A late-Holocene (<2600 BP) glacial advance in the south-central Andes (29°S), northern Chile. *The Holocene* **8**, 473–479.

Grosjean M., Valero-Garcés B. L., Geyh M. A., Messerli B., Schotterer U., Schreier H. and Kelts K. (1997) Mid- and late-Holocene limnogeology of Laguna del Negro Francisco, northern Chile, and its palaeoclimatic implications. *The Holocene* **7**, 151–159.

Grotzinger J. P. (1990) Geochemical model for Proterozoic stromatolite decline. *American Journal of Science* **290**, 80–103.

Grotzinger J. P. and Knoll A. H. (1999) Stromatolites in Precambrian carbonates: evolutionary mileposts or environmental dipsticks? *Annual Review of Earth and Planetary Sciences* **27**, 313–358.

Grotzinger J. P. and Rothman D. H. (1996) An abiotic model for stromatolite morphogenesis. *Nature* **383**, 423–425.

Ibarra Y. and Corsetti F. A. (2016) Lateral Comparative Investigation of Stromatolites: Astrobiological Implications and Assessment of Scales of Control. *Astrobiology* **16**, 271–281.

Kalkowsky E. (1908) Oolith und Stromatolith im norddeutschen Buntsandstein. *Zeitschrift der deutschen geologischen Gesellschaft*, 68–125.

Kim S. T. and O'Neil J. R. (1997) Equilibrium and nonequilibrium oxygen isotope effects in synthetic carbonates. *Geochimica et Cosmochimica Acta* **61**, 3461–3475.

Knoll A. H., Canfield D. E. and Konhauser K. (2012) *Fundamentals of geobiology*., John Wiley & Sons.

Kump L. R. and Arthur M. A. (1999) Interpreting carbon-isotope excursions: carbonates and

organic matter. *Chemical Geology* **161**, 181–198.

Des Marais D. J., Nuth J. A., Allamandola L. J., Boss A. P., Farmer J. D., Hoehler T. M., Jakosky B. M., Meadows V. S., Pohorille A., Runnegar B. and Spormann A. M. (2008) The NASA Astrobiology Roadmap. *Astrobiology* **8**, 715–730.

Mlewski E. C., Pisapia C., Gomez F., Lecourt L., Soto Rueda E., Benzerara K., Ménez B., Borensztajn S., Jamme F., Réfrégiers M. and Gérard E. (2018) Characterization of Pustular Mats and Related Rivularia-Rich Laminations in Oncoids From the Laguna Negra Lake (Argentina). *Frontiers in microbiology* **9**, 996.

Peters K., Walters C. and Moldowan J. (2005) *The biomarker guide: biomarkers and isotopes in the environment and human history*.,

Peters S. E., Husson J. M. and Wilcots J. (2017) The rise and fall of stromatolites in shallow marine environments. *Geology* **45**, 487–490.

Petryshyn V. A., Juarez Rivera M., Agić H., Frantz C. M., Corsetti F. A. and Tripati A. E. (2016) Stromatolites in Walker Lake (Nevada, Great Basin, USA) record climate and lake level changes ~35,000years ago. *Palaeogeography, Palaeoclimatology, Palaeoecology* **451**, 140–151.

Riding R. (2006) Microbial carbonate abundance compared with fluctuations in metazoan diversity over geological time. *Sedimentary Geology* **185**, 229–238.

Riding R. (2000) Microbial carbonates: the geological record of calcified bacterial–algal mats and biofilms. *Sedimentology* **47**, 179–214.

Riding R. and Liang L. (2005) Geobiology of microbial carbonates: metazoan and seawater saturation state influences on secular trends during the Phanerozoic. *Palaeogeography, Palaeoclimatology, Palaeoecology* **219**, 101–115.

Solari M. A., Hervé F., Le Roux J. P., Airo A. and Sial A. N. (2010) Paleoclimatic significance of lacustrine microbialites: A stable isotope case study of two lakes at Torres del Paine, southern Chile. *Palaeogeography, Palaeoclimatology, Palaeoecology* **297**, 70–82.

Spear J. R. and Corsetti F. A. (2013) The evolution of geobiology in the context of living stromatolites. In pp. 549–565.

Summons R. E. and Lincoln S. A. (2012) Biomarkers: Informative Molecules for Studies in Geobiology. In *Fundamentals of Geobiology* John Wiley & Sons, Ltd, Chichester, UK. pp. 269–296.

Valero-Garces B., Grosjean M., Schwalb A., Geyh M., Messerli B. and Kelts K. (1996) Limnogeology of Laguna Miscanti: evidence for mid to late Holocene moisture changes in the Atacama Altiplano (Northern Chile). *Journal of Paleolimnology* **16**, 1–21.

Zeebe R. and Wolf-Gladrow D. (2001) *CO2 in Seawater: Equilibrium, Kinetics, Isotopes*., Elsevier Science B.V., Amsterdam.

Chapter 2: Geospatial insights into the controls of microbialite formation at Laguna Negra, Argentina

Scott R. Beeler[1], Fernando J. Gomez[2], Alexander S. Bradley[1]

[1]Department of Earth and Planetary Science, Washington University in St. Louis, Saint Louis, Missouri, 63130, USA

[2]CICTERRA-CONICET, Facultad de Ciencias Exactas, Fisicas, y Naturales, Universidad Nacional de Córdoba, Córdoba, X5000, Argentina

2.1 Abstract

Microbialites provide a record of the interaction of microorganisms with their environment and constitute a record of microbial life and environments through geologic time. Our capacity to interpret this record is limited by an incomplete understanding of the microbial, geochemical, and physical processes that influence microbialite formation and morphogenesis. The modern system Laguna Negra in Catamarca Province, Argentina contains microbialites in a zone of carbonate precipitation associated with gradients in physico-chemical conditions and microbial community structure, making it an ideal location to study how these processes interact to drive microbialite formation. Previous work at Laguna Negra has primarily focused on linking carbonate formation and morphology to environmental variability at the micro- to meso- scale. In this study we investigated the geospatial relationships between carbonate morphology, geochemistry, and microbial community at the macro- to mega- scale. Our approach combined high resolution imagery with field observations and geochemical measurements. We mapped the distribution of carbonate morphologies, allochtonously derived cobbles and boulders, and correlated these with sedimentary matrices and geochemical parameters. Our work shows that the macroscale distribution of different carbonate morphologies correlates with microbial mats distributions — a result consistent with previous microscale observations. No statistically significant relationships were found between microbial mat distribution and other parameters measured in this study. Spatial variability in the size and abundance of mineralized structures was observed and is interpreted to be due to variability of physical processes, however the specific cause of this variability is unresolved. (e.g. wind/water action, freeze/thaw, or salt deposition). Overall, our results provide insight into the interpretation of microbialite occurrence

and distributions in the geologic record. This highlights the utility of geospatial statistics to probe the controls of microbialite formation in other environments.

2.2 Introduction

Microbialites are sedimentary structures formed as a result of the interaction of microbial life with their environment (Burne & Moore, 1987). Although relatively rare today, microbialites were common for the majority of Earth's history and provide one of the most complete archives of geobiological information through geologic time (Hofmann, 1973; Riding, 2000; Peters *et al.*, 2017). Changes in the abundance and morphology of microbialites have been recognized through time and space in the geologic record and are commonly interpreted in terms of changes in environmental and/or geobiological processes at both the local and global scales (Grotzinger & Knoll, 1999; Riding & Liang, 2005). However, a mechanistic understanding of the processes controlling microbialite formation and growth remains incomplete often hindering our ability to interpret the meaning of microbialites in the geologic record (Bosak *et al.*, 2013). Development of more robust formational models for microbialites is thus crucial to fully realize the geobiological information they preserve.

The study of microbialites is traditionally undertaken using a multiscale framework where observations are made at the micro- (millimeter or less), meso- (centimeter), macro- (decimeter), and mega- (meter) scales (Shapiro, 2000). Utilizing this multiscale approach combined with lateral comparative analyses of their variability allows for more robust interpretation of the meaning of microbialites than is possible when analysis is only undertaken at one scale (Ibarra & Corsetti, 2016). Accordingly, models for microbialite formation and growth should be developed within this same multiscale framework. This requires an understanding of how the microbial, geochemical, and physical processes leading to microbialite

formation vary across spatial scales and how their interactions contribute to the characteristics of microbialites across these same spatial scales (Grotzinger & Knoll, 1999; Bosak *et al.*, 2013).

Study of modern microbialite forming environments enables the analysis of microbial, geochemical, and physical processes alongside the mineralized structures they produce. Previous studies of these environments have produced a wide body of literature, which provide the foundation of our understanding of microbialite formation and morphogenesis (e.g. Golubic, 1991; Andres & Pamela Reid, 2006; Jahnert & Collins, 2012; Pace *et al.*, 2016). However, only a relatively small number of modern environments containing microbialites have been studied compared to the expansive amount found in the rock record, and the suitability of many of these settings as genuine analogs for ancient environments is controversial (Grotzinger & Knoll, 1999; Bosak *et al.*, 2013). Among the most notable of these differences is the discrepancy in microfabrics between modern and ancient microbialites (Kazmierczak & Kempe, 2006; Frantz *et al.*, 2015). These observations highlight the need for study of additional environments where microbialite formation occurs ideally in settings containing microbialites with microfabrics more comparable to ancient examples.

The hypersaline lake Laguna Negra in Catamarca Province, Argentina is a relatively understudied analog environment which contains microbialites with microfabrics comparable to those found in Precambrian examples implying its utility as a more suitable analog for ancient microbialite formation (Gomez *et al.*, 2014). Microbialites form in a zone of freshwater input at the lake's margin alongside abiogenic carbonate precipitates and allochthonous mineralized structures, and the occurrence of these different structure types is laterally variable at the megascale. The variability in structure types is associated with changes in the presence and structure of microbial mats, gradients in geochemical parameters, and shifts in physical

conditions (Gomez *et al.*, 2014, 2018; Mlewski *et al.*, 2018; Beeler et al., *in review*). The attributes make Laguna Negra an ideal setting to study the how changes in microbial, geochemical, and physical processes affect the formation and growth of microbialites. Previous work at Laguna Negra has primarily focused on understanding the processes controlling the formation and morphogenesis of microbialites and abiogenic carbonates from the micro- to macro- scales or controls on isotopic signatures preserved within the carbonates (Gomez *et al.*, 2014, 2018; Buongiorno *et al.*, 2018; Mlewski *et al.*, 2018; Beeler et al.,*in review*).

In this study, we examined the relationship between environmental conditions and microbialite formation and morphogenesis at the macro- to mega- scale by employing an approach integrating high resolution aerial imagery, geochemical measurements, and ground observations into a geographic information system (GIS) data model. This model was utilized to visualize and statistically interrogate the geospatial relationships between environmental conditions and microbialite morphology. Our results offer insight into the processes controlling microbialite formation and distribution at Laguna Negra and provide a framework for future studies of the lake. Additionally, our work provides further insight into the manner in which environmental processes combine to affect the formation and distribution of microbialites at the macro- and mega- scales, which can be used to better interpret the meaning of variability at theses scales in the rock record.

2.3 Field Area

Laguna Negra is a closed-basin lake located in the Puna-Altiplano region of the Andes Mountains with hypersaline body waters (>300 ppt salinity). Input of more dilute waters into the lake from groundwater seeps and seasonal snowmelt spring occurs exclusively along its southeastern margin in an area termed the stromatolite belt. Input waters evolve due to

evaporation, degassing, and mineral precipitation leading to large gradients in geochemical parameters (Gomez et al., 2014; Beeler *et al., in review*). Waters within the stromatolite belt are supersaturated with respect to both calcite and aragonite and widespread precipitation of carbonate minerals occurs which occur as a range of morphologies (oncoids, laminar crusts, and gravels; Gomez *et al.*, 2014). Oncoids are discrete spheroidal to discoidal structures that contain concentric laminations with a low degree of inheritance between layers. Laminar crusts vary from discrete structures to laterally extensive pavements comprised of isopachous laminae with a high degree of inheritance. Gravels are discrete non-laminated aggregates. In addition to carbonate precipitates, angular boulders comprised primarily of volcanic rocks are also abundant within the stromatolite belt. Field observations indicate that the occurrence of different carbonate and non-carbonate structures varies spatially across the stromatolite belt and can to a first order be separated into spatially separate zones (Gomez *et al.*, 2014). However, the variability in occurrence of carbonate structures has not previously been analyzed in detail.

Mineralized structures are associated with various types of background matrices including carbonate muds, salt flats, grasses, and microbial mats. Three distinct types of microbial mats been described previously at Laguna Negra which can be recognized visually: stratified mats, greenish mats, and black pustular mats (Gomez et al., 2018). These visual changes have been shown to be associated with changes in the structure of microbial communities through 16S rRNA and microscopic analysis, and changes in these communities drive changes in the microfabrics preserved within oncoids (Gomez *et al.*, 2018; Mlewski *et al.*, 2018). Similar to mineralized structures, field observations have noted spatial trends in the occurrence of these matrix types, but these trends have also not been analyzed in detail.

Specifically, variability in the community structure of microbial mats have been identified and can be recognized due to visual

differences in mat color (Gomez *et al.*, 2018). Likewise, ground observations indicate that different matrix types association are variably associated different mineralized structure types, but this variability has also yet to be statistically analyzed (Gomez *et al.*, 2014).

2.4 Methods

Field data was collected at Laguna Negra in March 2017 to assess the spatial variability in the occurrence, size, and abundance of mineralized structures at Laguna Negra and their relationship with changes in environmental conditions. This was achieved using an approach combining aerial imagery with ground truth observations and geochemical measurements. Aerial imagery was collected using a DJI Phantom 4 Pro Quadcopter operated DroneDeploy mapping software at a 1.6 cm/pixel resolution. Aerial photos were assembled into an orthomosaic using PrecisionMapper software (Figure 2.1). Ground truth observations of mineralized structure and background matrix types were assessed at 15 locations around the stromatolite belt. Basic geochemical data (pH, conductivity, and dissolved inorganic carbon concentration) was also collected at each of these locations and interpolated to generate geochemical maps as described in Beeler et al. (*in review)*. All imagery, geochemical, and ground truth data were integrated into a GIS database in ArcMap (v.10.4.1) for further analysis.

Aerial imagery was used to assess variability in mineralized structure type, mineralized structure size and abundance, and matrix type across this stromatolite at 300 randomly distributed locations across the stromatolite belt. Locations for aerial imagery analysis were chosen using the Create Random Points tool with a three meter buffer generated around each point with the Buffer tool. The Create Random Points tool was run using a minimum allowed

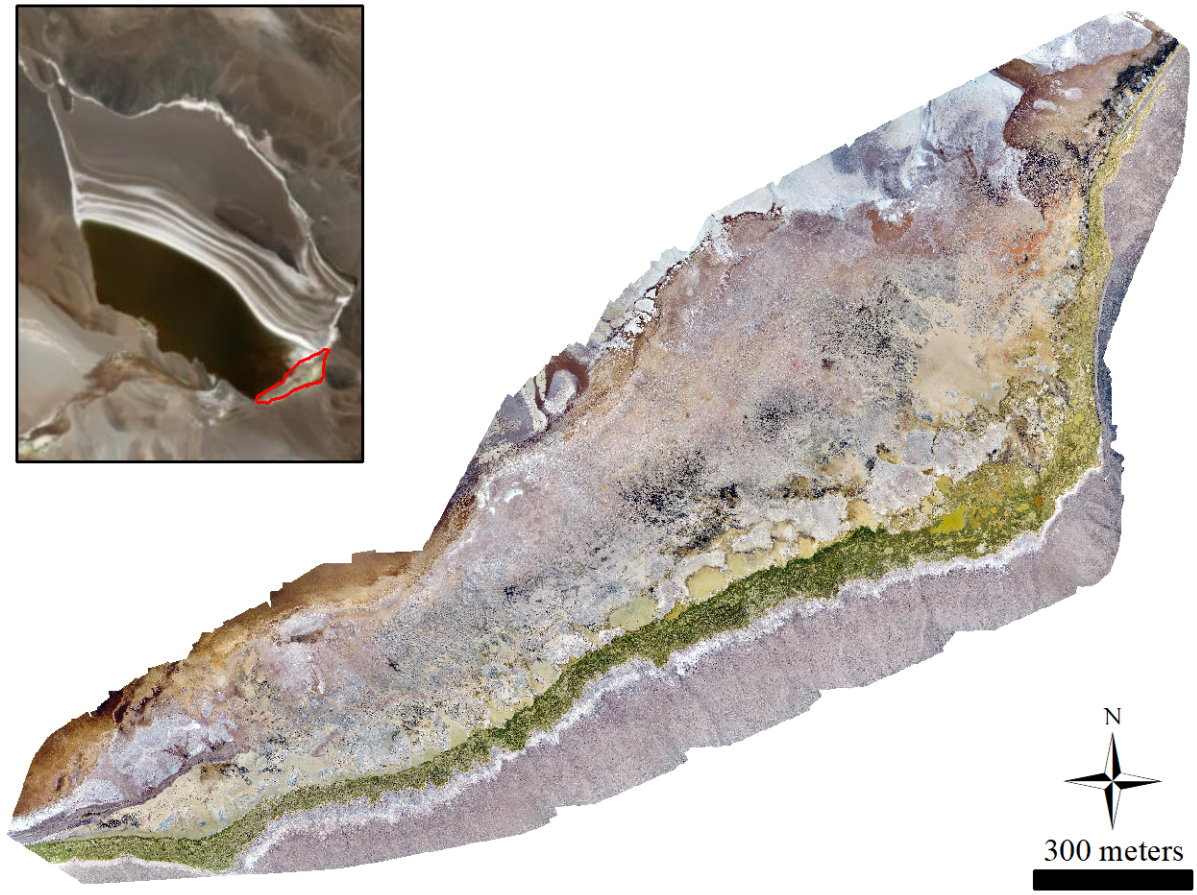

Figure 2.1: Aerial orthomosaic image of the stromatolite belt. Inset image shows the location of the stromatolite belt in the lake with inset imagery from ArcGIS world imagery.

distance of three meters to ensure no overlap between locations. The total area analyzed from all locations was 8481 m^2 which is ~1.5% of the total area of the stromatolite belt (557605 m^2), which gives a 1.1% confidence interval at the 95% confidence level. At each of the 300 locations the dominant type of discrete mineralized structure within the buffer was classified as either oncoid, boulder, laminar crust, gravel or none (Figure 2.2). The matrix type associated with these structures was classified as either grass, microbial mat, carbonate mud, or salt (Figure 2.3). Microbial mats were further classified following Gomez et al. (2018) as stratified, pustular, or greenish. Classification of both carbonate, matrix, and mat type was based off of aerial imagery and comparisons to ground truth observations. If multiple structure or matrix types were present

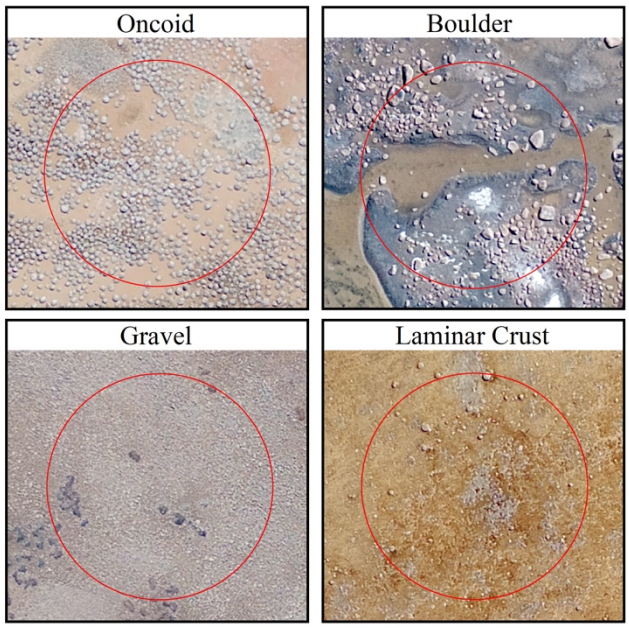

Figure 2.2: Examples of each of the mineralized structure types classifications. Red circles are the 3 meter buffers where analysis of size and abundance of the structures were performed.

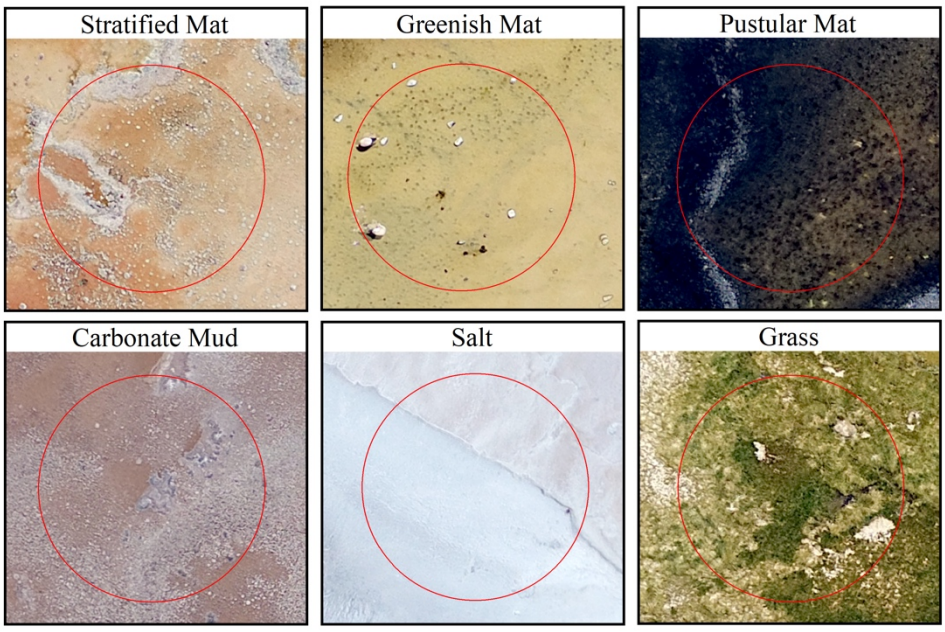

Figure 2.3: Examples of each of the background matrix types classifications. Red circles are the 3 meter buffers where analysis of size and abundance of the structures were performed.

within a buffer it was classified according to the most abundant structure or matrix type. If present, the abundance and size of large scale (>4 cm) mineralized structures were measured within the three meter buffer at each location using the CraterTools add-in software (Kneissl *et al.*, 2011). The number of mineralized structures and their average size were calculated within each buffer. Basic geochemical parameters (pH, DIC, TDS) at each location were generated from interpolated maps generated as described in Beeler et al., *in press* using field measurements.

Geospatial statistics were used to assess differences in the distribution, size, and abundance of mineralized structures and the distribution of matrix type and were calculated using the Spatial Statistics toolbox in ArcMap. Variability in the distribution of different mineralized structure and matrix types were assessed using the Median Center tool. Global spatial patterns in the average size and abundance of mineralized structures were assessed using the Getis-Ord General G statistic with the High/Low Clustering tool and the Global Moran's I statistic with the Spatial Autocorrelation tool. Local analysis of hotspots of high and low values of structure size and abundance were assessed using the Anselin Local Moran's I statistic with the Cluster and Outlier Analysis tool. The Anselin Local Moran's I statistic was ran through 9999 permutations and a False Discovery Rate (FDR) correction was used to minimize the risk of improper identification of false positives (Caldas de Castro & Singer, 2006). Both global and local patterns were assessed using a fixed distance band conceptualization with Euclidian distance as the distance method. A fixed distance band of 75 meters was used for structure density analyses and a band of 85 meters was used for size analyses. The threshold distance was selected as it is the maximum peak value calculated with the Incremental Spatial Autocorrelation tool that ensured that all locations had at least two neighbors for analysis. The relationship between different structure and mat types and their size, abundance, and environmental variables

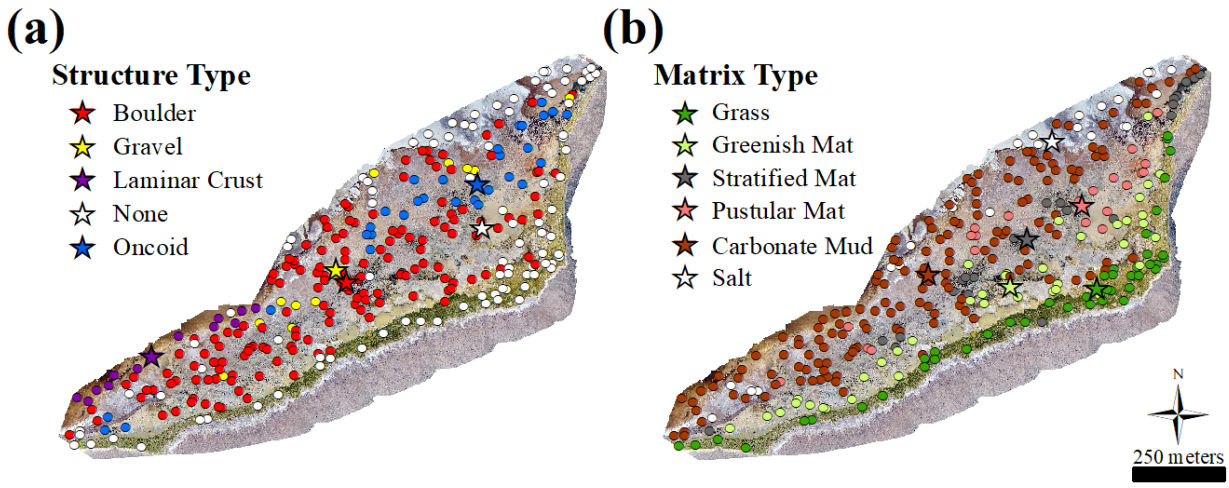

Figure 2.4: Spatial distribution of mineral structure types (a) and matrix types (b) across the stromatolite belt. Circles represent the locations of the 300 randomly distributed points for analysis and stars are the median center for each of the structure or matrix types identified within these points.

were assessed using analysis of variance (ANOVA) and post-hoc Tukey's honest significant difference (HSD) tests. Statistical

tests were carried out using R (version 3.3.3) and the agricolae package (de Mendiburu, 2017; R Core Team, 2017).

2.5 Results

2.5.1 Spatial Distribution of Structures and Matrix Types

The distribution of mineralized structures types varied across the lake edge indicated by the change in the median center of the occurrence of different structure types analyzed at the 300 randomly distributed locations (Figure 2.4a). Non-carbonate boulders were the most abundant mineralized structure type in the stromatolite belt occurring in 51.7% of locations analyzed and have a widespread distribution across the stromatolite belt that is slightly skewed to the southwest. Oncoids are the most abundant carbonate structure occurring in 10.0% of locations analyzed. Oncoids are most abundant in the northeastern part of the stromatolite belt, but also

occur along the southwestern margin of the lake. Laminar crusts occurred in 4.3% of locations measured and occur exclusively at the northwest edge of the stromatolite belt. Gravels occurred in 3.7% of locations in a narrow band that extends laterally across the stromatolite belt. In 30.4% of locations analyzed no large scale mineralized structures were observed and locations without mineralized structures were relatively evenly distributed across the stromatolite belt.

Similarly, the distribution of different matrix types at Laguna Negra displays clear patterns moving from the lake margin towards the body of the lake as evidenced by changes in the median center of the occurrence of different (Figure 2.4b). Grasses are dominant near the lake margin giving way to microbial mats followed by carbonate muds and eventually salt deposits. While the transition between matrix types is clear the contacts between different matrix types are gradational. Grasses were observed in 14.6% of locations analyzed and were concentrated primarily along the margin of the stromatolite belt where more dilute groundwater seeps occur. Microbial mats occurred in 27.6% of analyzed locations and were more abundant in locations more proximal to the groundwater seeps compared to other matrix types. Greenish mats were the most abundant mat type comprising 45.2% of mats. Greenish mats were widespread laterally but tended to occur more proximal to the groundwater seeps relative to other mat types. Stratified mats and pustular mats each comprised 27.4% of total mats. Stratified mats and pustular mats had nearly identical median centers, however the stratified and pustular mats were not distributed evenly and occurred in spatially distinct zones. Carbonate muds were the most abundant matrix type occurring in 49.7% of locations analyzed. Muds occurred more distally to groundwater inputs and were slightly more abundant towards the southeastern part of the stromatolite belt. Salt deposits occurred in 8.0% of locations analyzed and occurred distally from

groundwater inputs and were more abundant towards the northeastern portion of the stromatolite belt.

2.5.2 Association of Structure and Matrix Types

Mineralized structure types are variably associated with different types of background matrix types (Figure 2.5). Boulders were most commonly associated with carbonate mud (60.6% of locations) followed by microbial mats (33.0% of locations) with occasional association with salts (5.2% of locations) and grass (1.3% of locations). Oncoids were most commonly associated with microbial mats (60.0% of locations) followed by carbonate muds (26.7% of locations) and salt (13.3% of locations). No oncoids were observed associated with grasses. Laminar crusts were only observed to occur in association with carbonate muds. Gravels were primarily associated with sediments (90.9% of locations) and also occurred in association with a microbial mat (9.1% of locations). Locations containing no large scale mineralized structures most commonly contained grass (46.2% of locations) but were also lacking in locations containing carbonate muds (26.4% of locations), mats (14.3% of locations), and salt (13.2% of locations). The type of microbial mats that different structure types are associated with was also variable

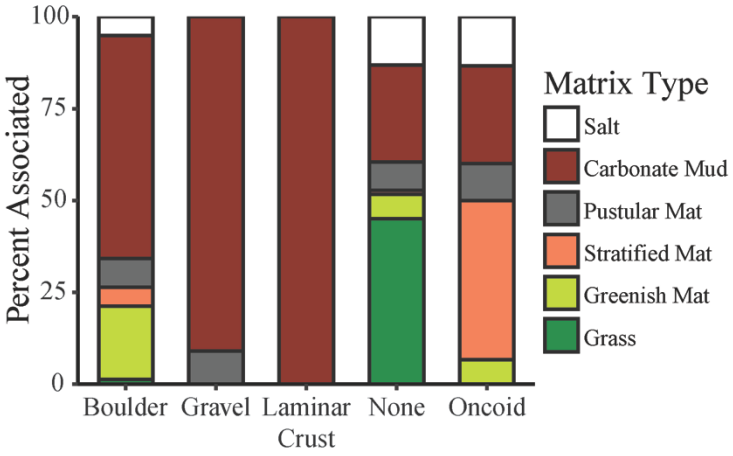

Figure 2.5: Association of different mineral structure types with different matrix types. Pearson's chi-squared test indicated a significant association between structure and matrix type.

Table 2.2: Pearson's chi squared residuals of the relationship between mineralized structure type and matrix types. Positive values indicate higher associations than expected from random distributions and negative values lower than expected from random distributions. Values higher than +3 and lower than -3 indicated significant differences than expected from random distributions.

	None	Boulder	Oncoid	Gravel	Laminar Crust
Grass	10.02	-6.67	-2.36	-1.38	-1.51
Greenish Mat	-2.18	3.73	-1.09	-1.31	-1.42
Stratified Mat	-2.73	-1.49	7.97	-0.95	-1.04
Pustular Mat	0.01	0.05	0.51	0.18	-1.06
Carbonate Mud	-5.32	3.93	-2.66	2.79	3.71
Salt	2.19	-1.87	1.14	-1.00	-1.09

across the stromatolite belt. Boulders most commonly occur in association with greenish mats (58.8% of locations with mats) with less common association with both pustular (23.5% of locations with mats) and stratified mat (17.6% of locations with mats). Oncoids are most commonly associated with stratified mats (72.2% of locations with mats) with less common - association with pustular (16.7% of locations with mats) and greenish mats (11.1% of locations with mats). Gravels were only found in association with a black pustular mat.

Pearson's Chi-squared test indicates a statistically significant relationship between structure and matrix types ($p < 2.2\ e^{-16}$). Pearson's residuals for each relationship (Table 1) provide insight into which relationships differ most greatly from those expected based on random associations with values >2 and <-2 indicating associations significantly greater or less than expected (Agresti, 2007). Locations without any mineralized structures were more commonly associated with grass and salt, and less commonly associated with carbonate muds,

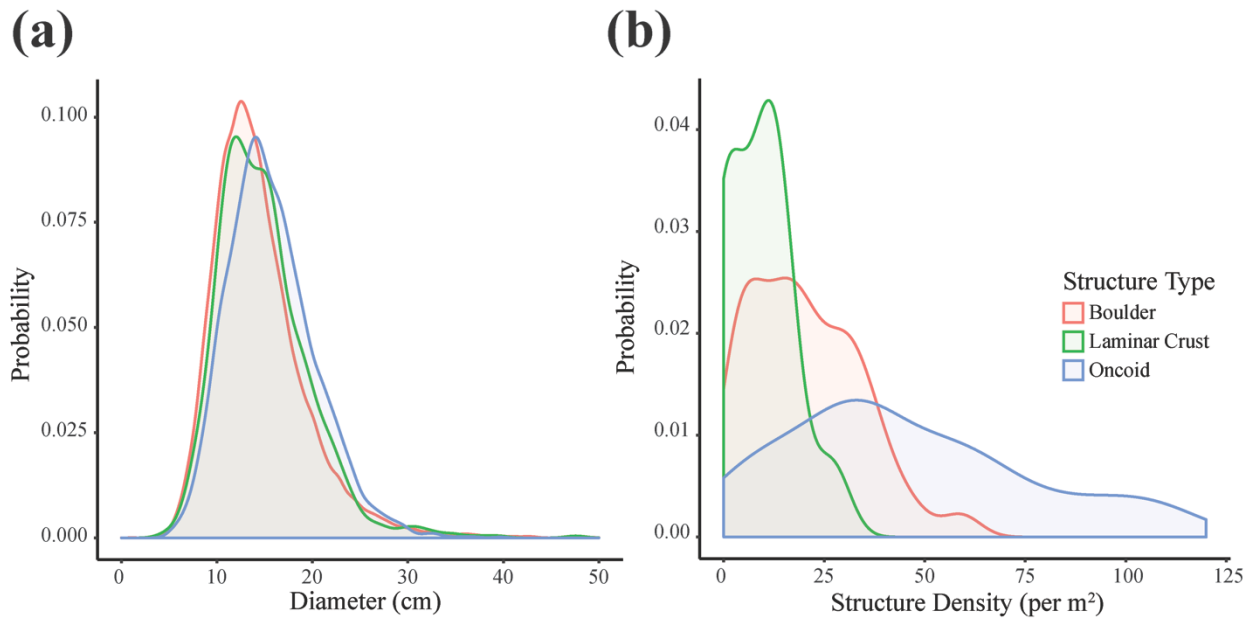

Figure 2.6: Probability density functions for the average diameter (a) and abundance (b) of different mineralized structure types. Post-hoc Tukey's HSD test indicate significant differences in average size between oncoids and other structure types but no significant difference between boulders and laminar crusts. Post-hoc Tukey's HSD also indicated significant differences in abundance between all structure types.

greenish mats, and stratified mats. Boulders were more commonly associated with greenish mats and carbonate muds, and less commonly associated with grasses. Oncoids are more commonly associated with stratified mats, and less commonly associated with grass and carbonate muds. Gravels and laminar crusts were more commonly associated with carbonate muds.

2.5.3 Variability in Abundance and Size of Mineralized Structures

The average diameter of large scale mineralized structures (>4 cm in diameter) varied between structure type (Figure 2.6a). Oncoids had the highest average diameter of 15.7 cm with a standard deviation of 4.6 cm. Laminar crusts had an intermediate average diameter of 14.9 cm with a standard deviation of 4.8 cm. Boulders had the lowest average diameter of 14.5 cm with a standard deviation of 5.1 cm. An analysis of variance of average size of structures showed significant differences in mean size between one or more of the structure types ($p < 2e^{-16}$). A post-hoc Tukey HSD test was used to test for the pairwise differences in structure size between

types and found significant differences in average size between each of the different mineralized structure types.

The average density of mineralized structures (abundance per m^2) within the buffers also varied between locations containing different mineralized structure types (Figure 2.6b). Oncoids had the highest average density of structures with 45.4 structures per m^2 and a standard deviation of 30.6 structures per m^2. Boulders had an intermediate density of structures with 20.4 structures per m^2 and a standard deviation of 13.8 structures per m^2. Laminar crusts had the lowest average density of structures with 8.9 structures per m^2 and a standard deviation of 8.1 structures per m^2. An analysis of variance of structure density showed significant differences in mean values between one or more structure types ($p < 2e^{-16}$). A post-hoc Tukey HSD test of pairwise comparisons showed locations containing oncoids had a significantly higher density of mineralized structures than both laminar crusts and boulders. There was no significant difference in the average density of mineralized structures between locations containing laminar crusts or boulders.

The global spatial statistics of Global Moran's I and Getis-Ord General G enable identification of spatial patterns for values across the lake edge by comparing the variability of nearby features to the variability of the overall dataset (Mitchel, 2005). The Global Moran's I statistic tests whether an attribute value for a location (in this case average structure size or abundance) are clustered, dispersed, or randomly distributed across the lake edge, however it cannot identify whether clustering, if present, is of high or low values. The Global Moran's I statistic is a number between -1 and +1 with a value of -1 indicating perfect dispersion and a value of +1 indicating complete clustering. The related statistic of Getis-Ord General G can resolve whether these high or low values are spatially clustered but is unable to resolve between

random or dispersed patterns if no clustering is present. Higher G values compared to the expected G value for a random distribution indicate clustering of high values while lower G values indicate clustering of low values. The significance of both Moran's I and General G is tested by calculating a z-score comparing the measured values to those expected from a random distribution. Using the two statistics in conjunction increases their utility by providing insight into the both the spatial patterns and their magnitude. However, Moran's I and General G are both global statistics meaning they analyze the overall pattern of clustering, but they cannot determine the location of high or low clusters within a dataset. The Anselin Local Moran's I decomposes the Global Moran's I statistic to identify localized hot spots of similar values or outliers with values significantly different from their neighbors (Anselin, 1995). This enables location and mapping of areas with significant clusters, which can then be compared with other spatial information allowing for better interpretation of the meaning of spatial trends. It should be noted that these clusters only represent the most extreme locations of clustering as the Anselin Local Moran's I statistic can fail to identify local clusters when clustering is present on the global scale as is the case with Laguna Negra (Tiefelsdorf & Boots, 2010). In addition, a conservative approach with a False Discovery Rate correction was used to identify cluster, which may artificially exclude significant clusters (Caldas de Castro & Singer, 2006).

The average size of mineralized structures at the analyzed locations was variable across the stromatolite belt (Figure 2.7a). The Global Morans I statistic for average structure size across the stromatolite belt was 0.13 with a z-score = 3.93 ($p < 8.7e^{-5}$) indicating significant clustering of similar values. The observed General G for average structure size was 0.0439 with an expected G of 0.0441 yielding a z-score of -0.46 ($p = 0.65$) indicating there is not significant clustering of high values only or low values only. Anselin's Local Moran's I identified a significant cluster of

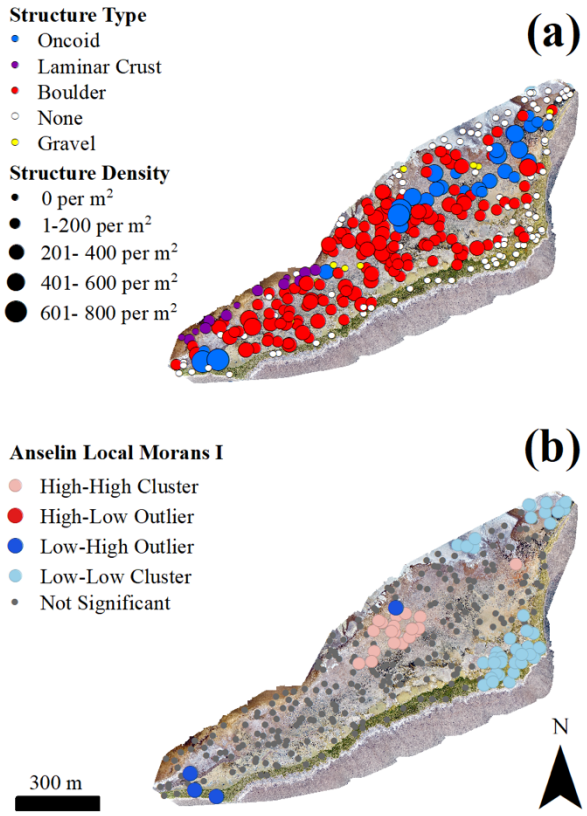

Figure 2.8: (a) Variability in the abundance of mineralized structures within three meter buffers of analyzed locations. (b) Anselin Local Moran's I showing locations containing clusters or outliers of structure abundance.

high value outliers near the central portion of the stromatolite belt and a significant cluster of low values in the northeastern edge (Figure 2.7b). Both the high cluster and low cluster areas consisted of boulders.

The density of mineralized structures within the analyzed buffers was also variable across the stromatolite belt (Figure 2.8a). The density of mineralized structures across the stromatolite belt is significantly clustered as indicated by a Global Morans I statistic of 0.35 with a z-score of 9.63 ($p < 5\ e^{-6}$). The observed General G statistic for average structure density was 0.0437 with an expected G of 0.0264 yielding a z-score of 12.4 ($p < 5e^{-6}$) indicating that high values are significantly clustered. Anselin's Local I identified one cluster of high values, three clusters of low values, and several low value outliers (Figure 2.8b). Clusters of high values occurred in the

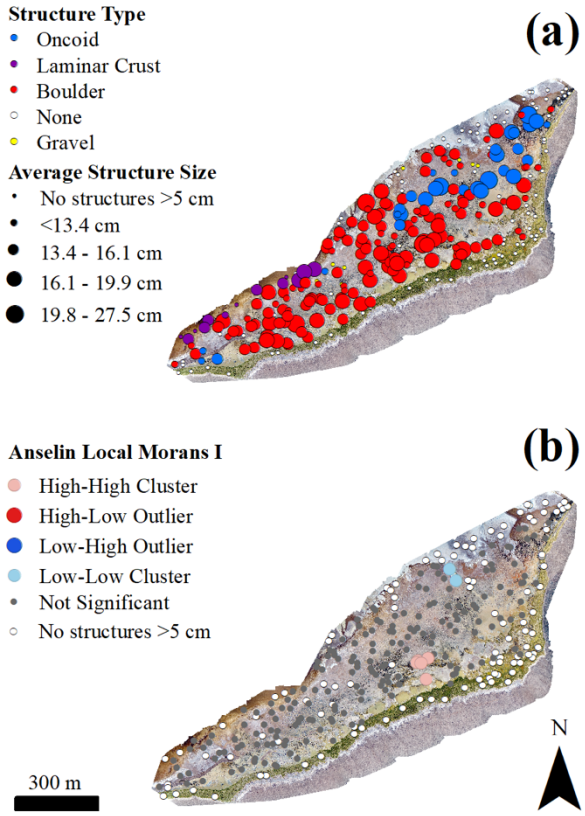

Figure 2.7: (a) Variability in the average size of mineralized structures within three meter buffers of analyzed locations. (b) Anselin Local Moran's I showing locations containing clusters or outliers of average structure size.

central portion of the stromatolite belt and were comprised of a mixture of oncoids and boulders. Low value clusters occurred near the groundwater source and in the northeastern portion in the lake at the edge of the salt flat and were areas where no large scale mineralized structures occurred. Low value outliers occurred in the southwestern portion of the stromatolite belt and consisted of locations containing no large scale mineralized structures that occurred nearby areas containing oncoids.

2.5.4 Geochemical Variability Associated with Structure and Matrix Types

Different mineralized structure types were associated with waters of different geochemical compositions (Figure 2.9a-c). Analysis of variance of the geochemical properties of waters indicated significant differences in TDS ($p < 2.2e^{-8}$), pH ($p < 1.3\ e^{-8}$), and DIC ($p < 6.5e^{-5}$)

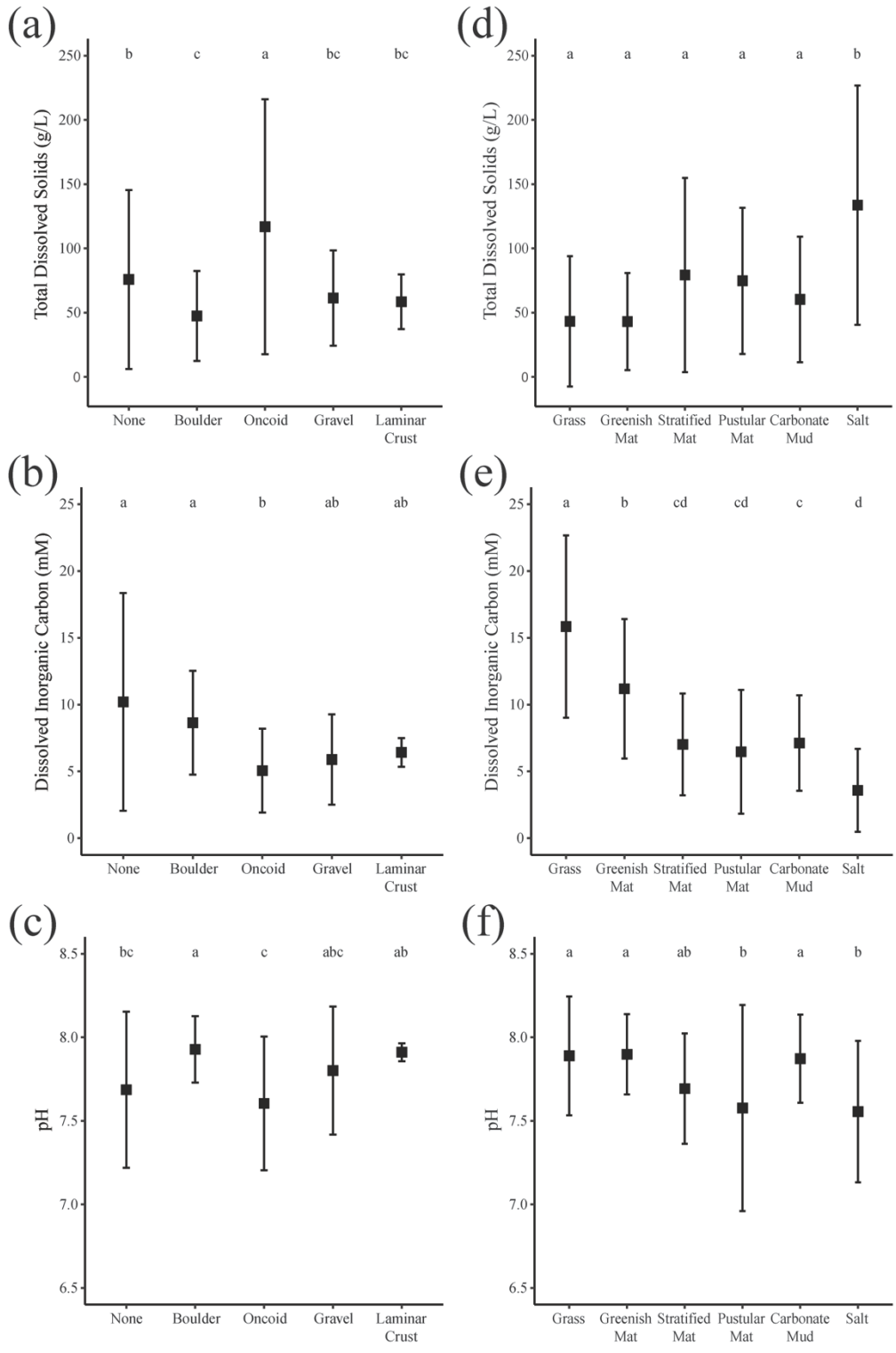

Figure 3: Variation in the geochemistry of waters associated with different mineralized structure types (a-c) and matrix types (d-f). Letters indicate significant differences in the mean geochemical composition of waters associated with different mineral structure or matrix types determined using a post-hoc Tukey HSD test.

on average in locations with different structure types. Post-hoc Tukey HSD testing showed that locations with oncoids were associated with waters of significantly higher average TDS than all other structure types structures. Locations containing boulders were associated with waters with significantly lower average TDS than those with no structures. There were no significantly distinguishable differences in average TDS between all other structure types. Locations containing oncoids were associated with waters with a significantly lower average pH than locations containing boulders or laminar crusts. Locations containing oncoids were associated with waters with a significantly lower average dissolved inorganic carbon (DIC) concentrations than locations containing boulders or no structures. No other statistically distinguishable differences in average DIC concentrations were observed between other mineralized structure types. Locations containing boulders were associated with waters with a significantly higher pH than locations containing oncoids or no structures. Laminar crusts were associated with waters of a significantly higher average pH than oncoids. No statistically distinguishable differences in average pH of waters were observed between other structure types.

Likewise, different matrix types were associated with waters of different geochemical compositions (Figure 2.9d-f). Locations containing salt were associated with waters of significantly higher average TDS than other matrix types. No other statistically distinguishable differences in average structure type were observed between other matrix types. Locations containing grass were associated with waters containing significantly higher DIC concentrations than locations containing other matrix types. Locations containing salt were associated with waters with significantly lower DIC concentrations compared to locations containing other matrix types. Locations containing salt were associated with waters with significantly lower

average pH than locations containing carbonate mud or grass. The average pH in locations containing mats, carbonate muds, or grass were not statistically distinguishable.

2.6 Discussion

2.6.1 Controls on the Distribution of Mineralized Structure Types

Our results show that at Laguna Negra microbialites and other mineralized structure types have variable distributions across the stromatolite belt with mineralized structure types tending to occur in spatially distinct zones (Figure 2.4a). However, the contacts between these different zones are gradational and there is no clear succession between mineralized structure types. Variability in mineralized structure type is associated with changes in matrix type, geochemistry, and physical parameters suggesting that a combination of these processes is responsible for the distribution of the various structure types. Analysis of the covariation between these parameters, the mineralogical and morphological characteristics of the structures, and their spatial distributions provides insight in to the processes controlling the distribution of the structures across the stromatolite belt.

Boulders have the most widespread distribution across the stromatolite belt, and their distribution is slightly skewed to the southwestern corner. The mineralogy of boulders suggests that they are allochthonous in origin and sourced from the surrounding country rock, and therefore their distribution must be dependent on the transport of these materials into the stromatolite belt through geologic processes. The large size and high angularity of boulders is consistent with a proximal source of boulders to the stromatolite belt. Skewness in the distribution of boulders coincides with variability in geomorphology surrounding the lake as the microbial belt is bracketed on its southern margin by the base of an alluvial fan and on its eastern margin by a ridge. These results indicate that the distribution of boulders is driven by variability

in the delivery of material into the stromatolite belt by this alluvial fan. Significant differences in the geochemistry of waters associated with boulders versus waters associated with other structure types were also observed, however it is difficult to generate a mechanism that would lead to a causal link between these parameters. Therefore, the most likely explanation for the distribution of boulders across the stromatolite belt is geomorphic variability driving variability in the delivery of material.

The other mineralized structure types at Laguna Negra are comprised of carbonate minerals (primarily calcite with minor aragonite) suggesting an autochthonous origin. These structures have been interpreted to have variable degrees of microbial contribution to their formation based upon morphological evidence with laminar crusts and gravels interpreted to have formed as a result of abiogenic carbonate precipitation (Gomez *et al.*, 2014). Our results are consistent with this interpretation as all locations containing laminar crusts and all but one location containing gravels are associated with carbonate muds and Pearson's residuals indicate a greater association with carbonate muds than expected based on a random distribution (Figure 2.5, Table 1). The spatial distribution of these structures is variable with laminar crusts occurring exclusively at the northwestern edge of the stromatolite belt whereas gravels have a widespread lateral distribution NE-SW across the stromatolite belt. Geochemical variability in waters from which carbonates precipitate could provide a possible explanation for their distribution, however there is no statistically significant difference in the basic geochemical parameters measured in this study between waters associated with the different matrix types (Figure 2.9). This does not rule out a geochemical driver of variability in the morphology of these abiotic carbonate precipitates as variability in parameters not measured in this study such as carbonate saturation state and the presence of inhibitors to calcite precipitation such as iron, magnesium, or sulfate

(Reddy & Nancollas, 1976; Grotzinger & James, 2000). Additionally, a seasonal stream providing influx of meltwaters that was not active during our sampling is present in the northwestern corner of the lake edge and could provide localized changes in chemistry seasonally. However, the similarity of carbon and oxygen isotopic compositions preserved in carbonates to those in lake waters measured in this study suggest geochemical conditions at the lake have remained relatively constant through time (Beeler et al., *in review*). A more detailed geochemical study and analysis of its temporal variability would help to enhance our understanding of possible geochemical controls on the occurrence of abiogenic carbonate structures.

Oncoids are the other dominant carbonate structure type at the lake and have been interpreted to have a biogenic origin based on petrographic analyses (Gomez *et al.*, 2014, 2018; Mlewski *et al.*, 2018). Our results are consistent with these observations as oncoids most commonly occur in association with microbial mats and Pearson's residuals indicate that oncoids are more commonly associated with stratified mats than expected based on a random distribution (Figure 2.5, Table 2.1). Oncoids have a somewhat limited distribution with the majority of locations containing oncoids concentrated in the northeastern portion of the stromatolite belt. The distribution of stratified mats is likewise skewed towards the northeastern corner of the lake and provides a possible explanation for oncoids predominately forming in this portion of the lake. It should be noted that not all locations containing oncoids are associated mats, and microbial mats occur in locations that do not contain oncoids. Intrastructure variability in microfabrics related to changes in microbial community structures has been observed within oncoids and suggests a temporally dynamic microbial ecosystem at Laguna Negra (Gomez *et al.*, 2018). We hypothesize that oncoid formation occurs in the zone where microbial mats,

particularly stratified mats, most commonly occur even if microbial mats are not always present in that location. Additional work focusing on the temporal variability in lake conditions and mat distribution would serve to test this hypothesis.

2.6.2 Controls on the Distribution of Matrix Types

Our results indicate that variability in the spatial distribution of matrix types is associated with changes in the distribution of biogenic versus abiogenic carbonate structure types at Laguna Negra. Therefore, understanding the controls of variability in matrix type is necessary to understand what drives the distribution of the different carbonate mineral precipitates. Laguna Negra's matrix types follow a succession from grasses to microbial mats to mineral precipitates (Figure 2.4b). These transitions occur alongside large geochemical gradients that have previously been recognized at Laguna Negra (Gomez *et al.*, 2014; Beeler et al., *in review*). Geochemical and biological processes are intimately linked with geochemistry acting as a control on which organisms may survive in an environment, and in turn biological processes altering the geochemistry of an environment through their metabolic processes (De Wit & Bouvier, 2006; Druschel & Kappler, 2015). Likewise, the geochemical evolution of waters in evaporative settings generates sequential patterns of mineral precipitation, and mineral precipitation may also alter geochemical parameters (Bąbel & Schreiber, 2014). Thus, the geochemical evolution of lake waters could represent a possible control on the distribution of matrix types at Laguna Negra.

Salinity changes are one potential control on matrix distribution types as increasing salinity has been shown to increase mortality rates in marsh grasses such as those found at Laguna Negra, and variability in salinity has been shown to drive changes in microbial community structure in other settings (Linthurst & Blum, 1981; Gulzar *et al.*, 2003; Lozupone &

Knight, 2007; Bolhuis *et al.*, 2013). Progressive evaporation leading to changes in salinity is also associated with changes in mineralogy during progressive precipitation of evaporite minerals (McCaffrey *et al.*, 1987). Large increases in salinity occur across the stromatolite belt with brackish input waters becoming over 20 times more concentrated as they evolve into lake waters through progressive evaporation (Beeler et al., *in review*). Locations containing salt deposit were on average associated with waters of significantly higher salinities compared to those containing carbonate muds (Figure 2.9d), which we interpret to be due to changes in the saturation state of minerals following an evaporative sequence. In contrast, the average salinity associated with different matrix types is not significantly different between locations containing marsh grasses, different mat types, or carbonate muds (Figure 2.9d). Therefore, despite the large spatial variability in salinity across the stromatolite belt these changes do not appear to drive changes in the distribution of these matrix types.

Changes in pH represent another potential control on the distribution of matrix types as pH has been shown to be a major contributor to the structure of microbial communities globally (Fierer & Jackson, 2006). Additionally, successive mineral precipitation during evaporation is also associated with changes in pH (Bąbel & Schreiber, 2014). An overall decrease in pH occurs across the stromatolite belt from slightly alkaline at the groundwater source to neutral pH in the lake body (Beeler et al.,*in review*) . Significant differences were found in the average pH of waters associated with greenish versus pustular mats (Figure 2.9f). Diatoms, which are the dominant primary producer at Laguna Negra, are highly sensitive to pH, thus differences in pH could explain the variability in the structure of the mat types (Birks *et al.*, 1990; Gomez *et al.*, 2018). However, while there are significant differences in the average pH of waters associated with greenish versus pustular mats the overall pH ranges are highly variable and overlapping.

This indicates that pH is not acting as a strict control on mat structure, and therefore we do not interpret pH changes as a cause of changes in mat type. A significant decrease in pH was also observed in locations containing salts versus those containing carbonate muds (Figure 2.9f), which is consistent with a control of successive precipitation of minerals following an evaporite sequence (Bąbel & Schreiber, 2014).

The concentration of DIC could also control the distribution of matrix types as inorganic carbon may act as a limiting nutrient in some settings and also acts as a control on the saturation state of carbonate minerals (Riebesell *et al.*, 1993; Appelo *et al.*, 2005). DIC concentration decrease across the stromatolite belt from extremely high values at the groundwater source (25 mM) to low values nearest the lake body (1.6 mM) due to a combination of degassing, evaporation, and carbonate precipitation (Beeler et al., in review). The average DIC concentration of associated waters is significantly different between structure types indicating it is a potential driver of the variability in matrix types (Figure 2.9e). While DIC concentrations associated with grasses and different mat types do have significant differences it is unlikely that this change is due to carbon limitation as DIC concentrations across the entire stromatolite belt are an order of magnitude higher than those found in locations where carbon is a limiting nutrient (Riebesell *et al.*, 1993). In contrast, significant differences between carbonate muds, which largely consist of carbonate muds, and salt can be explained by DIC loss driving a change in the saturation state of carbonate minerals.

Together these results indicate that differences in the distribution of the "sedimentological" matrix types (i.e. carbonate muds and salt) can be explained through the geochemical evolution of waters following an evaporative sequence. In contrast, the basic geochemical parameters measured in this study are incapable of explaining the variability in the

distribution of the "biological" matrix types (i.e. grass and microbial mats). While the geochemistry of waters associated with these matrix types show differences, no causal mechanisms are apparent that can link this variability to changes in their distributions. However, this does not rule out a geochemical control of mat distributions as parameters not analyzed in this study such as the availability of nutrients or electron acceptors could still drive the distribution of "biological" matrix types if they co-vary with these changes.

Physical parameters such as wind shear or wave action has also been shown to control the distribution of microbial mats in other environments and could be a potential driver of mat distributions at Laguna Negra (Bouougri & Porada, 2012; Cuadrado *et al.*, 2014). Some of the highest wind speeds on Earth have been recorded in the Puna-Altiplano region suggesting high winds could potentially disrupt mats at Laguna Negra (Milana, 2009). High speed winds in the Puna-Altiplano region predominately blow from NW-SE, and while detailed meteorological data is lacking at Laguna Negra field observations suggest similar wind paths at Laguna Negra (Bridges *et al.*, 2015). Winds blowing from NW-SE would run parallel to the direction of matrix succession consistent with wind driven changes in their distribution (Figure 2.4b). Collection of more detailed meteorological data and information regarding the different mat types resistance to wind shear are necessary to more rigorously test the role of wind in shaping matrix distributions at Laguna Negra.

2.6.3 Controls on the Size and Abundance of Mineralized Structures

In addition to spatial differences in their distribution, the average size and abundance of mineralized structures was significantly variably between structure types with oncoids having the largest average size and abundance, boulders intermediate values, and laminar crusts the lowest values (Figure 2.6). The differences in size and abundance of different structure types may

reflect variability in the processes controlling their formational mechanism, however these differences could also reflect spatial variability in processes that control their distribution across the stromatolite belt such as wind or water action that are independent of their formational mechanism. In order to constrain these differences, we analyzed the spatial variability in the average size and abundance of structures across the stromatolite belt using geospatial statistical techniques (Figures 2.7-8).

Global Moran's I indicated significant clustering of similar values for both average size and abundance of structures across the stromatolite belt. General G did not show significant clustering of high or low values for average structure size, which in conjunction with the significant result for Global I indicates that clustering of both high and low values is occurring rather than clustering of either high or low values. In contrast, the General G statistic indicated significant clustering of high values was identified for the abundance of mineralized structures. Anselin Local Moran's I for the average size of structures identified a cluster of high values near the lake margin in the center of the stromatolite belt and a cluster of low values near the lake body towards the northeastern portion of the stromatolite belt (Figure 2.7b). Both high value and low value clusters of structure size are in areas containing boulders. Anselin Local Moran's I for the abundance of structures exhibited a cluster of high values centrally located in the stromatolite belt and low value clusters near the groundwater input and at the edge of the salt flat located in the northwest corner of the lake (Figure 2.8b). The cluster of high values occurred across an area containing both boulders and oncoids. Low value clusters occurred in areas containing either no mineralized structures or oncoids. The locations of clustering for mineralized structures of similar size and abundance do not follow any of the spatial trends established for differences in mineralized structure type, matrix type, or geochemistry. This suggests that the control of this

clustering is not a result of changes in these parameters across the stromatolite belt. Similarly, visual analysis of variability in the average size and abundance of mineralized structures does not indicate any clear trends (Figures 2.7a and 2.8a). The interaction of physical processes such as wind and water action, freeze/thaw cycles, or salt deposition provide a potential explanation for the observed distributions. However, detailed data of variability in physical processes temporally make reconstructing their effects difficult and is beyond the scope of this project.

Regardless of its cause, the spatial clustering present at Laguna Negra does not appear to be related to changes in the distribution of mineralized structure types spatially type across the stromatolite belt. This implies that the observed variation in the size and abundance of different mineralized structure types is a result of variability in the processes governing their formation. The allochthonous origin of boulders indicates that their size and abundance is the result of physical rather than geochemical and/or microbial processes and represent a purely physically driven endmember. In contrast, the autochthonous origin of carbonate structures suggests that their size and abundance could also be affected by geochemical and/or microbial processes affecting mineral precipitation in addition to physical processes. Discrete mineralized structures found in areas containing laminar crusts were significantly smaller and less abundant than those in areas containing oncoids. We interpret these differences to be a result in the mode of carbonate precipitation as laminar crusts often form laterally extensive pavements rather than discrete structures. This difference in the mode of carbonate precipitation may be the result of localized microbial activity changing the manner in which carbonate is being precipitated (Dupraz & Visscher, 2005; Dupraz *et al.*, 2009) . Alternatively, variability in physical conditions such as changes in water depth, wind action, or freeze/thaw cycles could also disrupt the formation of laterally extensive pavements. Analysis of variability in lake conditions temporally

are necessary to fully resolve these differences and provide stronger interpretation of the meaning of variability in the size and abundance of different structure types.

2.7 Conclusions

Previous work at Laguna Negra has focused on understanding the formation and morphogenesis of microbialites and associated non-microbial carbonates from the micro- (millimeter or less) to macro- (decimeter) scales, and have linked variability at these scales to changes in the presence and structure of microbial communities (Gomez *et al.*, 2014, 2018; Mlewski *et al.*, 2018). The results of this study build upon this work and expand our knowledge into the processes that control their formation and distribution from the macro- to mega- (meter to kilometer) scales. Our results indicate that at these spatial scales the distribution of oncoids versus other carbonates is driven by changes in the distribution of microbial mats. This is consistent with microscale observations that morphological changes in microbialites are the result of changes in the structure and function of microbial communities and supports the interpretation of a biogenic origin for oncoids and an abiogenic origin of laminar crusts and gravels. While a significant relationship between the distribution of different carbonate types and matrix types was evident the processes controlling the distribution of matrix types remains unclear as none of the basic geochemical parameters measured in this study nor simple physical processes can fully explain the variable distributions of matrix types. Likewise, differences in the size and abundance between mineralized structure types were also observed that may reflect difference in biogeochemical or physical processes, however no clear causal relationship has been identified. Future studies at Laguna Negra focused on understanding the spatial and temporal variability of additional geochemical parameters and physical conditions are necessary to more fully resolve the cause of this variability.

Our results differ from observations made from other modern environments that have attributed variability in the spatial distribution of microbialites and other carbonates at the macro- to mega- scale in these settings to a combination of physical parameters such as accommodation space, wave energy, sediment flux, or tectonic processes (Eckman *et al.*, 2008; Jahnert & Collins, 2012; Bouton *et al.*, 2016). While physical processes do influence the size and abundance of mineralized structures and may act as an underlying control on the distribution of microbial mats at Laguna Negra they are not the primary influence on the spatial distribution of the microbialites directly. A microbial driver of the macro- to mega- scale distribution of microbialites contrasts with the canonical interpretation that microbial controls exert increasingly less influence at larger spatial scales (Trompette, 1982; Ginsburg, 1991; Andres & Reid, 2006). Analysis of spatial variability in the occurrence and characteristics of microbialites in the rock record should therefore consider the potential role of variability in microbial communities as a driver for their distributions.

2.8 References

Agresti A. (2007) *An introduction to categorical data analysis*., Wiley-Interscience.

Andres M. S. and Pamela Reid R. (2006) Growth morphologies of modern marine stromatolites: A case study from Highborne Cay, Bahamas. *Sedimentary Geology* **185**, 319–328.

Andres M. S. and Reid R. P. (2006) Growth morphologies of modern marine stromatolites: A case study from Highborne Cay, Bahamas. *Sedimentary Geology* **185**, 319–328.

Appelo C., Postma D. and Postma D. (2005) *Geochemistry, Groundwater and Pollution, Second Edition*., Taylor & Francis.

Bąbel M. and Schreiber B. . (2014) Geochemistry of evaporites and evolution of seawater. In *Treatise on Geochemistry* Elsevier, Amsterdam. pp. 483–560.

Birks H. J. B., Line J. M., Juggins S., Stevenson A. C. and Braak C. J. F. T. (1990) Diatoms and pH Reconstruction. *Philosophical Transactions of the Royal Society B: Biological Sciences* **327**, 263–278.

Bolhuis H., Fillinger L. and Stal L. J. (2013) Coastal Microbial Mat Diversity along a Natural Salinity Gradient ed. J. A. Gilbert. *PLoS ONE* **8**, e63166.

Bosak T., Knoll A. H. and Petroff A. P. (2013) The Meaning of Stromatolites. *Annual Review of Earth and Planetary Sciences* **41**, 21–44.

Bouougri E. H. and Porada H. (2012) Wind-induced mat deformation structures in recent tidal flats and sabkhas of SE-Tunisia and their significance for environmental interpretation of fossil structures. *Sedimentary Geology* **263**–**264**, 56–66.

Bouton A., Vennin E., Boulle J., Pace A., Bourillot R., Thomazo C., Brayard A., Désaubliaux G., Goslar T., Yokoyama Y., Dupraz C. and Visscher P. T. (2016) Linking the distribution of microbial deposits from the Great Salt Lake (Utah, USA) to tectonic and climatic processes. *Biogeosciences* **13**, 5511–5526.

Bridges N. T., Spagnuolo M. G., de Silva S. L., Zimbelman J. R. and Neely E. M. (2015) Formation of gravel-mantled megaripples on Earth and Mars: Insights from the Argentinean Puna and wind tunnel experiments. *Aeolian Research* **17**, 49–60.

Buongiorno J. (2014) Mineralized microbialites as archives of environmental evolution of a hypersaline lake basin: Laguna Negra, Catamarca Province, Argentina. *Masters Theses*, gbi.12327.

Burne R. V and Moore L. S. (1987) Microbialites: organosedimentary deposits of benthic microbial communities. *Palaios* **2**, 241–254.

Caldas de Castro M. and Singer B. H. (2006) Controlling the false discovery rate: A new

application to account for multiple and dependent tests in local statistics of spatial association. *Geographical Analysis* **38**, 180–208.

Cuadrado D. G., Perillo G. M. E. and Vitale A. J. (2014) Modern microbial mats in siliciclastic tidal flats: Evolution, structure and the role of hydrodynamics. *Marine Geology* **352**, 367–380.

Druschel G. K. and Kappler A. (2015) Geomicrobiology and Microbial Geochemistry. *Elements* **11**, 389–394.

Dupraz C., Reid R. P., Braissant O., Decho A. W., Norman R. S. and Visscher P. T. (2009) Processes of carbonate precipitation in modern microbial mats. *Earth-Science Reviews* **96**, 141–162.

Dupraz C. and Visscher P. (2005) Microbial lithification in marine stromatolites and hypersaline mats. *Trends in Microbiology* **13**, 429–438

Eckman J. E., Andres M. S., Marinelli R. L., Bowlin E., Reid R. P., Aspden R. J. and Paterson D. M. (2008) Wave and sediment dynamics along a shallow subtidal sandy beach inhabited by modern stromatolites. *Geobiology* **6**, 21–32.

Fierer N. and Jackson R. B. (2006) The diversity and biogeography of soil bacterial communities. *Proceedings of the National Academy of Sciences of the United States of America* **103**, 626–631.

Frantz C. M., Petryshyn V. A. and Corsetti F. A. (2015) Grain trapping by filamentous cyanobacterial and algal mats: Implications for stromatolite microfabrics through time. *Geobiology* **13**, 409–423.

Ginsburg R. (1991) Controversies about stromatolites: vices and virtues. *Controversies in Modern Geology*.

Golubic S. (1991) Modern Stromatolites: A Review. In *Calcareous Algae and Stromatolites* Springer Berlin Heidelberg, Berlin, Heidelberg. pp. 541–561.

Gomez F. J., Kah L. C., Bartley J. K. and Astini R. A. (2014) Microbialites in a high-altitude Andean lake: multiple controls on carbonate precipitation and lamina accretion. *Palaios* **29**, 233–249.

Gomez F. J., Mlewski C., Boidi F. J., Farías M. E. and Gérard E. (2018) Calcium Carbonate Precipitation in Diatom-rich Microbial Mats: The Laguna Negra Hypersaline Lake, Catamarca, Argentina. *Journal of Sedimentary Research* **88**, 727–742.

Grotzinger J. P. and James N. P. (2000) Precambrian Carbonates: Evolution of Understanding.

Grotzinger J. P. and Knoll A. H. (1999) Stromatolites in Precambrian carbonates: evolutionary mileposts or environmental dipsticks? *Annual Review of Earth and Planetary Sciences* **27**, 313–358.

Gulzar S., Khan M. A. and Ungar I. A. (2003) Salt Tolerance of a Coastal Salt Marsh Grass. *Communications in Soil Science and Plant Analysis* **34**, 2595–2605.

Hofmann H. J. (1973) Stromatolites: Characteristics and utility. *Earth-Science Reviews* **9**, 339–373.

Ibarra Y. and Corsetti F. A. (2016) Lateral Comparative Investigation of Stromatolites: Astrobiological Implications and Assessment of Scales of Control. *Astrobiology* **16**, 271–281.

Jahnert R. J. and Collins L. B. (2012) Characteristics, distribution and morphogenesis of subtidal microbial systems in Shark Bay, Australia. *Marine Geology* **303–306**, 115–136.

Kazmierczak J. and Kempe S. (2006) Genuine modern analogues of Precambrian stromatolites from caldera lakes of Niuafo‘ou Island, Tonga. *Naturwissenschaften* **93**, 119–126.

Kneissl T., van Gasselt S. and Neukum G. (2011) Map-projection-independent crater size-frequency determination in GIS environments—New software tool for ArcGIS. *Planetary and Space Science* **59**, 1243–1254.

Linthurst R. A. and Blum U. (1981) Growth modifications of Spartina alterniflora Loisel. by the interaction of pH and salinity under controlled conditions. *Journal of Experimental Marine Biology and Ecology* **55**, 207–218.

Lozupone C. A. and Knight R. (2007) Global patterns in bacterial diversity. *Proceedings of the National Academy of Sciences* **104**, 11436–11440.

McCaffrey M. A., Lazar B. and Holland H. D. (1987) The Evaporation Path of Seawater and the Coprecipitation of Br- and K+ with Halite. *SEPM Journal of Sedimentary Research* **Vol. 57**, 928–937.

de Mendiburu F. (2017) agricolae: Statistical Procedures for Agricultural Research.

Milana J. P. (2009) Largest wind ripples on Earth? *Geology* **37**, 343–346.

Mitchel A. (2005) The ESRI Guide to GIS analysis, Volume 2: Spartial measurements and statistics. *ESRI Guide to GIS analysis*.

Mlewski E. C., Pisapia C., Gomez F., Lecourt L., Soto Rueda E., Benzerara K., Ménez B., Borensztajn S., Jamme F., Réfrégiers M. and Gérard E. (2018) Characterization of Pustular Mats and Related Rivularia-Rich Laminations in Oncoids From the Laguna Negra Lake (Argentina). *Frontiers in microbiology* **9**, 996.

Pace A., Bourillot R., Bouton A., Vennin E., Galaup S., Bundeleva I., Patrier P., Dupraz C., Thomazo C., Sansjofre P., Yokoyama Y., Franceschi M., Anguy Y., Pigot L., Virgone A. and Visscher P. T. (2016) Microbial and diagenetic steps leading to the mineralisation of Great Salt Lake microbialites. *Scientific Reports* **6**, 31495.

Peters S. E., Husson J. M. and Wilcots J. (2017) The rise and fall of stromatolites in shallow marine environments. *Geology* **45**, 487–490.

R Core Team (2017) R: A language and environment for statistical computing.

Reddy M. M. and Nancollas G. H. (1976) The crystallization of calcium carbonate. *Journal of Crystal Growth* **35**, 33–38.

Riding R. (2000) Microbial carbonates: the geological record of calcified bacterial–algal mats and biofilms. *Sedimentology* **47**, 179–214.

Riding R. and Liang L. (2005) Geobiology of microbial carbonates: metazoan and seawater saturation state influences on secular trends during the Phanerozoic. *Palaeogeography, Palaeoclimatology, Palaeoecology* **219**, 101–115.

Riebesell U., Wolf-Gladrow D. A. and Smetacek V. (1993) Carbon dioxide limitation of marine phytoplankton growth rates. *Nature* **361**, 249–251.

Shapiro R. S. (2000) A comment on the Systematic Confusion of Thrombolites. *Palaios* **15**, 166–169.

Tiefelsdorf M. and Boots B. (2010) A Note on the Extremities of Local Moran's Iis and Their Impact on Global Moran's I. *Geographical Analysis* **29**, 248–257.

Trompette R. (1982) Upper Proterozoic (1800-570 Ma) stratigraphy: A survey of lithostratigraphic, paleontological, radiochronological and magnetic correlations. *Precambrian Research* **18**, 27–52.

De Wit R. and Bouvier T. (2006) "Everything is everywhere, but, the environment selects"; what did Baas Becking and Beijerinck really say? *Environmental Microbiology* **8**, 755–758.

Chapter 3: Controls of extreme isotopic enrichment in modern microbialites and associated abiogenic carbonates

Scott R. Beeler[1], Fernando J. Gomez[2], Alexander S. Bradley[1]

[1]Department of Earth and Planetary Science, Washington University in St. Louis, Saint Louis, Missouri, 63130, USA

[2]CICTERRA-CONICET, Facultad de Ciencias Exactas, Fisicas, y Naturales, Universidad Nacional de Córdoba, Córdoba, X5000, Argentina

This chapter is currently in review at *Geochimica et Cosmochimica Acta*

3.1 Abstract

Microbialites and abiogenic carbonates of the closed-basin hypersaline lake Laguna Negra (Catamarca Province, Argentina) are highly enriched in both ^{13}C and ^{18}O. These carbonates precipitate in the zone of recharge where lake water mixes with groundwater. We examined the processes controlling the isotopic evolution of input waters in order to better interpret the isotopic compositions of the carbonates. Large enrichments of ^{13}C in dissolved inorganic carbon and ^{18}O in water occur as input groundwater chemically evolves. These enrichments can be explained through the abiotic processes of water-equilibration, evaporation, degassing, and carbonate precipitation. The ^{13}C and ^{18}O contents of lake carbonates are consistent with equilibrium precipitation from lake water suggesting that the currently ongoing processes can explain the isotopic patterns observed in carbonates. Isotopic compositions of these microbialites are largely unrelated to the biological processes controlling microbialite formation – a pattern that may be generalizable to other settings. However, the isotopic compositions of these microbialites record information about their depositional environment.

3.2 Introduction

Microbialites are sedimentary structures arising from the interaction of microbial and geological processes that occur extensively throughout the rock record (Burne and Moore, 1987; Grotzinger and Knoll, 1999; Riding, 2000). These structures are among the oldest evidence of life on Earth and provide one of the best records of life, particularly in the Precambrian where a robust fossil record is lacking (Allwood et al., 2006; Schopf and Kudryavtsev, 2007; Nutman et al., 2016; Peters et al., 2017). Microbialites can provide insight into how life and the environment have co-evolved through geologic time. Microbialites have been proposed as a

target in the search for extraterrestrial life because they provide geological evidence of life that can potentially be recognized at outcrop scale (Cady et al., 2003; Des Marais et al., 2008). However, structures that are morphologically similar to microbialites can be formed abiotically confounding their utility as a tool to detect and understand life on early Earth and potentially other planets (Grotzinger and Rothman, 1996). Even in cases where biogenicity is clear our ability to interpret the biogeochemical information potentially preserved in microbialites is incomplete (Grotzinger and Knoll, 1999; Bosak et al., 2013). Additional lines of evidence in addition to morphology are therefore necessary to assess the biogenicity of microbialites and determine the biogeochemical information they may preserve.

The $\delta^{13}C$ and $\delta^{18}O$ of carbonate minerals that comprise microbialites are a compelling tool to understand the meaning of microbialites because they reflect environmental processes associated with their formation. If carbonate is precipitated in chemical equilibrium with dissolved inorganic carbon (DIC) and water, then the carbonate captures geochemical and hydrological processes. Microbial processes can also play a role, and the stable isotopic composition of carbon and oxygen of carbonate minerals have been analyzed to make inferences about the structure and function of microbial communities associated with microbialite formation (Andres et al., 2006; Brady et al., 2014; Birgel et al., 2015). Likewise, stable isotopic compositions have been suggested as a potential tool to assess the biogenicity of mineral structures on Mars (Banfield et al., 2001). The changes in isotopic values preserved in the laminated fabrics present in many microbialites have also been used as time series evidence of shifts in these processes through time (Nehza et al., 2009; Frantz et al., 2014; Petryshyn et al., 2016). At the broad scale, the isotopic composition of carbonate minerals are used as a tool to understand the evolution of biogeochemical cycles through geologic time (Kump and Arthur,

1999). Developing an understanding how isotopic signatures are generated and preserved in microbialites in modern environments can help to enhance our ability to interpret their meaning in ancient and potentially extraterrestrial examples.

The evaporative lake Laguna Negra (Catamarca Province, Argentina) contains microbialites with carbonate that is highly enriched in ^{13}C and ^{18}O. These isotopic compositions have been hypothesized to arise from the interactions of microbial, geochemical, and hydrological processes, and to some degree reflect the environmental conditions temporally at the lake (Gomez et al., 2014; Buongiorno et al., 2018). However, the lateral variability in the isotopic compositions of surface waters across the lake at a single time point are unconstrained complicating our understanding of how to interpret the temporal variability in the isotopic compositions preserved in the carbonates. Here we performed spatial analyses of isotopic and geochemical parameters in Laguna Negra waters to assess the degree and controls of isotopic variability at the lake. We then used this data to provide a framework for more robust interpretation of isotopic values of carbon and oxygen from carbonate minerals at Laguna Negra and other comparable sites.

3.3 Field Area

Laguna Negra is a closed basin lake located in the Puna-Altiplano region of the Andes mountains (Figure 3.1). Lake waters are hypersaline (up to >300 ppt) reflecting the strongly negative water balance of the region (Risacher et al., 2003; Risacher and Fritz, 2009) . Inputs of water into the lake occur only along its southeastern margin where more dilute groundwater and seasonal snowmelt mix with the hypersaline lake waters. Geochemical modeling reveals that mixing of these waters produces an increase in the saturation state of both calcite and aragonite in the mixing zone, and explains the observation that carbonate precipitation only occurs within

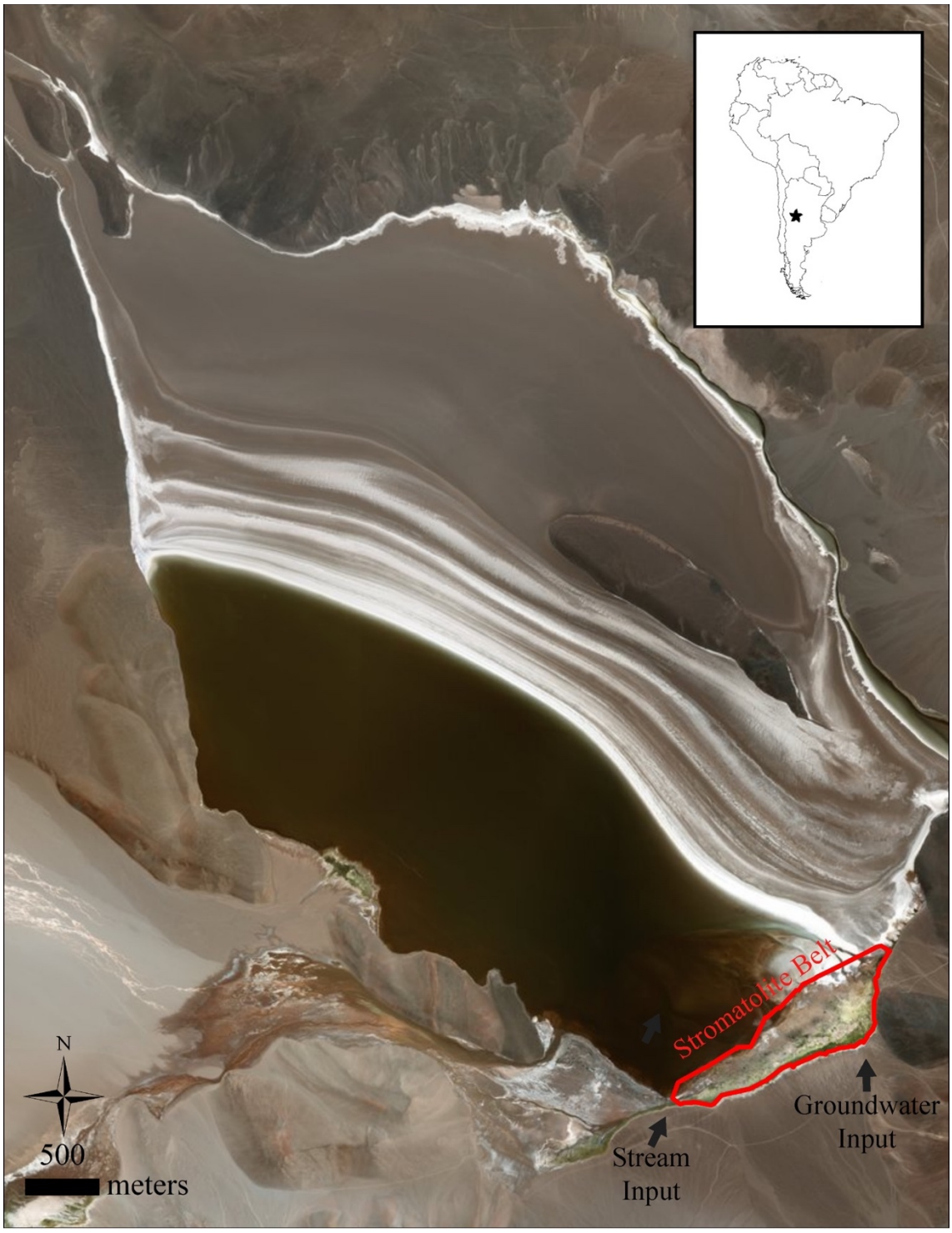

Figure 3.1: Aerial view of Laguna Negra indicating location of the microbialite belt where carbonate formation including microbialites and abiogenic carbonates form in a zone of input of more dilute water. Base image from ArcGIS World Imagery.

this region of the lake (Gomez et al., 2014). This zone of carbonate precipitation is referred to as the stromatolite belt, and include structures interpreted as microbialites in addition to morphologies interpreted as having formed without microbial influence (c.f. Gomez et al., 2014). Microbialitic morphologies found at Laguna Negra primarily occur as discrete spheroidal to discoidal laminated oncoids with occasional accretionary laminated stromatolites. In addition to microbialites, carbonates with morphologies interpreted to form abiogenically are also observed across the lake edge primarily in the form of gravels and laminar crusts. The occurrence of these different types of carbonate morphologies varies across the lake edge and tend to occur in spatially separated zones with microbialites primarily concentrated along the northeastern and central part of the stromatolite belt and transitioning into non-microbial carbonates moving westward. These variations in carbonate morphology are associated with changes in the occurrence and appearance of microbial mats. Petrographic evidence including changes in dominant microfabric type and the presence of microfossils between carbonate types of differing macrosopic morphologies is consistent with variable roles of biology in their formation (c.f. Gomez et al., 2014).

3.4 Materials and Methods

Waters were sampled in March 2017 from fifteen locations across the stromatolite belt to assess their geochemical and isotopic variability (Figure S3.1). Two samples were taken from areas identified as potential sources of inlet waters: a groundwater fed pool and surface stream likely fed from snowmelt. The remaining thirteen samples were taken from locations across the zone of mixing. Water samples were taken from surface waters using a polypropylene syringe equipped with PTFE tubing. Prior to sample collection the syringe and tubing were each rinsed three times with water from the sample location. Basic geochemical parameters (Temperature,

pH, and electrical conductivity) were measured *in situ* using a Myron L Ultrameter II handheld meter. Salinity (S) was calculated from electrical conductivity (EC) by the Ultrameter II algorithms with NaCl as the reference compound due to Na^+ and Cl^- being previously determined to be the dominant ions in Laguna Negra waters (Gomez et al., 2014). Salinity conversions by the Ultrameter II have a maximum range of 200 ppt so values above this range were calculated using a conversion factor of S=2*EC, which is the maximum value used by the Ultrameter II algorithm. The conversion for these high conductivity samples likely represents an underestimation of salinity, but this underestimation does not affect the interpretations made from this data. Samples were also collected for stable isotopic analysis of dissolved inorganic carbon (DIC) and oxygen and hydrogen of water. Samples for DIC analysis were collected by injecting waters into an evacuated 12 mL Exetainer vial filled with 1 mL of H_2SO_4 to evolve DIC into CO_2 for analysis. Additional water samples were also collected in 2 mL GC vials for isotopic analyses of oxygen and hydrogen of water. Isotopic composition and concentrations of DIC were measured using GasBench II system interfaced to a Delta V Plus IRMS at the UC Davis Stable Isotope Facility. The long term standard deviation of isotopic values is 0.1‰ with lithium carbonate and deep seawater utilized as reference materials. Hydrogen and oxygen isotopic compositions of water were measured using a Laser Water Isotope Analyzer V2 at the UC Davis Stable Isotope Facility. The long term standard deviation for isotopic values was <0.3‰ for ^{18}O and <2.0‰ for ^{2}H with a range of reference waters calibrated against IAEA reference waters.

Speciation of the carbonate system and carbonate alkalinity was calculated using measured values of [DIC] and pH and the equilibrium constants of Sass and Ben-Yaakov (1977). The Sass and Ben-Yaakov constants were chosen because they are calibrated across a

high range of salinities (0 to 330 parts per thousand) unlike other equilibrium constants in the literature, which are only calibrated across a more narrow range of salinities (typically 0 to ~40 parts per thousand). One drawback of the Sass and Ben-Yaakov constants is that they were determined only at a temperature of 30°C, and do not account for the effect of changing temperatures on equilibrium constants. Measured lake water temperatures at Laguna Negra were all ≤22.0°C and spatially variable, which may provide a source of error into speciation calculations performed using the Sass and Ben-Yaakov constants. To determine the importance of this error the speciation of the carbonate system of a solution was calculated accounting for temperature changes but not salinity changes using the equilibrium constants of Mehrbach et al. (1973) and compared to those calculated accounting for salinity but not temperature changes using the Sass and Ben-Yaakov constants (Figure S3.2). The variability in the concentration of carbonate species accounting for salinity with the Sass and Ben-Yaakov constants was substantially larger than the variability accounting for temperature changes using the Mehrbach constants. This indicates that salinity effects have a larger influence than temperature effects on the equilibrium constants in this system supporting the use of the Sass and Ben Yaakov constants.

The stable carbon and oxygen isotopic values expected for calcite precipitated in equilibrium with Laguna Negra waters were calculated at each sampling location. Stable oxygen isotopic values of an equilibrium calcite mineral were calculated with the oxygen isotope fractionation factor from Kim and O'Neil (1997) using measured water temperature and oxygen isotope values. Stable carbon isotope values of an equilibrium calcite mineral were calculated using the calcite-bicarbonate fractionation factor of Rubinson and Clayton (1969). The isotopic composition of bicarbonate was calculated using the mass balance formula of Zeebe and Wolf-

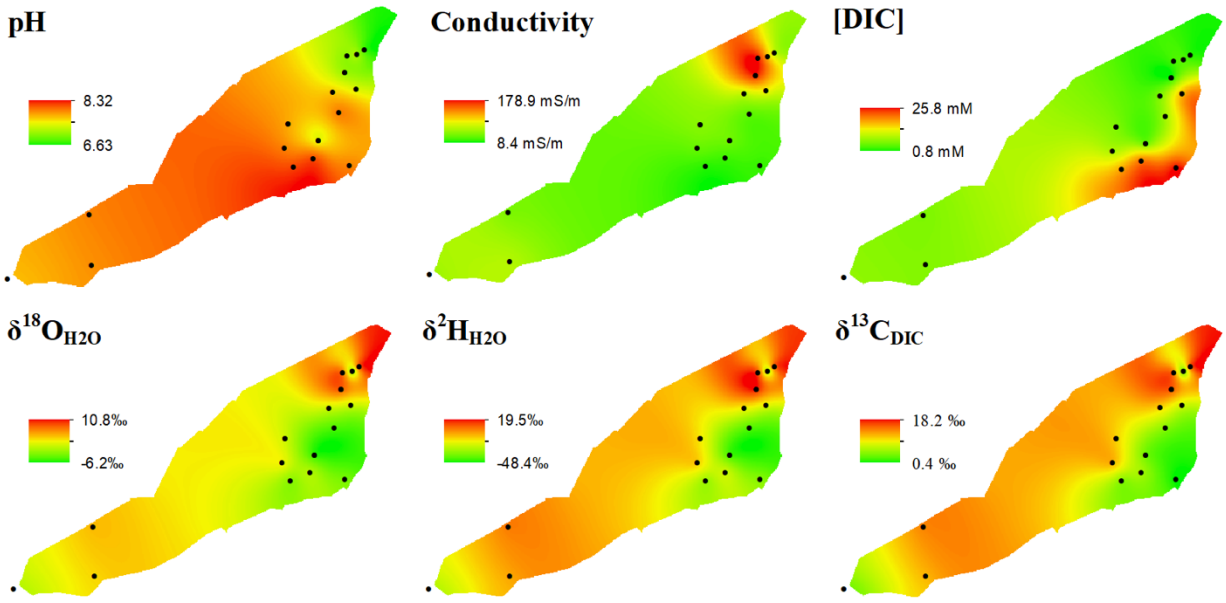

Figure 3.2: Spatial variability of geochemical and isotopic parameters across the stromatolite belt at Laguna Negra. Values are interpolated for the entire belt from measurements taken across the lake edge (black dots). In general, waters become more saline, acidic, DIC poor, and isotopically enriched moving away from the groundwater input source.

Gladrow (2001) using the fractionation factors of Mook (1986), measured $\delta^{13}C_{DIC}$ and DIC concentrations, and calculated concentrations of CO_2 (aq), HCO_3^-, and CO_3^{2-}.

Geochemical and isotopic data were integrated into a geographic information system (GIS) data model in ArcMap (v.10.5.1). Interpolated maps of geochemical and isotopic parameters were generated using the Spline tool using a cell size of 3.6 m/pixel. Interpolated maps of modeled values for $\delta^{13}C$ and $\delta^{18}O$ of calcite were generated using the Raster Calculator tool in ArcMap to perform the above calculations with the interpolated raster maps of measured values.

3.5 Results

Basic geochemical parameters measured across the stromatolite belt at Laguna Negra displayed a high degree of spatial variability (Table 3.1, Figure 3.2). Inlet waters sourced from the groundwater pond (LN-003) were dilute (EC = 8.88 mS/m) and moderately alkaline (pH =

Table 3.1: Geochemical parameters measured across the stromatolite belt

Sample	pH	Temperature (°Celcius)	Conductivity (mS/m)	Salinity (ppt)	[DIC] (mM)	Carbonate Alkalinity (meq/L)	$\delta^{13}C_{DIC}$ (‰,V-PDB)	$\delta^{2}H_{H2O}$ (‰,V-SMOW)	$\delta 18O_{H2O}$ (‰,V-SMOW
LN-003	7.92	19.2	17.2	15.8	25.0	30.6	0.45	-34.0	-3.15
LN-004	8.12	20.7	19.0	17.7	19.8	26.4	5.55	-22.5	-0.86
LN-005	8.15	17.9	13.7	12.3	17.5	23.2	4.29	-30.3	-2.47
LN-006	7.93	16.5	31.6	32.5	8.8	11.3	11.6	-9.5	1.72
LN-007	7.72	16.7	43.1	47.1	6.6	8.2	10.9	-13.6	0.43
LN-007b	7.82	17.7	45.7	50.4	5.1	6.6	9.73	-15.7	-0.12
LN-008	7.43	13.8	35.2	37.5	-	-	-	-43.9	-5.64
LN-008b	7.39	18.1	34.7	36.3	4.7	5.1	3.43	-42.9	-5.35
LN-009	7.14	3.1	115.4	236	3.6	6.3	3.79	-26.3	-1.18
LN-010	7.04	10.1	169.0	338	3.2	6.2	13.9	10.8	7.11
LN-011	7.18	16.7	157.6	315	1.6	3.1	15.1	10.9	7.02
LN-011b	6.99	21.5	176.5	353	-	-	-	21.0	8.61
LN-012	7.62	15.9	71.6	92.7	5.9	8.2	10.4	-14.2	0.56
LN-013	7.93	16.6	28.9	29.2	8.1	10.3	4.21	-41.6	-4.64
LN-014	7.35	20.0	90.1	133	16.5	23.1	7.59	-17.5	0.53
LN-015	7.68	21.7	51.1	57.0	7.0	8.8	2.62	-29.3	-1.18
LN-016	7.87	17.8	61.5	75.1	-	-	-	-	-
LN-017	7.92	18.4	39.6	42.7	5.7	7.6	13.5	3.0	4.28
LN-018	6.76	22.0	189.9	380	2.0	3.9	15.1	7.6	8.21

7.92). Waters measured from a surface stream (LN-015) were moderately alkaline (pH = 7.68) and substantially more saline (EC = 51.1 mS/m). In general, waters in stromatolite belt became more saline and less alkaline moving away from the groundwater inlet source. The northeastern corner of the stromatolite belt contained the most saline (EC up to 176.5 mS/m) and acidic (pH = 6.76) waters. Temperature also varied across the stromatolite belt, but the changes correlated with time of sampling indicating that ambient conditions likely control the temperature changes.

The stable oxygen and hydrogen isotopic composition of water were similarly variable. Input waters measured from the groundwater pool ($\delta^{18}O_{H2O}$ = -3.15‰, and $\delta^{2}H_{H2O}$ = -34.0‰) were depleted in heavy isotopes compared to other locations across the lake. Similar to the geochemical parameters, isotopic trends became more enriched in ^{18}O and ^{2}H moving away from the groundwater pool towards the lake ($\delta^{18}O_{H2O}$ up to +8.61‰ and $\delta^{2}H_{H2O}$ up to +21.0‰). Likewise, the concentration and isotopic composition of DIC was variable across the lake edge. The groundwater pool had the highest concentration ([DIC] = 25.0 mM) and most depleted isotopic composition ($\delta^{13}C_{DIC}$ = +0.45‰). These values are out of equilibrium with atmospheric values expected for T, S, and pH values for the ground water pool ([DIC] =1.34 mM and $\delta^{13}C_{DIC}$ = +1‰) calculated using the model of Zeebe and Wolf-Gladrow (2001). DIC concentrations decreased ([DIC] as low as 1.6 mM) and became highly enriched isotopically ($\delta^{13}C_{DIC}$ up to +15.06‰) moving away from the groundwater pool towards the lake.

3.6 Discussion

3.6.1 Controls on the Isotopic and Geochemical Variability of Laguna Negra Waters

The isotopic and geochemical trends of waters as they evolve across the stromatolite belt can provide insight the processes driving their evolution. Input of water into the lake has

previously been recognized to be primarily sourced from groundwater inlets with possible contribution from stream water inlets sourced from snowmelt (Gomez et al., 2014). Our results are consistent with groundwater inlets being the primary source of water into the lake as there are clear geochemical and isotopic trends from the groundwater inlets outwards towards the lake body (Figure 3.2). In contrast, the influence of the stream water input on geochemical and isotopic compositions of waters in the stromatolite belt showed comparatively limited influence. Stream input waters were more saline, DIC rich, and isotopically enriched than expected for meteoric waters indicating likely resulting from mixing with already evolved lake waters due to winds oriented upstream of the inlet source at the time of sampling. While this input may have local effects on the geochemical and isotopic compositions of waters near the input their overall effects on the trends observed across the stromatolite belt are limited compared to the influence of groundwater at least during the time our sampling (late austral summer). Accordingly, the influence of these streams was assumed to be negligible in the following calculations and modelling, however it is recognized that it may be a more important influence seasonally.

The isotopic values of water ($\delta^{18}O_{H2O}$ and $\delta^{2}H_{H2O}$) closer to zone of groundwater recharge are relatively depleted and become progressively enriched moving outwards towards the lakes indicating progressive loss of the light isotope as input waters evolve into lake waters. $\delta^{18}O_{H2O}$ and $\delta^{2}H_{H2O}$ strongly co-vary ($R^2 = 0.97$) across the lake edge along a trendline with a slope of 4.4 (Figure 3.3). These values are enriched relative to the isotopic compositions of meteoric waters in the region and project along trendline projects off of the local meteoric water line (Figure 3.3; Scheihing et al., 2017), which is characteristic of isotopic enrichment of waters driven by evaporation (Criss, 1999). This evaporative trend is also evident in the increase of

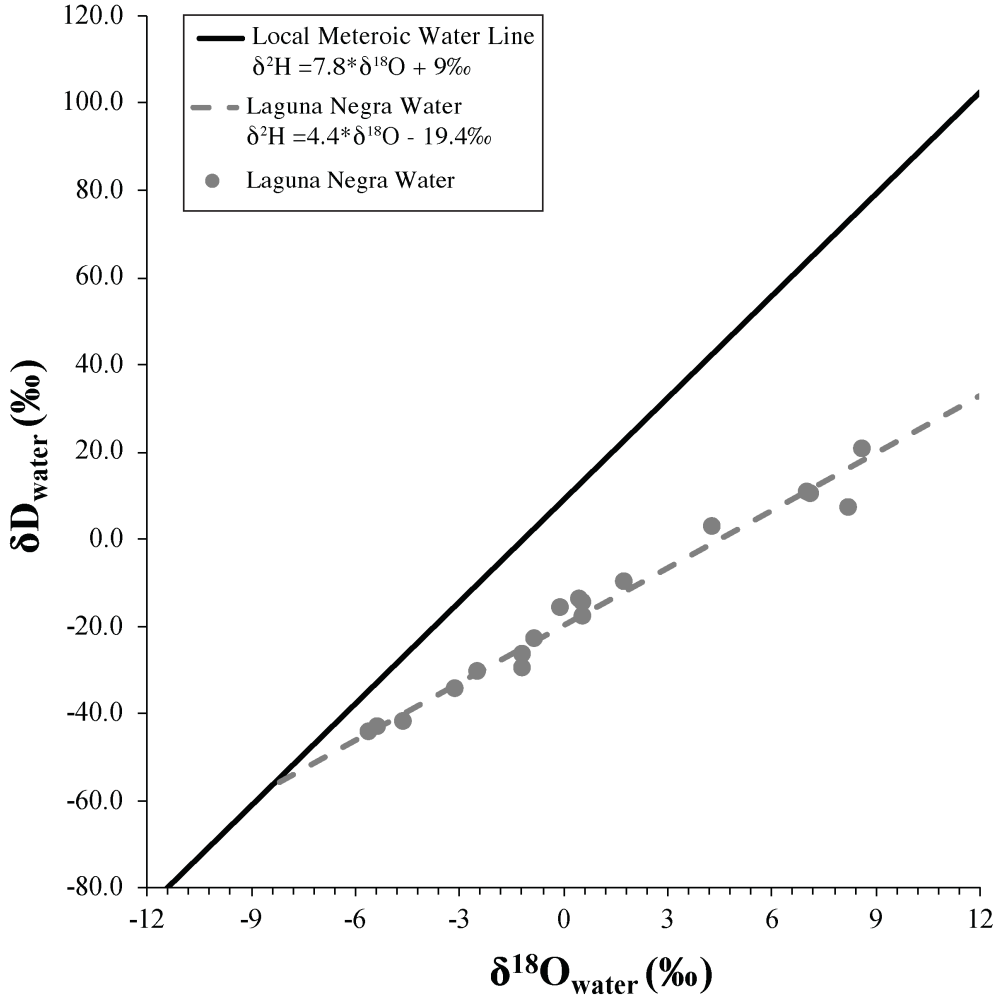

Figure 3.3: Measured isotopic values of oxygen and hydrogen from Laguna Negra water (grey points). Isotopic values follow a linear trend (grey dashed line) from the local meteoric water line (black line; Scheihing et al. 2017) implying evaporation is the primary control of the isotopic evolution of oxygen and hydrogen in water.

electrical conductivity observed moving outwards into the lake, which covaries ($R^2 = 0.68$) with changes in $\delta^{18}O_{H2O}$ (Figure S3.3) .

The evaporative trend seen in water isotopes predicts an increase in DIC concentration from groundwater source outwards into the lake if evaporation is also the only control of DIC dynamics at Laguna Negra (i.e. only water is lost with no other associated processes such as degassing occurring). Conversely, DIC concentrations decrease as water moves from the groundwater input into the lake. Thus, other processes must be responsible for carbon cycle

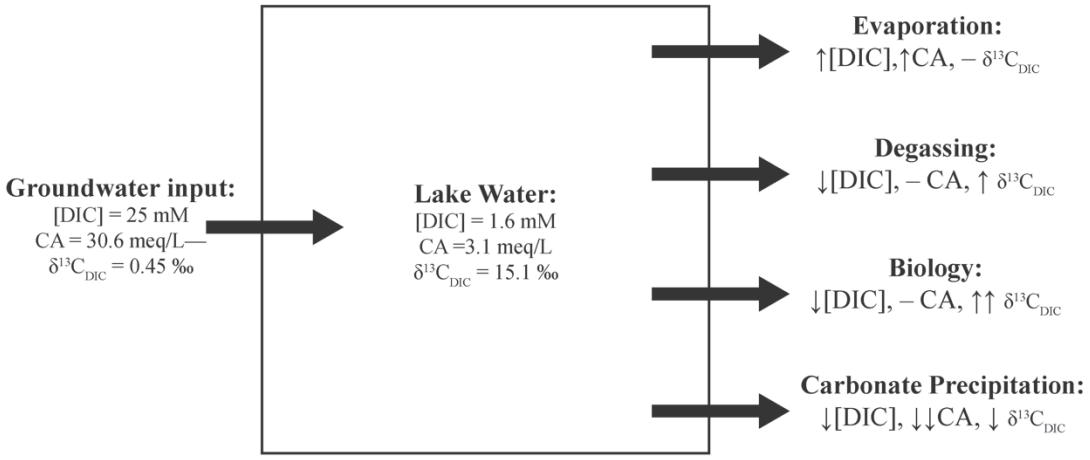

Figure 3.4: Box model used to investigate the processes that controlling the carbonate system at Laguna Negra. Groundwater is input into the lake and evolves into lake water through a combination of evaporation, degassing, biological processes, and carbonate precipitation. Outputs are described in terms of their effects on DIC concentration, carbonate alkalinity, and the isotopic composition as either increasing (↑), decreasing (↓), or no change (-)

dynamics at Laguna Negra in addition to evaporation. Degassing, carbonate precipitation, photosynthesis, and methanogenesis have all been observed or hypothesized to drive the loss of DIC at Laguna Negra and other similar hypersaline lakes (Valero-Garcés et al., 1999; Gomez et al., 2014; Birgel et al., 2015).

To determine the relative importance of these processes to DIC removal at Laguna Negra we developed a conceptual box model to probe the potential controls on the evolution of the carbonate system from the groundwater source to lake waters (Figure 3.4). In this model, groundwater is input into the lake and evolves to reach the lake water values through some combination of degassing, carbonate precipitation, and biological processes (photosynthesis and/or methanogenesis). Each of these processes drive associated changes in the [DIC], carbonate alkalinity, and $\delta^{13}C_{DIC}$ of lake waters as they evolve. To determine how these processes could combine to drive the evolution of groundwater inputs into lake body waters we compared the measured evolution of these parameters across the stromatolite belt with those

expected from these various processes. Specifically, we sought to determine whether the observed trends can be explained abiotically or if they require a biological mechanism for their formation.

The concomitant changes in alkalinity associated with changes in DIC concentrations can be used to constrain the processes responsible for DIC removal at Laguna Negra. DIC and carbonate alkalinity strongly co-vary ($R^2 = 0.99$) along a line with a slope of 1.27 (Figure S3.4; 95% CI [1.19, 1.34]). Degassing, photosynthesis, and methanogenesis each remove DIC without changing alkalinity while carbonate precipitation causes a decrease of two moles of alkalinity for each mole of DIC removed (Zeebe and Wolf-Gladrow, 2001). Therefore, the relative change in alkalinity vs. DIC can be used to determine the fraction of DIC removal by carbonate precipitation versus other processes. It should be noted that photosynthesis and methanogenesis cause a slight increase in alkalinity due nutrient uptake, however given the large size of the DIC pool at Laguna Negra the effect of this uptake on alkalinity is small and was not parameterized in this model (Zeebe and Wolf-Gladrow, 2001). Similarly, heterotrophic metabolisms may also increase DIC and alkalinity through remineralization of organic matter (Soetaert et al., 2007). However, the large decrease in DIC and alkalinity across the stromatolite belt indicates that processes removing DIC operate at substantially faster rates than these processes, thus heterotrophic processes are not included in our calculations. The fraction of DIC lost to carbonate precipitation (f_{cp}) necessary to explain the loss of alkalinity can be calculated following a method modified from that of Barkan et al. (2001). This can be calculated using the equation:

$$f_{cp} = \frac{CA_{Exp} - CA_{Meas}}{2(DIC_{Exp} - DIC_{Meas})} \quad (3.1)$$

where CA_{meas} and DIC_{meas} are the measured concentrations of carbonate alkalinity and DIC for a water. CA_{Exp} and DIC_{Exp} are the concentrations of carbonate alkalinity and DIC expected for a water based on evaporation alone and are defined:

$$CA_{Exp} = \frac{CA_{Initial}}{(1-f_{Evap})} \qquad (3.2)$$

$$DIC_{Exp} = \frac{DIC_{Initial}}{(1-f_{Evap})} \qquad (3.3)$$

where $CA_{Initial}$ and $DIC_{Initial}$ are the concentrations of carbonate alkalinity and DIC of the initial input water and f_{Evap} is the fraction of water removed due to evaporation.

Using this approach, we calculated f_{cp} across the stromatolite belt to assess the amount of DIC loss that can be attributed to carbonate precipitation. In this scenario, $DIC_{Initial}$ and $CA_{Initial}$ were defined as LN-003 (inlet water sample) and DIC_{Meas} and CA_{Meas} were defined as LN-011 (the sampling point with the lowest concentration of DIC). f_{Evap} was calculated for Laguna Negra as the percentage of water needed to evaporate to account for the change in salinity assuming evaporation is the only control on salinity yielding a value of 0.94 from ground water pool (LN-003) to lake water (LN-011). The calculated value of f_{Evap} is most likely an underestimation, because mineral precipitation is decreasing salinity by removing ions from solution. To account for any error in f_{Evap} values of 0.8 to 0.99 were utilized for our calculation of CA_{Exp} and DIC_{Exp}. Calculation of f_{cp} with these parameters yields a value of 0.61 (± 0.1 for different values of f_{Evap}) meaning that 61% ± 1% of the DIC loss at Laguna Negra overall can be attributed to carbonate precipitation. DIC removal by carbonate precipitation also predicts a decrease in pH as the removal of CO_3^{2-} shifts the carbonate equilibrium towards CO_3^{2-} liberating H^+:

$$H_2CO_3^* \rightleftharpoons HCO_3^- + H^+ \rightleftharpoons CO_3^{2-} + 2H^+ \qquad (3.4)$$

Thus, DIC removal primarily through carbonate precipitation at Laguna Negra also accounts for the decrease in pH moving outwards towards the lake from the groundwater ponds.

Similarly, the fractionation factor associated with the isotopic evolution of DIC can provide insight into the processes driving its removal. The processes likely to be controlling the evolution of DIC at Laguna Negra, carbonate precipitation, degassing, photosynthesis, and methanogenesis each contain distinct fractionation factors allowing them to be used as a fingerprint for their respective process on the isotopic evolution of Laguna Negra waters (Zhang et al., 1995; Botz et al., 1996; Hayes, 2001). The total fractionation factor associated with DIC removal was calculated using a Rayleigh fractionation model for the evolution of DIC and $\delta^{13}C_{DIC}$ in this system. In the Rayleigh model, the fractionation of (ε) is approximately equal to the slope of the regression between the natural log of the fraction of DIC remaining in the system

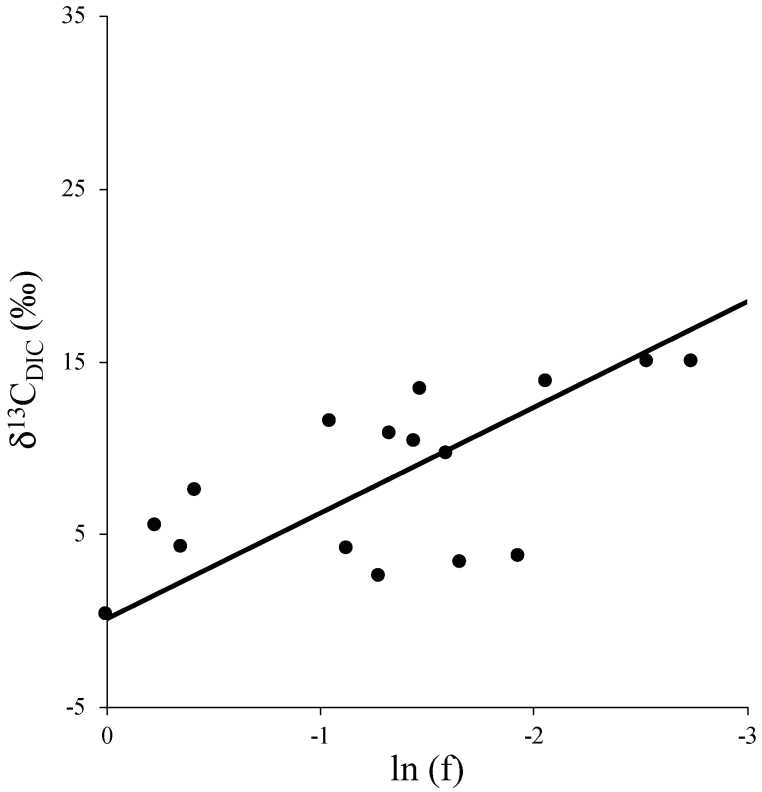

Figure 3.5: Regression of ln(f) (the natural log of the fraction of DIC remaining) vs. $\delta^{13}C_{DIC}$ for measured lake waters used to calculate the fractionation factors of lake waters (ε_{LN}). The slope of the regression is 3.9 (R^2 =0.41, 95% CI [1.2 ,6.6]).

(f) versus the isotopic composition of the DIC. Ordinary least squares regression for values recorded at Laguna Negra yields a slope of 3.9 (R^2 =0.41, 95% CI [-1.2 , 6.6]; Figure 3.5).Therefore, for Laguna Negra waters as DIC is removed from the system the isotopic composition of the remaining pool increases with a fractionation factor (ε_{LN}) of ~3.9‰ (95% C.I. [-1.2‰ , 6.6‰]).

Since the amount of DIC lost from calcite precipitation (f_{cp}) and its associated fractionation (ε_{cp}) are known (Romanek et al., 1992), the fractionation of DIC from processes other than calcite precipitation (ε_{other}) can be calculated using a mass balance approach using the equation:

$$\varepsilon_{other} = \frac{\varepsilon_{LN} - \varepsilon_{cp} * f_{cp}}{1 - f_{cp}} \qquad (3.5)$$

This approach yields a combined fractionation factor of 11.3‰ for processes other than calcite precipitation that remove DIC at Laguna Negra. This is higher than the equilibrium fractionation factor expected for degassing across the range of temperatures measured during our sampling is 8.2 to 10.2‰ (Zhang et al., 1995). However, fractionation factors of up to 19.4‰ have been obtained during evaporation of Dead Sea waters that have been attributed to non-equilibrium gas-transfer kinetic fractionations (Stiller et al., 1985). Given the high concentrations of DIC and degree of evaporation occurring it is reasonable to expect similar kinetic fractionations from degassing at Laguna Negra could be driving fractionations above the equilibrium value. Large fluxes of DIC from degassing are also consistent with DIC removal primarily through carbonate precipitation, because carbonate precipitation generates one mole of CO_2 for every mole of carbonate precipitated. Degassing driven through carbonate precipitation has been observed previously in the Dead Sea (Barkan et al., 2001; Golan et al., 2017). Therefore, the evolution of

DIC at Laguna Negra can be explained through the abiotic processes of degassing and carbonate precipitation alone.

It should be noted that this observation does not rule out a role for biological processes in the removal and isotopic evolution of DIC at Laguna Negra. For instance, photosynthetic algae, which have been observed to be the dominant primary producers at Laguna Negra, can account for this change as they typically produce fractionations of ~17-30‰ (Fry, 1996). Methanogenesis also produces very large fractionations (up to ~80‰) and could also play a role in producing large carbon isotopic enrichments as has been suggested in similar systems (Talbot and Kelts, 1990; Botz et al., 1996; Birgel et al., 2015). However, it does demonstrate that the highly enriched carbon isotope values of waters at Laguna Negra do not require a biological mechanism for their formation.

3.6.2 Interpreting the Carbonate Isotopic Record at Laguna Negra

The processes controlling the isotopic evolution of Laguna Negra's waters provide a framework for interpreting the isotopic signals preserved in calcite structures at the lake. While the isotopic composition of carbon and oxygen in calcite largely reflect the isotopic composition of the water from which they precipitated additional fractionation also occurs during precipitation that can vary in magnitude due to physicochemical conditions (Zeebe and Wolf-Gladrow, 2001).To account for these fractionations and enable more direct comparison to values measured previously from oncoids and laminar crusts at Laguna Negra the isotopic values of carbon and oxygen were modeled for a calcite precipitated in equilibrium with waters measured in this study. The modeled isotopic values of carbon and oxygen of a theoretical calcite mineral ($\delta^{13}C_{TC}$ and $\delta^{18}O_{TC}$) follow the same trends observed from the waters directly (Figure 3.6). This

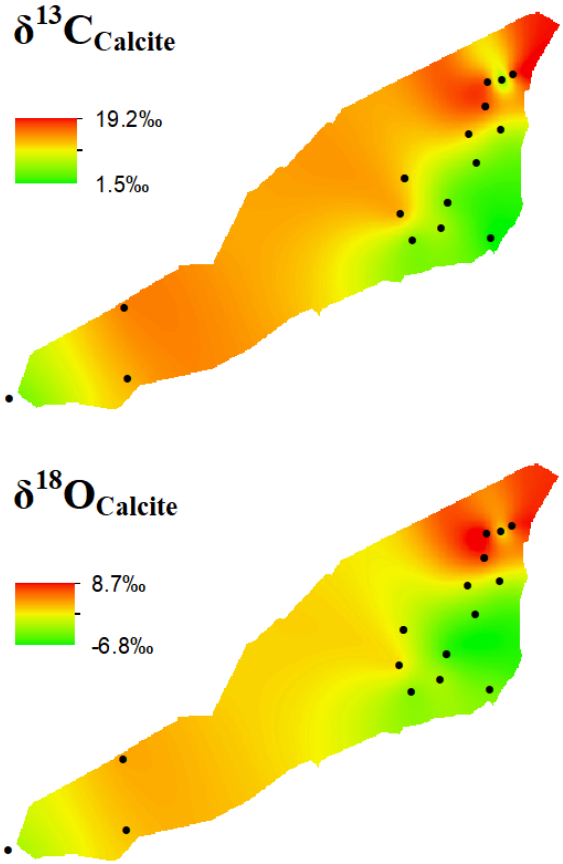

Figure 3.6: Spatial variability of modeled $\delta^{13}C_{Calcite}$ and $\delta^{18}O_{Calcite}$ formed in equilibrium with water measured in this study. Maps are interpolated from measured values (black dots).

implies that the isotopic evolution of the lake's waters spatially should be preserved in the isotopic composition of calcite structures across the lake edge. The values of $\delta^{13}C_{TC}$ and $\delta^{18}O_{TC}$ co-vary ($R^2 = 0.76$) along a trendline with a slope of 1.15 (95% CI [0.87,1.51]) by reduced major axis regression. This covariance is characteristic of closed-basin lakes and reflects the dual effects of physical and biological processes on the isotopic evolution of lake waters as described above (Talbot, 1990; Li and Ku, 1997).

Isotopic values measured from carbonate minerals at Laguna Negra ($\delta^{13}C_{MC}$ and $\delta^{18}O_{MC}$) by Buongiorno et al. (2018) display similar co-variant trends to those of the modeled values from lake water (Figure 3.7). Considering the complete isotopic dataset of all oncoids and laminar

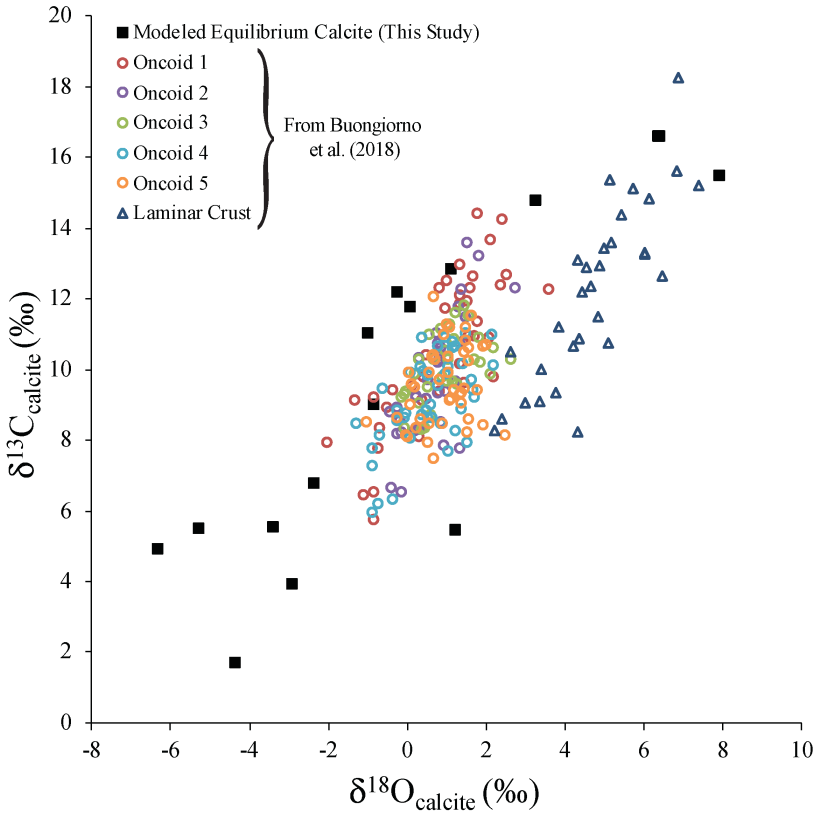

Figure 3.7: Comparison of modeled values for carbon and oxygen isotope values from a calcite formed in equilibrium with water measured in this study (closed squares) to those measured previously from oncoids and laminar crusts in Buongiorno et al. (2018).

crusts together shows that the isotopic values co-vary along a trendline of the same slope (m = 1.15; 95% C.I. [1.05,1.26]) by reduced major axis regression to that of the theoretical carbonate values, but their covariance is weaker ($R^2 = 0.50$). It should be noted that the range of isotopic compositions measured from carbonate minerals is more limited relative to the range of modeled isotopic values. This disparity could be a result of the fact oncoids and laminar crusts are unevenly distributed spatially across the stromatolite belt, with laminar crusts occurring towards the northwestern corner of the stromatolite belt and oncoids located in the central to northeastern portion, which could restrict the possible range these structures may record (Gomez et al., 2014). Similarly, this disparity could be an artefact of the more limited spatial distribution of sample locations for carbonates in Buongiorno et al. (2018) compared to this study. In any case, the

similar slope of the trendline for $\delta^{18}O_{TC}$ versus $\delta^{13}C_{TC}$ and $\delta^{18}O_{MC}$ versus $\delta^{13}C_{MC}$ suggests that the isotopic trends observed in the complete dataset of oncoids and laminar crusts preserve the trends of the isotopic evolution of lake waters spatially across the microbialite belt. Thus, the enrichment of ^{13}C and ^{18}O in carbonate minerals from Laguna Negra is also the result of the abiotic processes driving enrichment of the water.

The slope of the trendline of $\delta^{18}O$ versus $\delta^{13}C$ for individual structures are variable from the slope of the trend for theoretical calcite and the completed measured calcite dataset (Gomez et al., 2014). This implies that the isotopic variability within individual structures records localized changes in isotopic composition temporally rather than the overall spatial evolution trend seen in the theoretical and complete measured dataset. Therefore, individual structures should preserve a record of local environmental change, and supports the use of microbialites as time-series records of environmental evolution in Laguna Negra and other environments (Nehza et al., 2009; Frantz et al., 2014; Petryshyn et al., 2016). However, while the trends in the isotopic value record the temporal evolution of environmental conditions the absolute values rely primarily on the spatial evolution of lake waters. Analysis of values of the complete dataset alongside values from individual structures is necessary to correctly interpret the meaning of isotopic values in terms of both spatial and temporal dynamics.

The laminated nature of oncoids, which have previously been dated to an age of 2442 ± 252 years before present, preserve a time series of carbonate precipitation at the lake (Gomez et al., 2014). Therefore, the equivalence of slopes between measured carbonate isotopic values and those modeled for conditions during our study suggests that the environmental conditions observed in our study have persisted or at least recurred throughout this time. If the environmental conditions are not persistent and recur at specific time scales this could provide

insight into the timescales at which carbonates precipitate. Additional work investigating the variability of lake conditions over different time scales (i.e. daily, seasonally, yearly) would enhance our ability to understand the isotopic record preserved in Laguna Negra carbonates.

3.6.3 Implications for Interpreting Microbialite Biogenicity

Microbialites constitute one of the oldest and most complete records of life on Earth making them valuable tools for understanding the co-evolution of life and the environment through geologic time (Riding, 2000; Peters et al., 2017). The identification of microbialites is commonly based upon morphological lines of evidence, however morphologically similar structures may also be formed through entirely abiotic processes complicating their interpretation (Buick et al., 1981; Grotzinger and Rothman, 1996). Distinguishing microbialites from these abiotic mimics is crucial for our ability use microbialites as biosignatures in the geologic record. This is particularly significant for the most ancient examples which are among the oldest evidence of life on Earth, but whose biological origin is controversial (Allwood et al., 2006; Nutman et al., 2016; Allwood et al., 2018). Likewise, being able to assess the biogenicity of alleged microbialites is critical for their use as a target in astrobiological investigations (Cady et al., 2003; Des Marais et al., 2008). Identifying additional lines of evidence of biological activity associated with the formation of a potential microbialites is thus necessary to enable more confident assessment of its biogenicity (Grotzinger and Knoll, 1999).

Enriched carbon isotopic signatures in carbonate minerals may be generated as result of microbial processes, and the presence of these enrichments have been used as evidence of microbial activity, and even specific metabolisms, in both ancient and modern microbialites (Brady et al., 2010; Birgel et al., 2015; Nutman et al., 2016). However, the carbon isotopic signatures generated through biological activity are non-unique and may also be generated

through abiotic processes (Sumner, 2001). The results of this study demonstrate this point as the highly enriched carbon isotopic compositions occurring in Laguna Negra's carbonates being formed through abiotic processes. Furthermore, while these enrichments are abiotic in origin they occur within microbialites of demonstrable biogenicity (Gomez et al., 2014). Therefore, similarly large fractionations associated with possible microbialites should not necessarily be taken as evidence of biological activity, particularly if there is evidence for formation in an evaporative setting or the depositional setting is ambiguous.

3.6.4 Implications for the Geologic Carbon Isotopic Record

The carbon isotopic composition of carbonate minerals preserved in the geologic record is frequently utilized as a tool to understand variability in the global carbon cycle through Earth's history (Kump and Arthur, 1999; Bartley and Kah, 2004). However, these isotopic compositions may also reflect local environmental conditions complicating their interpretation (Melezhik et al., 1999). Developing a more robust understanding of the processes that drive localized enrichment in carbon isotopes in modern settings is necessary in order to better interpret local versus global effects in the geologic record. Our results show that at Laguna Negra degassing driven by evaporation and precipitation of carbonate minerals drives isotopic enrichments of $\delta^{13}C_{DIC}$ up to ~+15‰, and that these enrichments are in turn recorded in the carbonate minerals precipitated from the lake. Additionally, the degree of isotopic enrichment increases across the stromatolite belt in relation to the distance from the source, which as the lake evolves through time could be preserved as a stratigraphic isotope excursion. While the spatiotemporal extent of carbonate precipitation at Laguna Negra is limited, larger scale and longer lived evaporative basins are common throughout the geologic record where similar processes were operating and could in principle drive isotopic enrichments (Schreiber et al., 2007).

The magnitude of the carbon isotopic enrichments found at Laguna Negra are particularly noteworthy because they are comparable to the most highly enriched values found in the geologic record, the Paleoproterozoic Lomagundi carbon isotopic excursions (Schidlowski et al., 1976; Bekker, 2014). The Lomagundi isotopic excursions are observed globally and have thus been interpreted to reflect global scale changes in biogeochemical processes, however the excursions have also been suggested to have been generated or enhanced due to isotopic enrichment driven by local and/or diagenetic processes (Melezhik and Fallick, 1996; Hayes and Waldbauer, 2006; Planavsky et al., 2012). Many of the geologic units containing the Lomagundi excursion were deposited in restricted basins and contain stromatolites, and environmental processes such as evaporation or biological activity have been suggested as possible drivers of localized isotopic enrichment (Melezhik et al., 1999; Melezhik et al., 2005). Laguna Negra provides a comparable modern analog to study how these processes may combine to drive positive carbon isotopic excursions, and our results are consistent with the possibility of a local origin or enhancement of the Lomagundi excursion. Specifically, our work indicates that even the most extreme isotopic enrichments observed in the geologic record can be generated through a combination the abiotic processes of evaporation, degassing, and carbonate precipitation. Furthermore, despite the occurrence of these isotopic enrichments within microbialites and associated facies these signatures can be explained without a biological origin. Thus, the occurrence of the Lomagundi excursion within microbialites does not necessarily imply a biological role in the formation of the carbon isotope enrichments. Overall, these results emphasize that local physicochemical processes should be considered when interpreting the meaning of enriched carbon isotopic compositions in carbonates from the geologic record, particularly when there is evidence for deposition in an evaporative basin.

Finally, our work suggests that the information that can be gained from isotopic studies of carbonates is dependent upon the sampling technique employed. Analysis of the isotopic composition carbonate minerals across a stratigraphic section may provide insight into the temporal evolution of environmental, ecological, or hydrological conditions through time at that location. In addition, investigation of the isotopic variability laterally between contemporaneously deposited facies allows may provide insight into spatially variable processes within the depositional environment. The difference in information gained between sampling techniques highlights the need for measurement of lateral variability in isotopes of a single bed in addition to measurements vertically along a stratigraphic column. Together this data will enable a more complete understanding of the spatial and temporal evolution of the processes that control the isotopic signatures and ensure that isotopic trends are more properly interpreted.

3.7 Conclusions

The isotopic composition of dissolved inorganic carbon and oxygen in water can record information about microbial, geochemical, and hydrological processes, which can in turn be recorded in carbonate minerals precipitating from the water. We analyzed the spatial variability in the isotopic composition of lake waters at Laguna Negra and their relationship to the isotopic values preserved in carbonate minerals from the lake. Our results demonstrate that in Laguna Negra's carbonates oxygen isotopic enrichment is due solely to evaporation, while carbon isotopic enrichment results can be explained by the combined effects of carbonate precipitation and degassing. Therefore, despite their association with microbialites the isotopic signatures preserved at Laguna Negra can be explained without a biological mechanism. These results imply that similarly large fractionations found in the rock record or on other planets associated with possible microbialites should therefore not necessarily be interpreted as biological in origin

and should not be used as evidence for biogenicity of the structures. Constraining the depositional environment and analyzing several contemporaneously deposited facies within a microbialite forming environment is necessary to fully understand the processes responsible for the isotopic values preserved in microbialites and associated abiogenic carbonates. Placing the isotopic values measured in microbialites in the rock record or potentially other planets in the proper context of their depositional environment will allow for more robust interpretation of their meaning.

3.8 References

Allwood A. C., Rosing M. T., Flannery D. T., Hurowitz J. A. and Heirwegh C. M. (2018) Reassessing evidence of life in 3,700-million-year-old rocks of Greenland. *Nature* **563**, 241–244.

Allwood A. C., Walter M. R., Burch I. W. and Kamber B. S. (2007) 3.43 billion-year-old stromatolite reef from the Pilbara Craton of Western Australia: ecosystem-scale insights to early life on Earth. *Precambrian Research* **158**, 198–227.

Allwood A. C., Walter M. R., Kamber B. S., Marshall C. P. and Burch I. W. (2006) Stromatolite reef from the Early Archaean era of Australia. *Nature* **441**, 714–718.

Andres M. S., Sumner D. Y., Reid R. P. and Swart P. K. (2006) Isotopic fingerprints of microbial respiration in aragonite from Bahamian stromatolites. *Geology* **34**, 973–976.

Banfield J. F., Moreau J. W., Chan C. S., Welch S. A. and Little B. (2001) Mineralogical Biosignatures and the Search for Life on Mars. *Astrobiology* **1**, 447–465.

Barkan E., Luz B. and Lazar B. (2001) Dynamics of the carbon dioxide system in the Dead Sea. *Geochimica et Cosmochimica Acta* **65**, 355–368.

Bartley J. K. and Kah L. C. (2004) Marine carbon reservoir, Corg-Ccarb coupling, and the

evolution of the Proterozoic carbon cycle. *Geology* **32**, 129.

Bekker A. (2014) Lomagundi Carbon Isotope Excursion. In *Encylopedia of Astrobiology* pp. 1–6.

Birgel D., Meister P., Lundberg R., Horath T. D., Bontognali T. R. R., Bahniuk A. M., Rezende C. E., Vásconcelos C. and McKenzie J. A. (2015) Methanogenesis produces strong 13C enrichment in stromatolites of Lagoa Salgada, Brazil: a modern analogue for Palaeo-/Neoproterozoic stromatolites? *Geobiology* **13**, 245–266.

Bosak T., Knoll A. H. and Petroff A. P. (2013) The Meaning of Stromatolites. *Annual Review of Earth and Planetary Sciences* **41**, 21–44.

Botz R., Pokojski H.-D., Schmitt M. and Thomm M. (1996) Carbon isotope fractionation during bacterial methanogenesis by CO2 reduction. *Organic Geochemistry* **25**, 255–262.

Brady A. L., Laval B., Lim D. S. S. and Slater G. F. (2014) Autotrophic and heterotrophic associated biosignatures in modern freshwater microbialites over seasonal and spatial gradients. *Organic Geochemistry* **67**, 8–18.

Brady A. L., Slater G. F., Omelon C. R., Southam G., Druschel G., Andersen D. T., Hawes I., Laval B. and Lim D. S. S. (2010) Photosynthetic isotope biosignatures in laminated micro-stromatolitic and non-laminated nodules associated with modern, freshwater microbialites in Pavilion Lake, B.C. *Chemical Geology* **274**, 56–67.

Buick R., Dunlop J. S. R. and Groves D. I. (1981) Stromatolite recognition in ancient rocks: an appraisal of irregularly laminated structures in an Early Archaean chert-barite unit from North Pole, Western Australia. *Alcheringa: An Australasian Journal of Palaeontology* **5**, 161–181.

Buongiorno J., Gomez F. J., Fike D. A. and Kah L. C. (2018) Mineralized microbialites as

archives of environmental evolution, Laguna Negra, Catamarca Province, Argentina. *Geobiology*.

Burne R. V and Moore L. S. (1987) Microbialites: organosedimentary deposits of benthic microbial communities. *Palaios* **2**, 241–254.

Cady S. L., Farmer J. D., Grotzinger J. P., Schopf J. W. and Steele A. (2003) Morphological biosignatures and the search for life on Mars. *Astrobiology* **3**, 351–368.

Criss R. E. (1999) *Principle of Stable Isotope Distribution*., Oxford University Press.

Frantz C., Petryshyn V. and Marenco P. (2014) Dramatic local environmental change during the Early Eocene Climatic Optimum detected using high resolution chemical analyses of Green River Formation. *Palaeogeography, Palaeoclimatology, Palaeoecology* **405**, 1–15.

Fry B. (1996) 13C/12C fractionation by marine diatoms. *Marine Ecology Progress Series* **134**, 283–294.

Golan R., Lazar B., Wurgaft E., Lensky N., Ganor J. and Gavrieli I. (2017) Continuous CO2 escape from the hypersaline Dead Sea caused by aragonite precipitation. *Geochimica et Cosmochimica Acta* **207**, 43–56.

Gomez F. J., Kah L. C., Bartley J. K. and Astini R. A. (2014) Microbialites in a high-altitude Andean lake: multiple controls on carbonate precipitation and lamina accretion. *Palaios* **29**, 233–249.

Grotzinger J. P. (1990) Geochemical model for Proterozoic stromatolite decline. *American Journal of Science* **290**, 80–103.

Grotzinger J. P. and Knoll A. H. (1999) Stromatolites in Precambrian carbonates: evolutionary mileposts or environmental dipsticks? *Annual Review of Earth and Planetary Sciences* **27**, 313–358.

Grotzinger J. P. and Rothman D. H. (1996) An abiotic model for stromatolite morphogenesis. *Nature* **383**, 423–425.

Hayes J. (2001) Fractionation of carbon and hydrogen isotopes in biosynthetic processes. *Reviews in Mineralogy and Geochemistry* **43**, 225–277.

Hayes J. M. and Waldbauer J. R. (2006) The carbon cycle and associated redox processes through time. *Philosophical transactions of the Royal Society of London. Series B, Biological sciences* **361**, 931–50.

Kim S. T. and O'Neil J. R. (1997) Equilibrium and nonequilibrium oxygen isotope effects in synthetic carbonates. *Geochimica et Cosmochimica Acta* **61**, 3461–3475.

Kump L. R. and Arthur M. A. (1999) Interpreting carbon-isotope excursions: carbonates and organic matter. *Chemical Geology* **161**, 181–198.

Li H. C. and Ku T. L. (1997) δ13C-δ18O covariance as a paleohydrological indicator for closed basin lakes. *Palaeogeography, Palaeoclimatology, Palaeoecology* **133**, 69–80.

Des Marais D. J., Nuth J. A., Allamandola L. J., Boss A. P., Farmer J. D., Hoehler T. M., Jakosky B. M., Meadows V. S., Pohorille A., Runnegar B. and Spormann A. M. (2008) The NASA Astrobiology Roadmap. *Astrobiology* **8**, 715–730.

Melezhik V. A. and Fallick A. E. (1996) A widespread positive δ13Ccarbanomaly at around 2.33-2.06 Ga on the Fennoscandian Shield: A paradox? *Terra Nova* **8**, 141–157.

Melezhik V. A., Fallick A. E., Medvedev P. V. and Makarikhin V. V. (1999) Extreme 13Ccarb enrichment in ca. 2.0 Ga magnesite–stromatolite–dolomite–`red beds' association in a global context: a case for the world-wide signal enhanced by a local environment. *Earth-Science Reviews* **48**, 71–120.

Melezhik V. A., Fallick A. E., Rychanchik D. V. and Kuznetsov A. B. (2005) Palaeoproterozoic

evaporites in Fennoscandia: implications for seawater sulphate, the rise of atmospheric oxygen and local amplification of the δ13C excursion. *Terra Nova* **17**, 141–148.

Mook W. G. (1986) 13C in atmospheric CO2. *Netherlands Journal of Sea Research* **20**, 211–223.

Nehza O., Woo K. S. and Lee K. C. (2009) Combined textural and stable isotopic data as proxies for the mid-Cretaceous paleoclimate: A case study of lacustrine stromatolites in the Gyeongsang Basin, SE Korea. *Sedimentary Geology* **214**, 85–99.

Nutman A. P., Bennett V. C., Friend C. R. L., Van Kranendonk M. J. and Chivas A. R. (2016) Rapid emergence of life shown by discovery of 3,700-million-year-old microbial structures. *Nature* **537**, 535–538.

Peters S. E., Husson J. M. and Wilcots J. (2017) The rise and fall of stromatolites in shallow marine environments. *Geology* **45**, 487–490.

Petryshyn V. A., Juarez Rivera M., Agić H., Frantz C. M., Corsetti F. A. and Tripati A. E. (2016) Stromatolites in Walker Lake (Nevada, Great Basin, USA) record climate and lake level changes ~35,000years ago. *Palaeogeography, Palaeoclimatology, Palaeoecology* **451**, 140–151.

Planavsky N. J., Bekker A., Hofmann A., Owens J. D. and Lyons T. W. (2012) Sulfur record of rising and falling marine oxygen and sulfate levels during the Lomagundi event. *Proceedings of the National Academy of Sciences of the United States of America* **109**, 18300–5.

Riding R. (2000) Microbial carbonates: the geological record of calcified bacterial–algal mats and biofilms. *Sedimentology* **47**, 179–214.

Riding R. and Liang L. (2005) Geobiology of microbial carbonates: metazoan and seawater

saturation state influences on secular trends during the Phanerozoic. *Palaeogeography, Palaeoclimatology, Palaeoecology* **219**, 101–115.

Risacher F., Alonso H. and Salazar C. (2003) The origin of brines and salts in Chilean salars: a hydrochemical review. *Earth-Science Reviews* **63**, 249–293.

Risacher F. and Fritz B. (2009) Origin of Salts and Brine Evolution of Bolivian and Chilean Salars. *Aquatic Geochemistry* **15**, 123–157.

Romanek C. S., Grossman E. L. and Morse J. W. (1992) Carbon isotopic fractionation in synthetic aragonite and calcite: Effects of temperature and precipitation rate. *Geochimica et Cosmochimica Acta* **56**, 419–430.

Rubinson M. and Clayton R. N. (1969) Carbon-13 fractionation between aragonite and calcite. *Geochimica et Cosmochimica Acta* **33**, 997–1002.

Sass E. and Ben-Yaakov S. (1977) The carbonate system in hypersaline solutions: dead sea brines. *Marine Chemistry* **5**, 183–199.

Scheihing K., Moya C., Struck U., Lictevout E., Tröger U., Scheihing K. W., Moya C. E., Struck U., Lictevout E. and Tröger U. (2017) Reassessing Hydrological Processes That Control Stable Isotope Tracers in Groundwater of the Atacama Desert (Northern Chile). *Hydrology* **5**, 3.

Schidlowski M., Eichmann R. and Junge C. E. (1976) Carbon isotope geochemistry of the Precambrian Lomagundi carbonate province, Rhodesia. *Geochimica et Cosmochimica Acta* **40**, 449–455.

Schopf J. and Kudryavtsev A. (2007) Evidence of Archean life: stromatolites and microfossils. *Precambrian Research*.

Schreiber B. C., Lugli S., Baþel M. and Geological Society of London. (2007) *Evaporites*

through space and time., Geological Society.

Soetaert K., Hofmann A. F., Middelburg J. J., Meysman F. J. R. and Greenwood J. (2007) The effect of biogeochemical processes on pH. *Marine Chemistry* **105**, 30–51.

Stiller M., Rounick J. S. and Shasha S. (1985) Extreme carbon-isotope enrichments in evaporating brines. *Nature* **316**, 434–435.

Sumner D. Y. (2001) Microbial Influences on Local Carbon Isotopic Ratios and Their Preservation in Carbonate. *Astrobiology* **1**, 57–70.

Talbot M. R. (1990) A review of the palaeohydrological interpretation of carbon and oxygen isotopic ratios in primary lacustrine carbonates. *Chemical Geology: Isotope Geoscience Section* **80**, 261–279.

Talbot M. R. and Kelts K. (1990) Paleolimnological Signatures from Carbon and Oxygen Isotopic Ratios in Carbonates, from Organic Carbon-Rich Lacustrine Sediments: Chapter 6.

Valero-Garcés B. L., Delgado-Huertas A., Ratto N. and Navas A. (1999) Large< sup> 13</sup> C enrichment in primary carbonates from Andean Altiplano lakes, northwest Argentina. *Earth and Planetary Science Letters* **171**, 253–266.

Zeebe R. and Wolf-Gladrow D. (2001) *CO2 in Seawater: Equilibrium, Kinetics, Isotopes*., Elsevier Science B.V., Amsterdam.

Zhang J., Quay P. D. and Wilbur D. O. (1995) Carbon isotope fractionation during gas-water exchange and dissolution of CO2. *Geochimica et Cosmochimica Acta* **59**, 107–114.

3.9 Supplemental Figures and Tables

Figure S3.1: Locations sampled for geochemical and isotopic compositions in the stromatolite belt. Base image from ArcMap World Imagery.

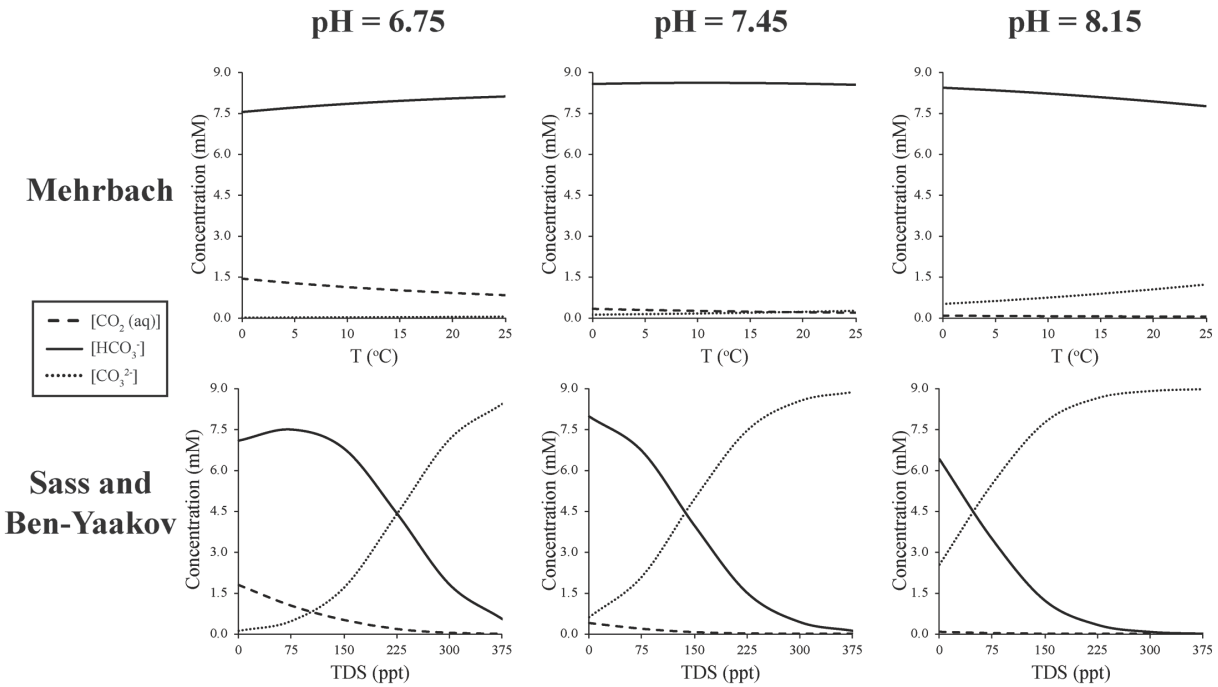

Figure S3.2: Variability in speciation of the carbonate system calculated using the equilibrium constants of Mehrbach et al. (1973), which accounts for temperature changes but not salinity changes, compared to those calculated using the Sass and Ben-Yaakov constants, which accounts for salinity but not temperature changes across the range of pH at Laguna Negra. These results indicate that salinity effects are substantially larger than temperature effects and supports use of the Sass and Ben-Yaakov constants to calculate carbonate speciation.

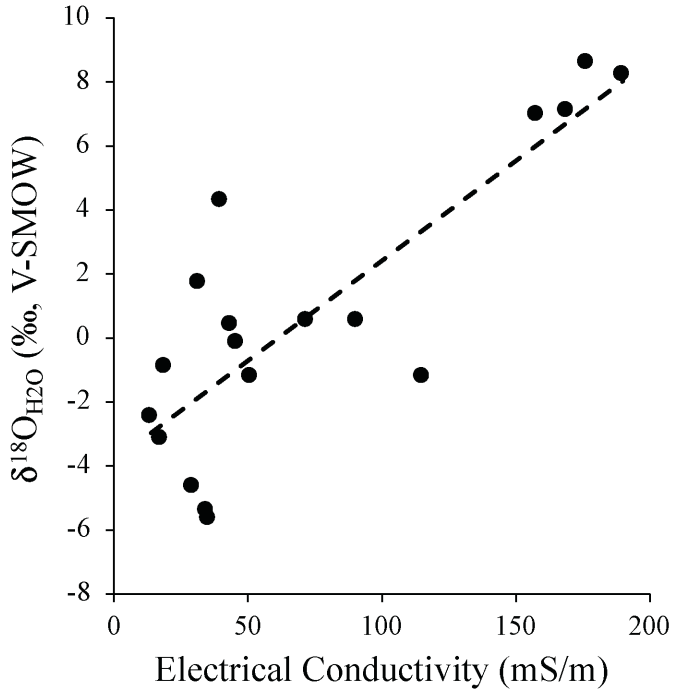

Figure S3.3: Relationship between electrical conductivity and $\delta^{18}O$ across the stromatolite belt. Values co-vary (R^2 = 0.68) consistent with evaporation driving isotopic enrichment at Laguna Negra.

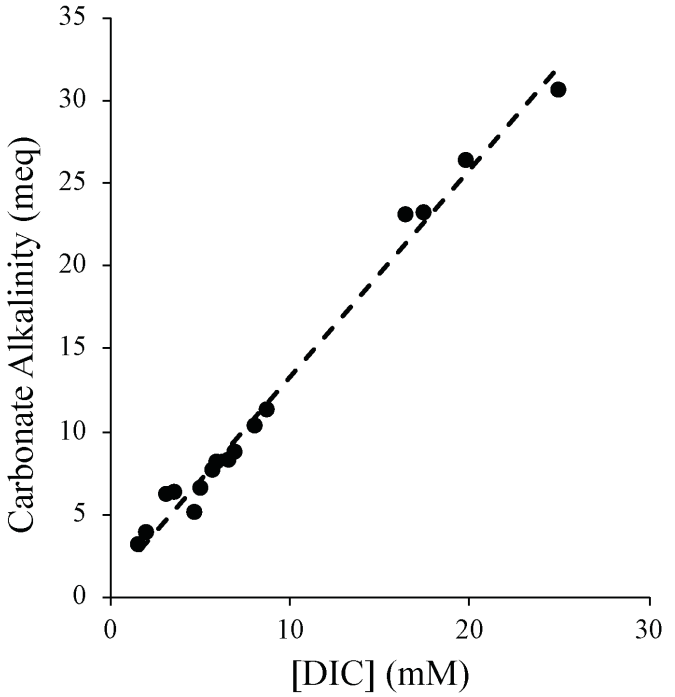

Figure S3.4: Relationship between [DIC] and carbonate alkalinity at Laguna Negra. Values co-vary (R^2 = 0.99) along line with a slope of 1.27.

Table S3.1: Metadata for locations sampled across the stromatolite belt

Sample	Location Type	Easting	Northing	Date	Time	Water Depth (mm)
LN-003	Groundwater Input	545083	6961624	March 6, 2017	15:37	150
LN-004	Stromatolite Belt	544944	6941652	March 6, 2017	16:15	9
LN-005	Stromatolite Belt	544867	6941619	March 6, 2017	16:50	5
LN-006	Stromatolite Belt	544832	6941691	March 6, 2017	17:14	16
LN-007	Stromatolite Belt	544846	6941787	March 6, 2017	17:40	12
LN-007b	Stromatolite Belt	544846	6941787	March 7, 2017	13:25	12
LN-008	Stromatolite Belt	544963	6941722	March 6, 2017	18:05	30
LN-008b	Stromatolite Belt	544963	6941722	March 7, 2017	13:15	15
LN-009	Stromatolite Belt	545113	6942057	March 7, 2017	9:10	5
LN-010	Stromatolite Belt	545074	6942051	March 7, 2017	9:45	1
LN-011	Stromatolite Belt	545067	6941984	March 7, 2017	11:12	18
LN-011b	Stromatolite Belt	545067	6941984	March 7, 2017	16:11	11
LN-012	Stromatolite Belt	545021	6941910	March 7, 2017	11:45	10
LN-013	Stromatolite Belt	545042	6941830	March 7, 2017	12:12	8
LN-014	Stromatolite Belt	545109	6941921	March 7, 2017	13:48	5
LN-015	Stream Inlet	543761	6941186	March 7, 2017	14:55	30
LN-016	Stromatolite Belt	544085	6941239	March 7, 2017	15:14	5
LN-017	Stromatolite Belt	544076	6941435	March 7, 2017	15:30	5
LN-018	Stromatolite Belt	545142	6942074	March 7, 2017	15:56	4

Chapter 4: Resolving the relative roles of temperature and hydrological change in oxygen isotopic trends preserved in lacustrine microbialites

Scott R. Beeler[1], Fernando J. Gomez[2], Kathryn Snell[3], Alexander S. Bradley[1]

[1]Department of Earth and Planetary Science, Washington University in St. Louis, Saint Louis, Missouri, 63130, USA

[2]CICTERRA-CONICET, Facultad de Ciencias Exactas, Fisicas, y Naturales, Universidad Nacional de Córdoba, Córdoba, X5000, Argentina

[3] Department of Geological Sciences, University of Colorado, Boulder, CO, USA, 80304, USA

4.1 Abstract

Geochemical trends preserved in the carbonate minerals comprising lacustrine microbialites provide a potential archive of terrestrial paleoenvironmental information that has previously been underutilized. However, in order to confidently utilize microbialites for this purpose the fidelity with which they record paleoenvironmental signals requires further investigation. The modern microbialites of Laguna Negra, Argentina provides a useful setting to test these relationships, because the climate of the region has been independently constrained allowing for comparison of trends preserved in the microbialites to regional records. Previous work at Laguna Negra found a decreasing temporal trend in the oxygen isotopic composition preserved in microbialites. This trend was interpreted to reflect changes in lake water oxygen isotopes due to an increasingly positive water balance at the lake through time, which is consistent with regional records of increasing effective moisture through the late Holocene. However, in addition to changes in the isotopic composition of the waters from which they precipitate, the oxygen isotopic composition of carbonate minerals may also vary due to changes in their temperature of precipitation complicating the interpretation of these trends. To resolve this issue, we utilized clumped isotope thermometry paired with stable oxygen isotope analysis of the carbonates to reconstruct both the temperature and oxygen isotopic composition of the waters from which the microbialites precipitated. Our results indicate that carbonate precipitation temperatures were relatively consistent, particularly when compared to the high degree of temperature variability at the lake, and that the oxygen isotopic compositions in carbonates comprising the microbialites showed no relationship with temperature changes. In contrast, the reconstructed water oxygen isotopic compositions showed a significant correlation with the oxygen isotopic compositions measured from the microbialites. These results support previous interpretations of oxygen isotopic trends

in the carbonates at the lake being driven by an increased water balance in the lake through time. Overall, this work lends further support to the utilization of microbialites as paleoenvironmental archives.

4.2 Introduction

Microbialites are sedimentary structures whose formation occurs as a result of the interaction of microbial, geochemical, and physical processes, and may therefore provide a geological archive of these processes (Burne and Moore, 1987; Riding, 2000). Study of microbialites has traditionally been used as a tool for understanding the co-evolution of life and its environment over geologic time scales (i.e. millions to billions of years) with particular focus on marine examples from the Precambrian (Grotzinger and Knoll, 1999; Schopf et al., 2007; Peters et al., 2017). Recently, younger lacustrine microbialites have begun to receive enhanced interest as archives of terrestrial paleoenvironmental information over shorter time scales (i.e. hundreds of years to tens of thousands of years) through analysis of proxy data preserved in the carbonate minerals comprising the structures (Solari et al., 2010; Ghinassi et al., 2012; Frantz et al., 2014; Petryshyn et al., 2015; Petryshyn et al., 2016). Laminated microbialites are especially intriguing for this purpose because they enable determination of time series trends analogous to the temporal paleoclimate reconstructions generated from speleothems or varve deposits (Meyers and Lallier-vergés, 1999; Lachniet, 2009). Utilizing microbialites as paleoclimate archives can serve to enhance the available records of terrestrial paleoclimate data, which will allow for an increase our understanding of climate systems over these time periods and enable the generation more accurate climate models.

However, as with any proxy record, concerns exist about the fidelity with which microbialites record paleoenvironmental signals. For lacustrine microbialites specific concerns

include the potential for overprinting of climatic or hydrological signals due to the microbial activity responsible for their formation or localized environmental conditions within the lake. Studying microbialites in systems where their geochemical trends can be compared to independently constrained regional climate records can provide insight into the accuracy of microbialite derived paleoclimate data. The high altitude, closed basin lake Laguna Negra located in the Andes Mountains provides an intriguing setting to study these relationships as it contains laminated microbialites and abiogenic carbonates that have formed over the last ~2000 years, a period where regional climate records are available (Gomez et al., 2014).

Previous work analyzing the stable oxygen isotopic composition ($\delta^{18}O_{carb}$) preserved in Laguna Negra's microbialites found a general decrease in $\delta^{18}O_{carb}$ of ~2-3‰ through time interpreted to be caused by a decrease in the isotopic composition of lake waters ($\delta^{18}O_{H2O}$) indicating an increasingly positive water balance at the lake (Buongiorno et al., 2018). This is consistent with regional climate records that suggest a general increase in effective moisture over the late Holocene (Valero-Garces et al., 1996; Grosjean et al., 1997; Grosjean et al., 1998). However, in addition to changes in $\delta^{18}O_{H2O}$, $\delta^{18}O_{carb}$ compositions may also reflect changes in the temperature of water from which the carbonates precipitated (Kim and O'Neil, 1997). Therefore, the decrease in $\delta^{18}O_{carb}$ observed in Laguna Negra's carbonates could have been enhanced or overprinted by changes in water temperature through time. Changes in water temperature unrelated to climatic variability present a particular concern at Laguna Negra as other lakes in the region, including those containing microbialites, are associated with active hot springs suggesting that hot spring input could have previously been important at Laguna Negra (Risacher and Eugster, 1979; Jones and Renaut, 1994). Unraveling the relative roles of changes

in temperature and $\delta^{18}O_{H2O}$ to the decreasing trend in $\delta^{18}O_{carb}$ at Laguna Negra is critical to proper interpretation of its paleoenvironmental meaning.

Carbonate clumped isotope (Δ_{47}) thermometry provides a method for determining the temperature at which a carbonate mineral precipitated independent of changes in $\delta^{18}O_{H2O}$ (Ghosh et al., 2006; Eiler, 2011; Affek, 2012). Additionally, when clumped isotope temperatures are paired with $\delta^{18}O_{carb}$ analyses the change in $\delta^{18}O_{H2O}$ through time can also be reconstructed. In this study, we employed paired carbonate clumped isotopic and $\delta^{18}O_{carb}$ analyses of microbialites from Laguna Negra in order to deconvolve the relative importance of temporal variability in the temperature and $\delta^{18}O_{H2O}$ of the lake waters from which the microbialites precipitated on the observed temporal trends in $\delta^{18}O_{carb}$. These analyses enable more robust reconstruction of the paleoenvironmental conditions associated with microbialite formation at the lake and their variability through time. Furthermore, these results provide insight into the utilization of microbialites as paleoclimate archives in other settings.

4.3 Methods

4.3.1 Field Area and Sample Collection

Laguna Negra is a hypersaline (>300 ppt salinity) closed basin lake located in the Puna-Altiplano region of the Andes Mountains in Catamarca Province, Argentina. Input of fresher waters into the lake occurs exclusively along the southeastern margin of the lake snowmelt in a zone referred to as the "stromatolite belt" with waters primarily sourced from groundwater springs and occasional seasonal streams. Evolution of the inlet waters within the stromatolite belt due to the combined effects of evaporation, carbonate precipitation, and degassing drive large

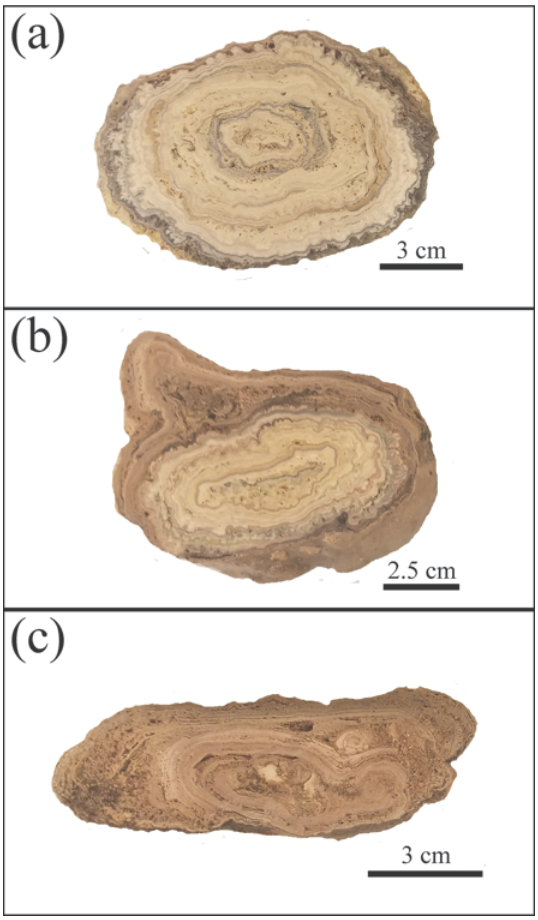

Figure 4.1: Morphologies of discrete carbon structure types found at Laguna Negra analyzed in this study: (a) oncoid, (b) oncoid with stromatolitic overgrowth, and (c) laminar crust

gradients in geochemical parameters and stable isotopic compositions (Beeler et al., *in review*). Likewise, the evolution of inlet waters and mixing with lake body waters increases the saturation state of both calcite and aragonite leading to widespread carbonate precipitation including both diffuse carbonate muds and discrete decimeter scale mineral structures (Gomez et al., 2014). Discrete carbonate structures occur as a range of morphologies (Figure 4.1) including both microbialites and abiogenic structures reflecting variability in their association with microbial mats (Beeler et al., *in prep*.; Gomez et al., 2018; Mlewski et al., 2018). Carbonate structures interpreted as microbialites are primarily represented by concentrically laminated oncoids with

occasional accretionary laminated stromatolitic overgrowths, whereas abiogenically precipitated carbonate structures primarily occur as laminated crusts.

The microbialites and abiogenic carbonates at Laguna Negra have previously been shown to have extreme enrichments in their stable oxygen and carbon isotopes ($\delta^{18}O_{carb}$ up to +9.3‰ and $\delta^{13}C_{carb}$ up to +18.3‰; Buongiorno et al, 2018). Likewise, waters of the stromatolite belt display large gradients in their stable carbon and oxygen isotopic compositions due to the combined effects of evaporation, degassing, and carbonate precipitation with comparably enriched values in the most evolved waters ($\delta^{18}O_{H2O}$ up to +8.61‰ and $\delta^{13}C_{DIC}$ up to +15.06‰; Beeler et al., *in review*). A similar covariant trend between $\delta^{18}O$ and $\delta^{13}C$ was observed in the overall carbonate and water datasets indicating that the carbonate isotopic compositions reflect the evolution of waters across the stromatolite belt (Beeler et al., *in review*). Additionally, intrastructure variability in the isotopic compositions of carbonates are interpreted to record information regarding paleoenvironmental conditions at the lake. Specifically, a general decreasing trend of ~2-3‰ in $\delta^{18}O_{carb}$ across laminae from the core (oldest) to edge (youngest) within oncoids has been interpreted to represent temporal changes in paleohydrological conditions at the lake (Buongiorno et al, 2018).

We sampled whole carbonate structures from eight locations across the stromatolite belt during March 2017 to assess their clumped isotopic and $\delta^{18}O_{carb}$ compositions. Samples collected represented the range of macroscopic morphologies found at the lake and consisted of six oncoids, an oncoid with a stromatolitic overgrowth, and a laminar crust. Geochemical data including $\delta^{18}O_{H2O}$ and temperature were also collected from each sampling location and were reported in Beeler et al. (*in review*). Following return to the laboratory whole structures were cut

into slabs and ~20 grams of sample powders were microdrilled from the core and edge of each sample for CO_2 analysis.

4.3.2 Clumped Isotopic Analyses

The clumped isotope paleothermometer is based on the temperature dependence of the abundance of ^{13}C-^{18}O bonds or isotopic "clumping" in carbonate minerals, wherein increased temperatures yield fewer ^{13}C-^{18}O bonds in the carbonate lattice relative to lower temperatures (Affek, 2012). Practically, the paleothermometer is based on measuring the ratio (R^{47}) of the rare mass 47 multiply substituted isotopologue of CO_2 ($^{13}C^{18}O^{16}O$) relative to the abundance of the common mass 44 isotopologue ($^{12}C^{16}O_2$) produced from the phosphoric dissolution of carbonate minerals (Eiler, 2011). Values are reported as Δ_{47} which is the per mil deviation of the measured ratio (R^{47}_{sample}) versus the value expected for a stochastic distribution ($R^{47}_{stochastic}$) and is defined as:

$$\Delta_{47} = \left(\frac{R^{47}_{sample}}{R^{47}_{stochastic}}\right) * 1000 \qquad (4.1)$$

Carbonate Δ_{47} compositions were determined using a Thermo Fisher MAT 253+ isotope ratio mass spectrometer at the University of Colorado, Boulder. Approximately 6 mg of carbonate powders of each sample were reacted in phosphoric acid bath at 90°C to generate CO_2 for analysis. CO_2 trapping, purification, and analysis were performed following previously established protocols (Huntington et al., 2009; Dennis et al., 2011). Each sample was analyzed in replicate and compared to a suite of gas and mineral standards. In addition, the stable oxygen isotopic values of each sample was simultaneously determined during Δ_{47} analyses.

4.3.3 Calculation of Temperature and Water Isotope Values

Carbonate precipitation temperatures are calculated from Δ_{47} values by applying a calibration developed from empirical Δ_{47}-T relationships, however at present there is no universally agreed upon calibration utilized for this conversion. In order to explore the range of estimated precipitation temperatures generated utilizing different Δ_{47}-T calibrations we calculated precipitation temperatures using several published calibrations (Ghosh et al., 2006; Dennis et al., 2011; Zaarur et al., 2013). Values are reported as the mean and standard error of estimated precipitation temperatures from replicate samples. $\delta^{18}O_{H2O}$ for the waters from which the carbonates precipitated was calculated using the calcite-H_2O fractionation-temperature relationship of Kim and O'Neil (1997) and reconstructed carbonate precipitation temperatures. Previous work at Laguna Negra has shown that carbonate mineral structures are comprised primarily of calcite with only minor aragonite components, which supports the use of the calcite fractionation factor (Buongiorno et al., 2018). $\delta^{18}O_{H2O}$ values are reported as mean and standard error of the mean reconstructed from replicate samples. Variability in reconstructed $\delta^{18}O_{H2O}$ due to differences in estimated precipitation temperatures from the use of different calibrations was determined by calculating $\delta^{18}O_{H2O}$ using temperatures estimated from each of the calibrations. Reported results and figures presented in the text use temperature and $\delta^{18}O_{H2O}$ values reconstructed using the Zaarur et al. (2013) calibration, which was chosen because it was the intermediate of the three calibrations used. The importance of changes in the absolute values of reconstructed temperature and oxygen isotopes between calibrations for interpretations drawn from the data is considered in the discussion.

4.4 Results

The results of clumped and stable oxygen isotopic analyses of Laguna Negra carbonates are presented in Table 4.1. Measured stable oxygen isotopic values from carbonates analyzed were generally enriched with $\delta^{18}O_{carb}$ of -0.16‰ to +4.80 (Figure 4.2). $\delta^{18}O_{carb}$ compositions were similar across all samples except for the laminar crust, whose core was enriched by ~3‰ relative to all other samples analyzed. A decrease in oxygen isotopes from the core versus edge of structures was observed in four of the structures analyzed, however two samples contained increased values from core to edge with two others showing no change. Δ_{47} temperatures from Laguna Negra carbonates ranged between 1.5 ˚C (± 1.3 ˚C) to 13.5 ˚C (± 4.9 ˚C) (Table 4.2; Figure 4.3). No distinguishable trend in precipitation temperature from the core versus edge of the sample was observed for all but one oncoid sample whose precipitation temperatures were higher for the core versus the edge. Reconstructed $\delta^{18}O_{H2O}$ values ranged between -1.99‰ (± 0.52‰) and +3.76‰ (± 0.75‰) (Table 4.3; Figure 4.4). A decrease in $\delta^{18}O_{H2O}$ from the core versus edge was observed in two oncoids and the laminar crust while all other samples showed had no distinguishable difference between core and edge. Linear regression indicates a significant co-variant relationship between $\delta^{18}O_{carb}$ and reconstructed $\delta^{18}O_{H2O}$ (R^2=0.72, p-value = 0.00003). In contrast no significant relationship was found between $\delta^{18}O_{carb}$ and Δ_{47} temperatures (R^2=0.003, p-value = 0.83)(Figure 4.5).

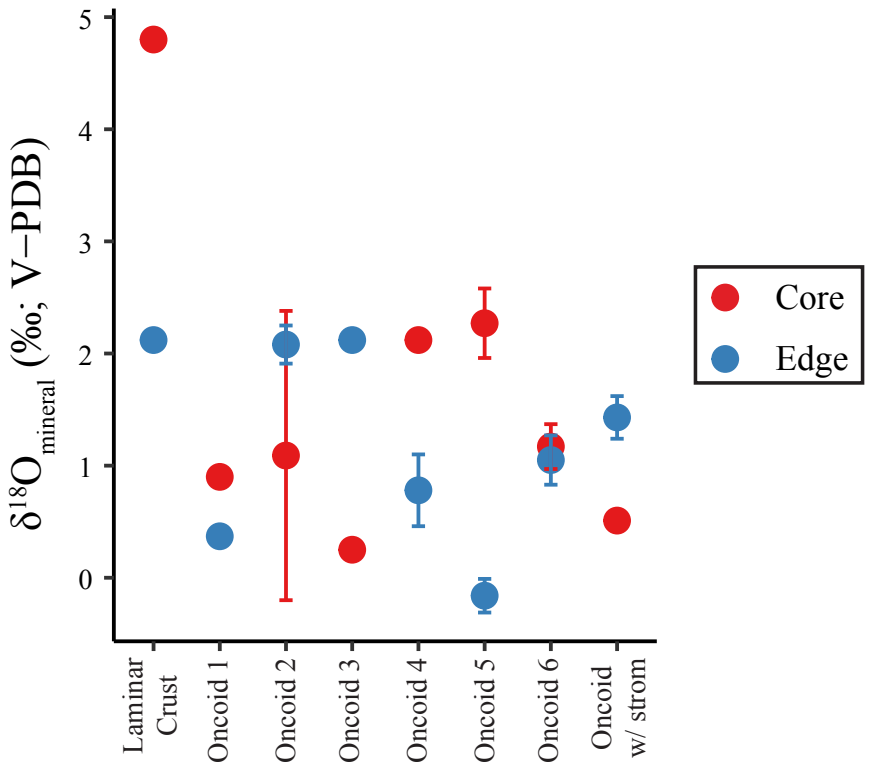

Figure 4.2: Stable oxygen isotopic compositions from the core versus edge of carbonate structures. Points represent mean values of replicate analyses with error bars of one standard deviation.

Table 4.3: Δ_{47} and $\delta^{18}O_{carb}$ values measured from Laguna Negra carbonates. Oxygen isotopic compositions are reported relative to the V-PDB standard.

Sample ID	Description	Location	Δ_{47}	SE	$\delta^{18}O_{carb}$ (‰)	SD
LN-009	Oncoid 1	Core	0.768	0.014	0.90	0.01
		Edge	0.782	0.018	0.37	0.01
LN-010C	Oncoid 2	Core	0.789	0.043	1.09	1.29
		Edge	0.766	0.021	2.08	0.17
LN-011	Oncoid 3	Core	0.776	0.008	0.25	0.06
		Edge	0.799	0.049	2.12	0.04
LN-012	Oncoid 4	Core	0.786	0.004	2.12	0.06
		Edge	0.814	0.007	0.78	0.32
LN-013	Oncoid 5	Core	0.772	0.025	2.27	0.31
		Edge	0.766	0.012	-0.16	0.15
LN-014	Oncoid 6	Core	0.784	0.026	1.17	0.20
		Edge	0.758	0.022	1.05	0.22
LN-017B	Laminar Crust	Core	0.775	0.016	4.80	0.02
		Edge	0.768	0.003	2.12	0.07
LN-018B	Oncoid with stromatolite	Core	0.754	0.023	0.51	0.08
		Edge	0.791	0.021	1.43	0.19

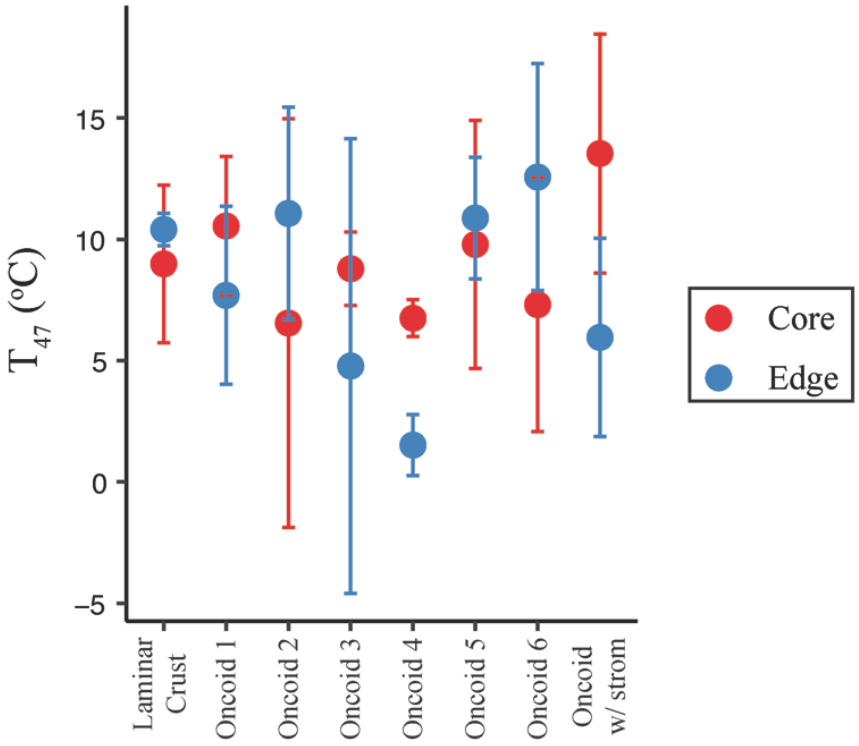

Figure 4.3: Precipitation temperature for core versus edge of carbonate samples reconstructed using clumped isotope thermometry. Points represent mean values of replicate analyses with error bars of one standard error of the mean. Temperatures were calculated using the calibration of Zaarur et al. (2013).

Table 4.4: Measured water temperatures and reconstructed carbonate precipitation temperatures from clumped isotopes using various Δ_{47}-T calibrations.

Sample ID	Description	T (ºC) Measured water	Location	TΔ_{47} (ºC) Zaarur et al. (2013)	SE	TΔ_{47} (ºC) Ghosh et al. (2006)	SE	TΔ_{47} (ºC) Dennis et al. (2011)	SE
LN-009	Oncoid 1	3.1	Core	10.55	2.86	13.80	2.60	2.80	4.00
			Edge	7.69	3.67	11.25	3.35	-1.20	5.10
LN-010C	Oncoid 2	10.1	Core	6.55	8.42	10.15	7.65	-2.65	11.65
			Edge	11.07	4.38	14.25	3.95	3.50	6.20
LN-011	Oncoid 3	16.7	Core	8.79	1.52	12.25	1.35	0.30	2.10
			Edge	4.78	9.37	8.55	8.55	-5.00	12.90
LN-012	Oncoid 4	15.9	Core	6.75	0.76	10.40	0.70	-2.55	1.05
			Edge	1.52	1.26	5.65	1.15	-9.70	1.70
LN-013	Oncoid 5	16.6	Core	9.79	5.11	13.10	4.60	1.75	7.15
			Edge	10.88	2.51	14.15	2.25	3.25	3.55
LN-014	Oncoid 6	20.0	Core	7.31	5.23	10.85	4.75	-1.70	7.30
			Edge	12.57	4.68	15.65	4.25	5.70	6.70
LN-017B	Laminar Crust	18.4	Core	8.99	3.25	12.45	2.95	0.55	4.55
			Edge	10.41	0.67	13.70	0.60	2.55	0.95
LN-018B	Oncoid with stromatolite	22.0	Core	13.54	4.93	16.50	4.40	7.05	7.05
			Edge	5.96	4.08	9.65	3.75	-3.60	5.60

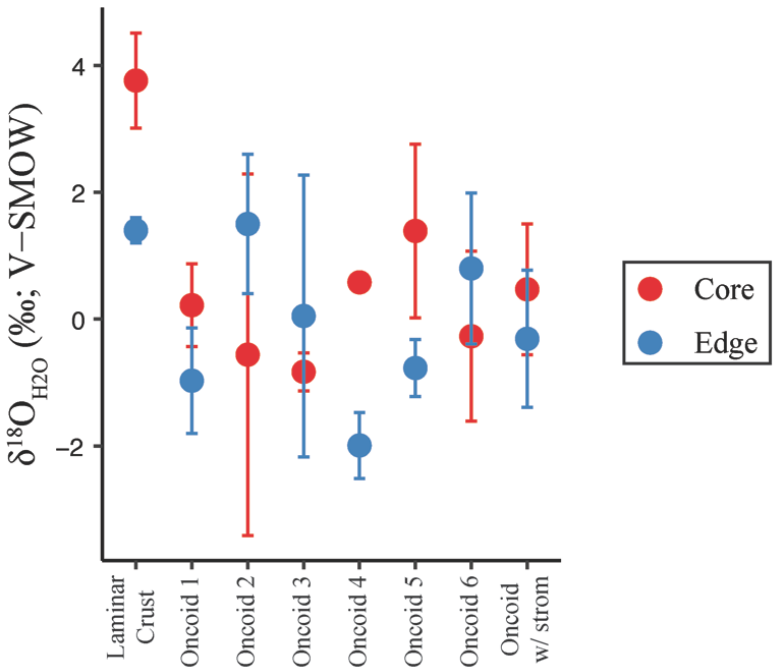

Figure 4.4: Reconstructed water oxygen isotopic compositions from which carbonates precipitated for the core versus edge of carbonate samples. Points represent mean values of replicate analyses with error bars of one standard error of the mean. Water oxygen isotopic compositions were calculated using measured carbonate oxygen isotopic compositions and precipitation temperatures calculated using the calibration of Zaarur et al. (2013).

Table 4.5: Measured $\delta^{18}O_{H2O}$ and reconstructed $\delta^{18}O_{H2O}$ water values generated using measured $\delta^{18}O_{carb}$ values and reconstructed precipitation temperatures using various Δ_{47}-T calibrations.

Sample ID	Description	$\delta 18O_{H2O}$ (‰) Measured	Location	$\delta^{18}O_{H2O}$ (‰) Zaarur et al. (2013)	SE	$\delta^{18}O_{H2O}$ (‰) Ghosh et al. (2006)	SE	$\delta^{18}O_{H2O}$ (‰) Dennis et al. (2011)	SE
LN-009	Oncoid 1	-1.18	Core	0.22	0.65	0.94	0.58	-1.58	0.95
			Edge	-0.97	0.83	-0.17	0.74	-3.08	1.23
LN-010C	Oncoid 2	7.11	Core	-0.56	2.85	0.27	2.63	-2.81	3.78
			Edge	1.50	1.10	2.21	0.98	-0.25	1.58
LN-011	Oncoid 3	7.02	Core	-0.83	0.30	-0.05	0.26	-2.81	0.46
			Edge	0.05	2.22	0.93	1.97	-2.39	3.26
LN-012	Oncoid 4	0.56	Core	0.58	0.14	1.41	0.12	-1.64	0.22
			Edge	-1.99	0.52	-1.02	0.49	-4.78	0.66
LN-013	Oncoid 5	-4.64	Core	1.39	1.37	2.14	1.24	-0.49	1.93
			Edge	-0.77	0.45	-0.05	0.38	-2.53	0.73
LN-014	Oncoid 6	0.53	Core	-0.27	1.34	0.53	1.20	-2.43	1.92
			Edge	0.80	1.19	1.47	1.07	-0.78	1.71
LN-017B	Laminar Crust	4.28	Core	3.76	0.75	4.54	0.67	1.77	1.11
			Edge	1.40	0.20	2.13	0.18	-0.41	0.27
LN-018B	Oncoid with stromatolite	8.21	Core	0.47	1.03	1.12	0.89	-1.01	1.56
			Edge	-0.31	1.08	0.54	0.98	-2.61	1.52

4.5 Discussion

4.5.1 Interpretation of Laguna Negra Paleoenvironmental Records

Previous work at Laguna Negra identified a decrease in $\delta^{18}O_{carb}$ across sequential laminae in oncoids and laminar crusts (Buongiorno et al.,2018). This trend was interpreted to be the result of decreasing $\delta^{18}O_{H2O}$ of the waters from which they precipitated due to an increasingly positive water balance at the lake through time (Buongiorno et al., 2018). However, because changes in $\delta^{18}O_{carb}$ can be the result of both changes in the temperature and $\delta^{18}O_{H2O}$ of the waters from which the structure precipitated, it is possible that this trend could have been overwritten or enhanced due to coincident changes of water temperature through time rather than changes in $\delta^{18}O_{H2O}$. In order to deconvolve the relative importance of changes in $\delta^{18}O_{H2O}$ and temperature to the observed decrease in $\delta^{18}O_{carb}$ we utilized clumped isotope thermometry paired with $\delta^{18}O_{carb}$ analyses to assess the precipitation temperature of Laguna Negra carbonates and enable reconstruction of changes in $\delta^{18}O_{H2O}$.

$\delta^{18}O_{carb}$ measured from oncoids in this study were generally comparable to the values measured by Buongiorno et al. (2018) with values ranging between ~0 to +2‰. The laminar crust measured in this study had a relatively depleted oxygen isotopic composition compared to that of Buongiorno et al. (2018), however was still relatively enriched compared to the oncoids. This is consistent with previous interpretations that relative changes in the isotopic composition of laminar crusts versus oncoids reflect spatial variability in isotopic compositions of waters in the microbialite (Beeler et al., *in review*.; Buongiorno et al., 2018). The previously observed decrease from the core versus edge of the structure (oldest to youngest layers) in $\delta^{18}O_{carb}$ was found in four of eight structures analyzed in this study, however no change or an increase from

core versus edge was found in the other samples (Figure 4.2a). This discrepancy could be the result of the lower intrastructural sampling density of this study compared to Buongiorno et al. (2018), which observed relatively high (~2-3‰) point to point variability in $\delta^{18}O_{carb}$ between successive laminae in addition to the overall decreasing trends. Alternatively, differences in preserved trends could be the result of age differences between oncoids analyzed in the studies leading to differences in the signals they record. Developing age models for Laguna Negra's carbonates is difficult as reservoir effects noted in similar lakes from the region complicate the use of ^{14}C indicating the need for U/Th based age models which is beyond the scope of this study (Valero-Garcés et al., 1999; Buongiorno et al., 2018).

Clumped isotope thermometry indicates that, including error, the temperature of precipitation for all samples analyzed falls between -5 and 18.5 ^{o}C with most values falling between ~5-15 ^{o}C (Figure 4.3). In comparison, field measurements of daytime variability in water temperatures measured during the field campaign varied between 3.1 ^{o}C – 22.0 ^{o}C (Table 4.2). Likewise, ~40 ^{o}C daily and ~60 ^{o}C variability in air temperatures have been measured regionally, although detailed meteorological data is lacking for Laguna Negra (Gomez et al., 2014). Given this high daily and seasonal variability in temperatures the relatively limited range of carbonate precipitation temperatures suggests that mineral formation is occurring, at least primarily, during specific temperature regimes. Unfortunately, variability in the absolute range of values for reconstructed temperatures due to the Δ_{47}-T calibrations utilized and the lack of long term water temperature data for Laguna Negra prohibits determination of specific time intervals at which carbonate precipitation is occurring. However, regardless of the calibration utilized reconstructed precipitations temperatures do preclude a substantial contribution of hot spring input over the history of carbonate precipitation at Laguna Negra in contrast to observations of a

hydrothermal contribution to the formation of similar structures elsewhere in the region (Risacher and Eugster, 1979; Jones and Renaut, 1994).

Reconstructed $\delta^{18}O_{H2O}$ values, including error, ranged from -3.4 to +4.5‰ with most samples analyzed containing values between ~ -2 and +2‰ (Figure 4.4). In comparison, field measurements of variability in $\delta^{18}O_{H2O}$ of the waters from which carbonate samples were collected ranged between -4.6 and 8.2‰, which was interpreted to be driven by evaporative enrichment of input waters spatially across the microbialite belt (Beeler et al.,*in review*). The relatively narrow range of values preserved in carbonates versus measured lake values could be the result of changes in the saturation state of calcite across the stromatolite belt as the gradients in measured $\delta^{18}O_{H2O}$ are associated with gradients in other geochemical parameters including the concentration of dissolved inorganic carbon (Beeler et al., *in review*). However, while mineral saturation states have been shown to be variable across the stromatolite belt the relationship between mineral saturation and $\delta^{18}O_{H2O}$ has not been quantified (Gomez et al., 2014). Determining this relationship could provide further insight into the cause of the more limited range of reconstructed versus measured $\delta^{18}O_{H2O}$ and enable a better understanding of the processes governing microbialite formation at the lake. Intriguingly, reconstructed $\delta^{18}O_{H2O}$ were enriched relative to values from oncoids consistent with the interpretation that the isotopic variability observed between structure types is the result of spatial variability in geochemical conditions at the lake (Beeler et al.,*in review*; Buongiorno et al., 2018).

A decrease in reconstructed $\delta^{18}O_{H2O}$ values from the core versus edge of structures was observed in three of the eight structures analyzed with the remaining five showing no resolvable difference (Figure 4.4). Reconstructing $\delta^{18}O_{H2O}$ using temperatures generated with different Δ_{47}-T calibrations changes the absolute values of $\delta^{18}O_{H2O}$, but regardless of the calibration used the

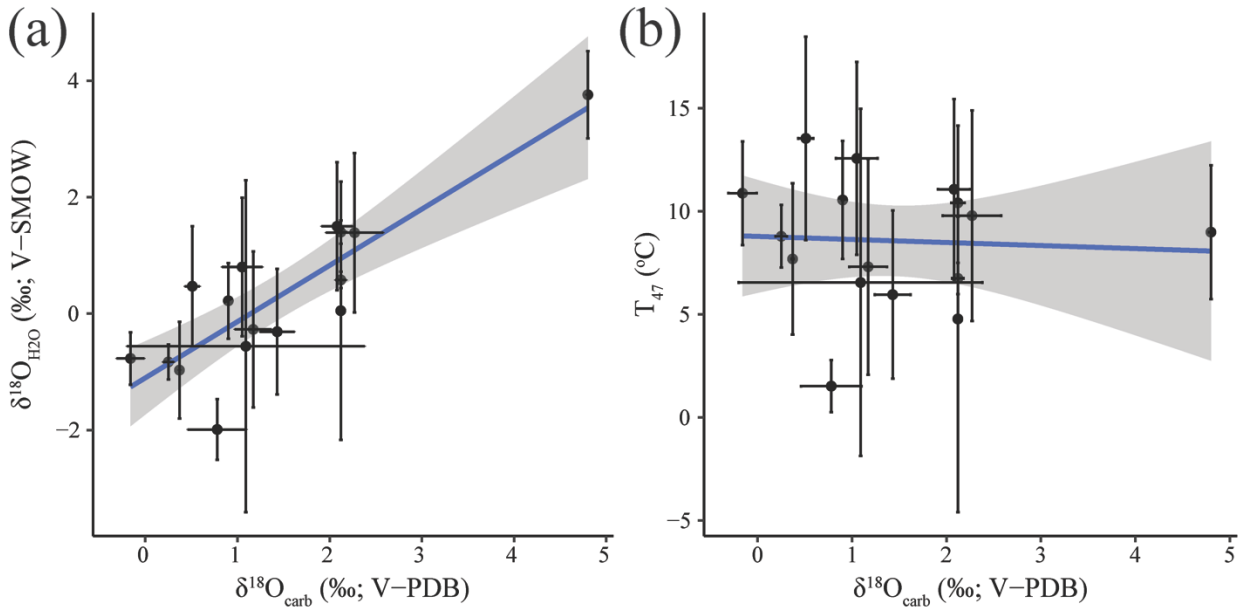

Figure 4.5: Linear regression of carbonate oxygen values versus (a) reconstructed water oxygen isotope values and (b) reconstructed precipitation temperatures. Significant co-variation was observed between carbonate oxygen isotopes and water isotopes (R^2=0.72, p = 0.00003) but no relationship was observed between carbon oxygen isotopes and temperature (R^2=0.003, p= 0.83).

observed trends were consistent. All three structures which displayed the decreased core to edge trend in reconstructed $\delta^{18}O_{H2O}$ also showed a decreasing trend in $\delta^{18}O_{carb}$ indicating that the decreasing trend observed in $\delta^{18}O_{carb}$ is reflective of changes in $\delta^{18}O_{H2O}$. One of these samples, Oncoid 4, also showed a resolvable decrease in its precipitation temperature from core versus edge.

To better deconvolve the overall effects of temperature versus $\delta^{18}O_{H2O}$ changes on $\delta^{18}O_{carb}$ recorded in the carbonates, linear regressions of $\delta^{18}O_{H2O}$ and temperature versus $\delta^{18}O_{carb}$ were performed for the entire datasets (Figure 4.5). A significant co-variant relationship was found between $\delta^{18}O_{carb}$ and $\delta^{18}O_{H2O}$, but no relationship was observed between $\delta^{18}O_{carb}$ and precipitation temperature. The lack of a significant relationship between $\delta^{18}O_{H2O}$ and temperature indicates that temperature variability is not responsible for the decreasing trends in $\delta^{18}O_{carb}$

observed previously and corroborates the interpretation of changes in $\delta^{18}O_{carb}$ in terms of changes in $\delta^{18}O_{H2O}$ due to an increase in water balance at the lake through time (Buongirono et al. 2018).

4.5.2 Implications for Microbialites as Paleoclimate Archives

The potential of lacustrine microbialites to act as terrestrial paleoenvironmental archives has begun to receive increased attention and has shown potential to expand our available climate records (Solari et al., 2010; Frantz et al., 2014; Petryshyn et al., 2016). In order to confidently utilize these structures in this manner a more robust understanding of the accuracy of the proxy data they preserve is required. The microbialites of Laguna Negra provide a valuable case study into the preservation of paleoenvironmental signals within a modern lacustrine setting with a relatively well constrained paleoclimatic history. Our results confirm previous work indicating that the trends in $\delta^{18}O_{carb}$ preserved within sequential laminae in Laguna Negra's microbialites and abiogenic carbonates preserve paleoenvironmental information that is consistent with regional climate records (Buongiorno et al., 2018). While differences in the $\delta^{18}O_{carb}$ of microbialites versus abiogenic carbonates were observed our results are consistent with previous work suggesting these changes are the result of variability in abiotic processes spatially across the lake (Beeler et al., *in review*.; Buongiorno et al., 2018). This indicates that the $\delta^{18}O_{carb}$ values preserved in microbialites are not being overprinted by the microbial communities that play an active role in their formation. Collectively, these results provide further validation that microbialites may act as faithful archives of paleoenvironmental conditions and supports their use in this manner.

Future work focusing on understanding the rate of laminae formation remains necessary in order to fully realize the potential of microbialites as paleoclimate archives, because understanding the time intervals represented by an individual lamina is critical for their use in

paleoclimate reconstructions. Previous work investigating the tempo of laminae formation in microbialites suggests that individual laminae may form over time scales ranging from days to years (Chivas et al., 1990; Berelson et al., 2011; Petryshyn et al., 2012). At Laguna Negra an absolute age model for the rate of microbialite formation is lacking due to complications with dating methods (Gomez et al., 2014; Buongiorno et al., 2018). However, the precipitation temperatures recorded within Laguna Negra's microbialites are relatively consistent when compared to the large range of daily and seasonal temperatures at the lake suggesting that the Laguna Negra microbialites form only at specific time intervals. This provides evidence that the environmental conditions preserve longer scale (yearly or longer) time averaged paleoclimate data rather than diurnal or seasonal variability, however more work generating more robust age models of microbialite formation at Laguna Negra is necessary to confirm this interpretation.

4.6 Conclusions

We utilized clumped isotope thermometry to reconstruct the temperature and $\delta^{18}O_{H2O}$ compositions of the waters from which microbialites and abiogenic carbonates precipitated at Laguna Negra. These results were used to deconvolve the relative importance of changes in temperature and $\delta^{18}O_{H2O}$ on the $\delta^{18}O_{carb}$ preserved within the mineral structures. Our results confirm previous interpretations that the decreased trends in $\delta^{18}O_{carb}$ within individual microbialites at Laguna Negra records changes in paleoenvironmental conditions that are consistent with regional records (Valero-Garces et al., 1996; Grosjean et al., 1997; Grosjean et al., 1998; Buongiorno et al., 2018). These results provide further validation that microbialites can act as faithful archives of paleoenvironmental conditions. Analyzing microbialites in other settings may therefore provide additional terrestrial paleoclimate data which can be used to develop more robust climate models and a better understanding of global climate systems.

4.7 References

Affek H. P. (2012) Clumped Isotope Paleothermometry: Principles, Applications, and Challenges. *The Paleontological Society Papers* **18**, 101–114.

Beeler S. R., Gomez F. J. and Bradley A. S. Controls of extreme isotopic enrichment in modern microbialites and associated abiogenic carbonates. *Geochimica et Cosmochimica Acta*.

Beeler S. R., Gomez F. J. and Bradley A. S. Geospatial insights into the controls of microbialite formation at Laguna Negra, Argentina. *in prep*.

Berelson W. M., Corsetti F. A., Pepe-Ranney C., Hammond D. E., Beaumont W. and Spear J. R. (2011) Hot spring siliceous stromatolites from Yellowstone National Park: Assessing growth rate and laminae formation. *Geobiology* **9**, 411–424.

Buongiorno J., Gomez F. J., Fike D. A. and Kah L. C. (2018) Mineralized microbialites as archives of environmental evolution, Laguna Negra, Catamarca Province, Argentina. *Geobiology*.

Burne R. V and Moore L. S. (1987) Microbialites: organosedimentary deposits of benthic microbial communities. *Palaios* **2**, 241–254.

Chivas A. R., Torgersen T. and Polach H. A. (1990) Growth rates and Holocene development of stromatolites from Shark Bay, Western Australia. *Australian Journal of Earth Sciences* **37**, 113–121.

Dennis K. J., Affek H. P., Passey B. H., Schrag D. P. and Eiler J. M. (2011) Defining an absolute reference frame for 'clumped' isotope studies of CO2. *Geochimica et Cosmochimica Acta* **75**, 7117–7131.

Eiler J. (2011) Paleoclimate reconstruction using carbonate clumped isotope thermometry. *Quaternary Science Reviews* **30**, 3575–3588.

Frantz C., Petryshyn V. and Marenco P. (2014) Dramatic local environmental change during the Early Eocene Climatic Optimum detected using high resolution chemical analyses of Green River Formation. *Palaeogeography, Palaeoclimatology, Palaeoecology* **405**, 1–15.

Ghinassi M., D'Oriano F., Benvenuti M., Awramik S., Bartolini C., Fedi M., Ferrari G., Papini M., Sagri M. and Talbot M. (2012) Shoreline fluctuations of Lake Hayk (northern Ethiopia) during the last 3500 years: Geomorphological, sedimentary, and isotope records. *Palaeogeography, Palaeoclimatology, Palaeoecology* **365–366**, 209–226.

Ghosh P., Adkins J., Affek H., Balta B., Guo W., Schauble E. A., Schrag D. and Eiler J. M. (2006) 13C–18O bonds in carbonate minerals: A new kind of paleothermometer. *Geochimica et Cosmochimica Acta* **70**, 1439–1456.

Gomez F. J., Kah L. C., Bartley J. K. and Astini R. A. (2014) Microbialites in a high-altitude Andean lake: multiple controls on carbonate precipitation and lamina accretion. *Palaios* **29**, 233–249.

Gomez F. J., Mlewski C., Boidi F. J., Farías M. E. and Gérard E. (2018) Calcium Carbonate Precipitation in Diatom-rich Microbial Mats: The Laguna Negra Hypersaline Lake, Catamarca, Argentina. *Journal of Sedimentary Research* **88**, 727–742.

Grosjean M., Geyh M. A., Messerli B., Schreier H. and Veit H. (1998) A late-Holocene (<2600 BP) glacial advance in the south-central Andes (29°S), northern Chile. *The Holocene* **8**, 473–479.

Grosjean M., Valero-Garcés B. L., Geyh M. A., Messerli B., Schotterer U., Schreier H. and Kelts K. (1997) Mid- and late-Holocene limnogeology of Laguna del Negro Francisco, northern Chile, and its palaeoclimatic implications. *The Holocene* **7**, 151–159.

Grotzinger J. P. and Knoll A. H. (1999) Stromatolites in Precambrian carbonates: evolutionary

mileposts or environmental dipsticks? *Annual Review of Earth and Planetary Sciences* **27**, 313–358.

Huntington K. W., Eiler J. M., Affek H. P., Guo W., Bonifacie M., Yeung L. Y., Thiagarajan N., Passey B., Tripati A., Daëron M. and Came R. (2009) Methods and limitations of "clumped" CO2isotope (Δ47) analysis by gas-source isotope ratiomass spectrometry. *Journal of Mass Spectrometry* **44**, 1318–1329.

Jones B. and Renaut R. (1994) Crystal fabrics and microbiota in large pisoliths from Laguna Pastos Grandes, Bolivia. *Sedimentology* **41**, 1171–1202.

Kim S. T. and O'Neil J. R. (1997) Equilibrium and nonequilibrium oxygen isotope effects in synthetic carbonates. *Geochimica et Cosmochimica Acta* **61**, 3461–3475.

Lachniet M. S. (2009) Climatic and environmental controls on speleothem oxygen-isotope values. *Quaternary Science Reviews* **28**, 412–432.

Meyers P. A. and Lallier-vergés E. (1999) Lacustrine Sedimentary Organic Matter Records of Late Quaternary Paleoclimates. *Journal of Paleolimnology* **21**, 345–372.

Mlewski E. C., Pisapia C., Gomez F., Lecourt L., Soto Rueda E., Benzerara K., Ménez B., Borensztajn S., Jamme F., Réfrégiers M. and Gérard E. (2018) Characterization of Pustular Mats and Related Rivularia-Rich Laminations in Oncoids From the Laguna Negra Lake (Argentina). *Frontiers in microbiology* **9**, 996.

Peters S. E., Husson J. M. and Wilcots J. (2017) The rise and fall of stromatolites in shallow marine environments. *Geology* **45**, 487–490.

Petryshyn V. A., Corsetti F. A., Berelson W. M., Beaumont W. and Lund S. P. (2012) Stromatolite lamination frequency, Walker Lake, Nevada: Implications for stromatolites as biosignatures. *Geology* **40**, 499–502.

Petryshyn V. A., Juarez Rivera M., Agić H., Frantz C. M., Corsetti F. A. and Tripati A. E. (2016) Stromatolites in Walker Lake (Nevada, Great Basin, USA) record climate and lake level changes ~35,000years ago. *Palaeogeography, Palaeoclimatology, Palaeoecology* **451**, 140–151.

Petryshyn V. A., Lim D., Laval B. L., Brady A., Slater G. and Tripati A. K. (2015) Reconstruction of limnology and microbialite formation conditions from carbonate clumped isotope thermometry. *Geobiology* **13**, 53–67.

Riding R. (2000) Microbial carbonates: the geological record of calcified bacterial–algal mats and biofilms. *Sedimentology* **47**, 179–214.

Risacher F. and Eugster H. (1979) Holocene pisoliths and encrustations associated with spring-fed surface pools, Pastos Grandes, Bolivia. *Sedimentology* **26**, 253–270.

Schopf J. W., Kudryavtsev A. B., Czaja A. D. and Tripathi A. B. (2007) Evidence of Archean life: stromatolites and microfossils. *Precambrian Research* **158**, 141–155.

Solari M. A., Hervé F., Le Roux J. P., Airo A. and Sial A. N. (2010) Paleoclimatic significance of lacustrine microbialites: A stable isotope case study of two lakes at Torres del Paine, southern Chile. *Palaeogeography, Palaeoclimatology, Palaeoecology* **297**, 70–82.

Valero-Garces B., Grosjean M., Schwalb A., Geyh M., Messerli B. and Kelts K. (1996) Limnogeology of Laguna Miscanti: evidence for mid to late Holocene moisture changes in the Atacama Altiplano (Northern Chile). *Journal of Paleolimnology* **16**, 1–21.

Valero-Garcés B. L., Delgado-Huertas A., Ratto N. and Navas A. (1999) Large 13 C enrichment in primary carbonates from Andean Altiplano lakes, northwest Argentina. *Earth and Planetary Science Letters* **171**, 253–266.

Zaarur S., Affek H. P. and Brandon M. T. (2013) A revised calibration of the clumped isotope thermometer. *Earth and Planetary Science Letters* **382**, 47–57.

Chapter 5: Biomarker analysis of microbialites and their associated microbial communities from the modern analog environment Laguna Negra, Argentina

Scott R. Beeler[1], Fernando J. Gomez[2], Alexander S. Bradley[1]

[1]Department of Earth and Planetary Science, Washington University in St. Louis, Saint Louis, Missouri, 63130, USA

[2]CICTERRA-CONICET, Facultad de Ciencias Exactas, Fisicas, y Naturales, Universidad Nacional de Córdoba, Córdoba, X5000, Argentina

5.1 Abstract

Microbialites provide geologic evidence of microbial processes, however interpreting the meaning of these structures in the rock record is often difficult. Analyzing the composition of lipids preserved in microbialites may provide insight into the microbial communities associated with their formation, however the degree to which the lipids preserved in microbialites are representative of these communities is uncertain. To address this question, we measured fatty acid and sterol profiles, and compound-specific isotopic compositions of fatty acids, in microbialites and abiogenic carbonates and their associated extant microbial communities at the modern lake Laguna Negra. Fatty acid and sterol compositions measured from extant microbial mats are consistent with an ecosystem at Laguna Negra in which primary productivity is dominated by diatoms with minor contributions from cyanobacteria, and the presence of a diverse heterotrophic bacterial community. However, the fatty acid and sterol profiles preserved in carbonates at Laguna Negra differed from the microbial communities with which they are most commonly associated with in the lake today. If the patterns preserved in carbonates were analyzed from the rock record, where information regarding the extant microbial communities was unavailable, the biomarker profiles preserved in carbonates would most easily be interpreted as a bacterially dominated community with minor contributions from eukaryotic algae. We attribute the differences in biomarker profiles preserved in carbonates versus extant microbial communities to preferential loss of more labile compounds during early diagenetic loss rather than changes in microbial community structure or lake conditions through time. These results suggest that biomarkers preserved in microbialites in the rock record may not necessarily represent the microorganisms responsible for their formation even in samples that have not undergone late stage diagenesis. Analysis of biomarkers in microbialites from the rock record

may still provide information regarding the microbial communities associated with microbialite formation as demonstrated in previous studies but should be used in tandem with other approaches in order to provide a complete understanding of the biological role in microbialite formation.

5.2 Introduction

Sedimentary structures formed as a result of microbial action known as microbialites constitute one of the oldest and most complete records of life on Earth (Schopf and Kudryavtsev, 2007; Peters et al., 2017). The occurrence and morphological diversity of these structures has varied through geologic time and space and these changes may provide information regarding the co-evolution of life and its environment through Earth's history (Riding, 2000). Understanding how changes in the structure and function of microbial communities affect the formation and growth of microbialites is crucial to our ability to interpret their meaning in the geologic record (Bosak et al., 2013). Unfortunately, microbialites in the rock record rarely preserve direct evidence of the microorganisms associated with their formation hindering the knowledge that can be gained through their study (Grotzinger and Knoll, 1999).

Modern settings of microbialite formation can act as analogs for understanding their ancient counterparts by enabling the study of active environmental processes alongside their resultant mineral structures. Study of the structure and function of microbial communities in these settings and their effects on carbonate precipitation have provided a framework for understanding how microbial processes may drive the growth of these structures (Dupraz and Visscher, 2005; Dupraz et al., 2009). These studies often rely on the analysis of active microbial communities through geochemical tracers or the biomolecules produced by microorganisms (e.g. DNA, RNA, or proteins), which while abundant sources of information in modern settings do not

persist over geologic time scales (Briggs and Summons, 2014). Thus, while these studies provide knowledge into the formation of microbialites within modern settings direct comparisons of parameters measured in modern environments to geologic samples cannot be made.

Lipids provide a biomolecular bridge between modern settings and the rock record as their recalcitrance over geologic time scales allows for direct comparison of their compositions in both modern and ancient microbialites (Summons and Lincoln, 2012) . While the information that can be gained from lipids is typically less specific than that of other biomolecules, variability in their structural diversity and isotopic composition can be linked to changes in the organisms responsible for their formation (Brocks and Pearson, 2005; Peters et al., 2005). Analyzing these compounds within microbialites can therefore provide insight into the microorganisms associated with their formation (Spear and Corsetti, 2013). Accordingly, analyses of lipid biomarkers have been performed on microbialites in the geologic record and used to make inferences regarding the ancient microbial communities driving their formation and growth (Luo et al., 2015; Saito et al., 2015; Olcott Marshall and Cestari, 2015).

However, interpreting the meaning of lipids within microbialites in the rock record may be complicated by the fact that the lipids preserved in a microbialite are not necessarily representative of the organisms associated with their formation. Comparative studies of the relationships of lipids from living microbial communities to those preserved in their associated microbialites in modern settings are necessary to more fully understand their relationships. These studies have been carried out in several modern environments and have begun to better clarify the interpretation of lipids in microbialites found in the geologic record (e.g. Jahnke et al., 2004; Jungblut et al., 2009; Allen et al., 2010; Brady et al., 2014; Johnson et al., 2018). However, the generalizability of the knowledge gained from these studies is unclear since the number of

modern environments studied is severely limited compared to the vast number of microbialite environments in the rock record (Grotzinger and Knoll, 1999; Bosak et al., 2013). Study of additional modern analog environments is necessary to resolve these questions.

Laguna Negra, a hypersaline lake located in the Puna Region of the Andes Mountains of Catamarca Province, Argentina, contains a variety carbonate morphologies including forms interpreted as microbialites in addition to non-microbial carbonates (Gomez et al., 2014). Morphological changes at Laguna Negra have been shown to be related to changes in the presence and structure of microbial communities at the lake (Mlewski et al., 2018; Gomez et al., 2018). In this study, we analyzed the variability in the fatty acid and sterols profiles and the compound specific carbon isotopic compositions of fatty acids of carbonates and their associated microbial communities at Laguna Negra. These results allowed for investigation into the relationships of lipid compositions preserved in carbonates to the microbial communities associated with their formation at Laguna Negra and provides insight into the interpretation of the meaning of lipids preserved in microbialites from the geologic record.

5.3 Materials and Methods

5.3.1 Field Area and Sample Collection

Laguna Negra is a closed basin hypersaline (>300 ppt salinity) lake located in the Puna-Altiplano region of the Andes Mountains in Catamarca Province, Argentina. Carbonate precipitation at Laguna Negra occurs exclusively along the southeastern margin of the lake in a zone of input of more dilute waters referred to as the stromatolite belt (Gomez et al., 2014). Carbonate precipitates forming in the stromatolite belt occur as a range of macroscopic morphologies that have been interpreted to reflect changes in the degree of microbial contribution to their formation (Gomez et al., 2014; Mlewski et al., 2018; Gomez et al., 2018).

Carbonates interpreted to have a biogenic origin generally occur as concentrically laminated spheroidal to discoidal oncoids that occur both subaqueously and subaerially. In addition, some oncoids contain accretionary laminated stromatolites growing on top of oncoids that generally occur sediment/water interface. Abiogenically precipitated carbonates typically occur as laminated flat-lying laminar crusts that often form laterally extensive pavements.

Aerial mapping of carbonate structures types indicates their distributions are spatially variable across the stromatolite belt and this variability is related to variability in the distribution of microbial mats (Chapter 2.) Microbial mats occur as three visually distinct types: stratified mats, greenish mats, and pustular mats. Oncoids were more commonly associated with microbial mats, specifically stratified mats, whereas laminar crusts were more commonly associated with carbonate sediments that did not contain mats. The distribution of stromatolites was not analyzed through aerial mapping due to their subsurface occurrence, however field observations indicate they most commonly occur alongside greenish mats. Microscopic analysis of microbial mats at Laguna Negra indicates that both stratified and greenish mats are dominated by diatoms including Achnanthes brevipes sp., Halamphora sp., Denticula sp., Haloroundia Speciosa sp., Nitzschia sp., Navicula sp.,Surirella sp., and Striatula sp. with lesser contributions of cyanobacteria and other bacterial species (Gomez et al., 2018). 16S rRNA analysis of the mats indicated that stratified and greenish mats contained a diverse bacterial community that were broadly similar between mat types (Gomez et al., 2018). The structure of microbial communities in carbonate sediments that do not contain mats has not been analyzed.

Samples were taken of each of the predominant macroscale carbonate structure types at Laguna Negra (oncoids, stromatolites, and laminar crusts) to analyze variability in their lipid profiles. Likewise, samples of each of the types of microbial mats (stratified and greenish) and

sediments associated with the carbonates were also taken to analyze the variability between extant microbial communities present at the lake today and the lipid profiles preserved in carbonates. Carbonate samples were taken from locations across the stromatolite belt, wrapped in baked aluminum foil, and placed into plastic bags. Microbial mat and sediment samples were collected with a sterilized metal spatula and placed into sterile 50 mL conical centrifuge tubes. Microbial samples were refrigerated during transport until return to the lab. After return to the lab microbial mat and sediment samples were stored at 0^{o}C prior to extraction.

5.3.2 Lipid Extraction and Preparation

Following return to the lab lipids were extracted from representative samples of the three endmember carbonate morphologies and their associated microbial communities. Carbonate samples were cut into ~1 inch^3 chunks and sonicated in a 7:3 dichloromethane (DCM) to methanol solvent bath to remove any surface contaminants. Carbonates were then ground to a <10 micron particle size. Both carbonate and microbial mat samples were homogenized and extracted three times with a 7:3 DCM to methanol mixture using a MARS 6 Microwave Extraction System (CEM Corporation, Matthews, NC). Following extraction samples were reacted with activated copper shot to remove elemental sulfur compounds. Total lipid extracts were then separated by sequential elution through a silica gel column with solvents of increasing polarity into four fractions: (F1) hydrocarbons, (F2) ketones, esters, and aromatics, (F3) alcohols, and (F4) carboxylic acids. Following separation, the F4 fraction underwent methylation reactions to form fatty acid methyl ester derivatives (FAMEs) following the method of Rodriquez-Ruiz et al. (1998). The F3 fraction was reacted with N,O-bis(trimethylsilyl)trifluoroacetamide (BSTFA + TMCS) and pyridine to form trimethylsilyl (TMS) derivatives. Procedural blanks were prepared

in tandem throughout the extraction and preparation procedure and analyzed to ensure no contamination during these steps.

5.3.3 Compositional and Isotopic Analysis of Lipids

Samples were analyzed for their lipid compositions and relative abundances using gas chromatography/mass spectrometry (GC/MS) on an Agilent 7890A GC System operated in splitless mode equipped with a J&W DB-5 fused silica capillary column (30 m length, 0.25-mm inner diameter, and 0.25-um film thickness) coupled to an Agilent 5975C inert XL MS using He as a carrier gas. Mass spectrometry was performed using electron ionization scanning from 50-750 m/z at 1.08 scan/second. Data were analyzed using HP Chemstation, and identification of compounds was performed by comparison to reference spectra and elution patterns from published data. Samples were analyzed for their compound specific carbon isotope compositions using coupled gas chromatography-isotope ratio mass spectrometry on a Thermo Trace GC Ultra system equipped with a J&W DB-5 fused silica capillary column (30 m length, 0.25-mm inner diameter, and 0.25-um film thickness) coupled to a Delta V Plus Mass Spectrometer via a Delta GC Isolink. The $\delta^{13}C$ compositions were calculated by comparison to gas values of a known composition measured before and after introduction of the sample to the mass spectrometer and to an internal decanoic acid ($C_{10:0}$) standard of known isotopic values. Analytical precision was confirmed by measurement of a set of fatty acid and alkane standards of a known isotopic composition. Calculated $\delta^{13}C$ were corrected for the addition of methyl esters and TMS for fatty acids and alcohols respectively. Isotopic analyses were performed in triplicate and are reported as mean values of these analyses with one standard deviation of the propagated analytical uncertainty following the method of Polissar and D'Andrea (2014) . $\delta^{13}C$ values are reported

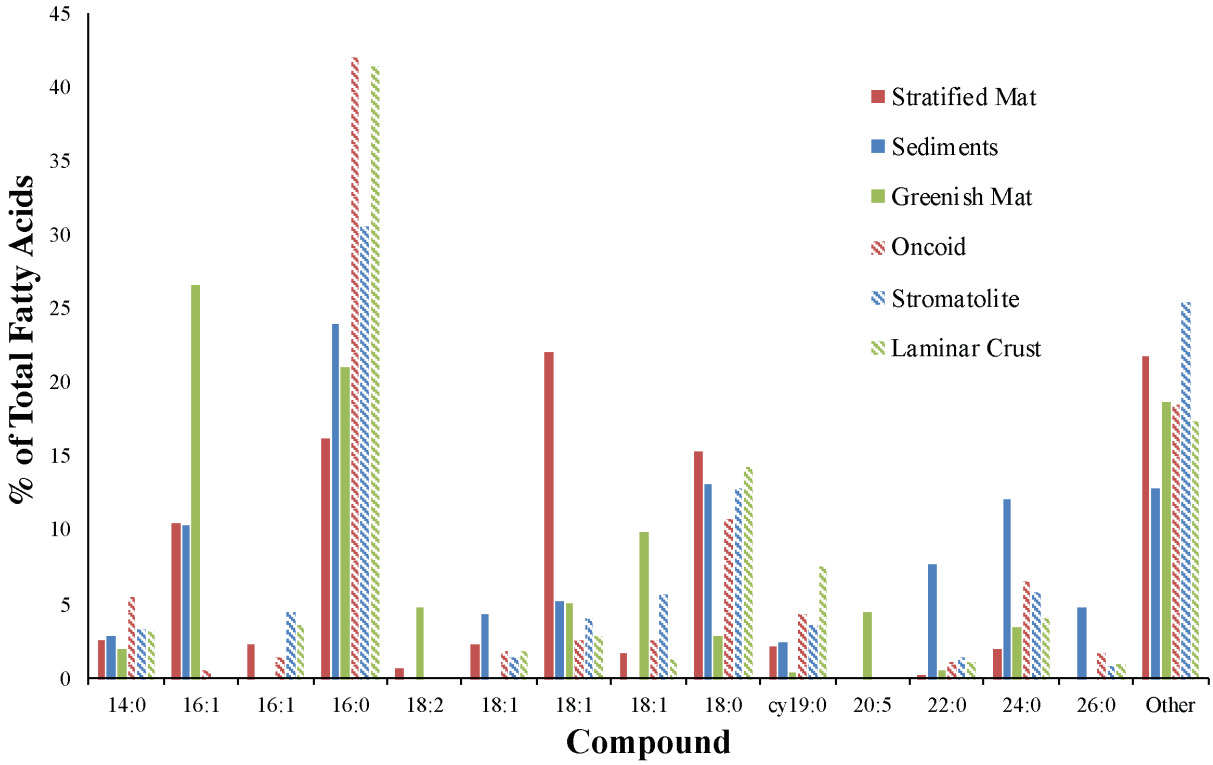

Figure 5.1: Relative abundance of the major fatty acids found in carbonates, microbial mats, and sediments at Laguna Negra. Other refers to the sum of all compounds with less than 3% relative abundance in all sample types analyzed.

relative to V-PDB. Principal component analysis of fatty acid and sterol profiles was performed using the prcomp function in R.

5.4 Results

5.4.1 Fatty Acid Compositions

Fatty acids in all samples were dominated by straight-chain saturated and monounsaturated homologues with even carbon numbers, and chain lengths between fourteen and twenty-sjx (Table 5.1; Figure 5.1). Short chain compounds ($<C_{20}$) were more abundant than long chain compounds ($\geq C_{20}$) with short chain compounds accounting for between 65-98 % of compounds in the samples analyzed. Specifically, saturated and monounsaturated C_{16} and C_{18} fatty acids were the most abundant compounds accounting for between 55-81% of total fatty

Table 5.6: Relative abundances (% of total) of fatty acids from all sample types analyzed.

	Stratified Mat	Sediment	Greenish Mat	Oncoid	Laminar Crust	Stromatolite
	n=2	n=2	n=2	n=6	n=2	n=2
Saturated Straight Chain						
C14:0	1.96 ± 0.03	0.45 ± 0.63	1.46 ± 0.60	3.40 ± 2.32	1.01 ± 1.43	2.82 ± 1.56
C15:0	0.80 ± 0.04	-	0.29 ± 0.41	0.29 ± 0.71	-	-
C16:0	16.18 ± 1.98	24.07 ± 1.41	21.09 ± 0.79	42.08 ± 11.39	41.41 ± 6.52	30.61 ± 3.06
C17:0	0.41 ± 0.17	-	0.65 ± 0.29	0.39 ± 0.46	-	0.81 ± 1.15
C18:0	15.33 ± 7.24	13.16 ± 3.02	2.93 ± 0.82	10.77 ± 2.37	14.40 ± 3.36	12.92 ± 0.84
C20:0	-	3.92 ± 0.29	0.36 ± 0.08	1.19 ± 0.63	1.51 ± 0.29	1.2 ± 0.28
C22:0	0.28 ± 0.09	7.75 ± 1.58	0.50 ± 0.16	1.17 ± 0.80	1.15 ± 1.63	1.46 ± 0.43
C24:0	2.00 ± 1.21	12.20 ± 0.28	3.51 ± 0.34	6.57 ± 1.39	4.04 ± 1.01	5.86 ± 1.36
C25:0	-	0.73 ± 1.03	-	-	-	-
C26:0	-	4.78 ± 1.92	-	1.66 ± 0.92	1.05 ± 1.48	0.9 ± 1.28
Total	36.96 ± 3.86	67.05 ± 1.31	30.79 ± 2.90	67.52 ± 7.47	64.58 ± 0.66	56.59 ± 3.43
Saturated Branched						
iC14:0	-	-	0.27 ± 0.38	0.13 ± 0.32	-	-
iC15:0	2.48 ± 0.34	1.28 ± 0.19	1.40 ± 0.67	2.11 ± 0.77	0.78 ± 1.11	1.63 ± 0.22
aC15:0	2.59 ± 0.16	2.88 ± 0.44	1.98 ± 0.68	5.51 ± 1.34	3.21 ± 1.59	3.31 ± 1.86
brC15:0	-	-	-	0.33 ± 0.64	-	-
iC16:0	2.83 ± 0.29	-	-	0.57 ± 0.65	0.43 ± 0.61	0.95 ± 1.34
meC17:0	1.47 ± 0.11	-	2.95 ± 0.96	2.08 ± 1.21	3.33 ± 0.29	3.89 ± 2.3
iC17:0	0.73 ± 0.26	-	0.64 ± 0.10	1.36 ± 0.22	1.41 ± 0.22	2.28 ± 0.13
aC17:0	0.76 ± 0.27	-	0.67 ± 0.05	1.42 ± 0.22	2.00 ± 0.17	2.62 ± 0.14
cyC17:0	0.82 ± 0.19	-	0.86 ± 0.27	1.53 ± 0.16	2.49 ± 1.84	1.45 ± 2.05
Phytanate	-	-	-	1.18 ± 0.79	2.95 ± 1.70	3.75 ± 2.44
iC19:0	3.06 ± 0.40	-	-	-	-	-
cyC19:0	2.21 ± 0.33	2.45 ± 1.11	0.42 ± 0.59	4.37 ± 1.81	7.65 ± 0.55	3.62 ± 3.81
iC23:0	-	1.17 ± 0.05	-	-	-	-
Total	16.95 ± 2.36	7.78 ± 1.70	9.19 ± 3.51	20.59 ± 4.24	24.24 ± 6.08	23.49 ± 6.48
Monounsaturated						
iC15:1	3.83 ± 1.25	0.99 ± 0.13	-	0.53 ± 0.61	-	0.98 ± 1.38
C16:1	10.49 ± 2.58	10.31 ± 0.77	26.61 ± 3.42	0.55 ± 1.34	-	-
C16:1	2.35 ± 0.63	-	-	1.47 ± 0.99	3.60 ± 1.10	4.55 ± 1.57
C16:1	2.05 ± 0.62	-	1.67 ± 0.37	1.40 ± 0.94	1.57 ± 2.21	3.15 ± 0.41
iC16:1	-	1.89 ± 0.23	-	-	-	-
aC16:1	-	0.41 ± 0.57	-	-	-	-
C17:1	-	0.59 ± 0.83	-	-	-	-
C18:1	2.24 ± 0.09	4.32 ± 1.71	-	1.91 ± 1.52	1.86 ± 0.49	1.49 ± 2.11
C18:1	22.12 ± 6.21	5.29 ± 0.56	5.06 ± 1.16	2.64 ± 1.43	2.82 ± 1.05	4.03 ± 1.21
C18:1	1.74 ± 2.46	-	9.88 ± 0.34	2.66 ± 1.36	1.33 ± 1.89	5.73 ± 3.34
C19:1	-	-	3.37 ± 1.39	-	-	-
C24:1	0.59 ± 0.36	1.38 ± 0.91	0.46 ± 0.04	0.31 ± 0.75	-	-
C24:1	-	-	0.54 ± 0.02	0.42 ± 0.65	-	-
Total	45.41 ± 1.59	25.17 ± 0.39	47.59 ± 2.54	11.88 ± 3.85	11.18 ± 6.75	19.93 ± 3.05
Polyunsaturated						
C16:2	-	-	3.18 ± 0.17	-	-	-
C18:2	0.68 ± 0.09	-	4.81 ± 1.46	-	-	-
C20:5	-	-	4.43 ± 2.23	-	-	-
Total	0.68 ± 0.09	-	12.42 ± 3.86	-	-	-

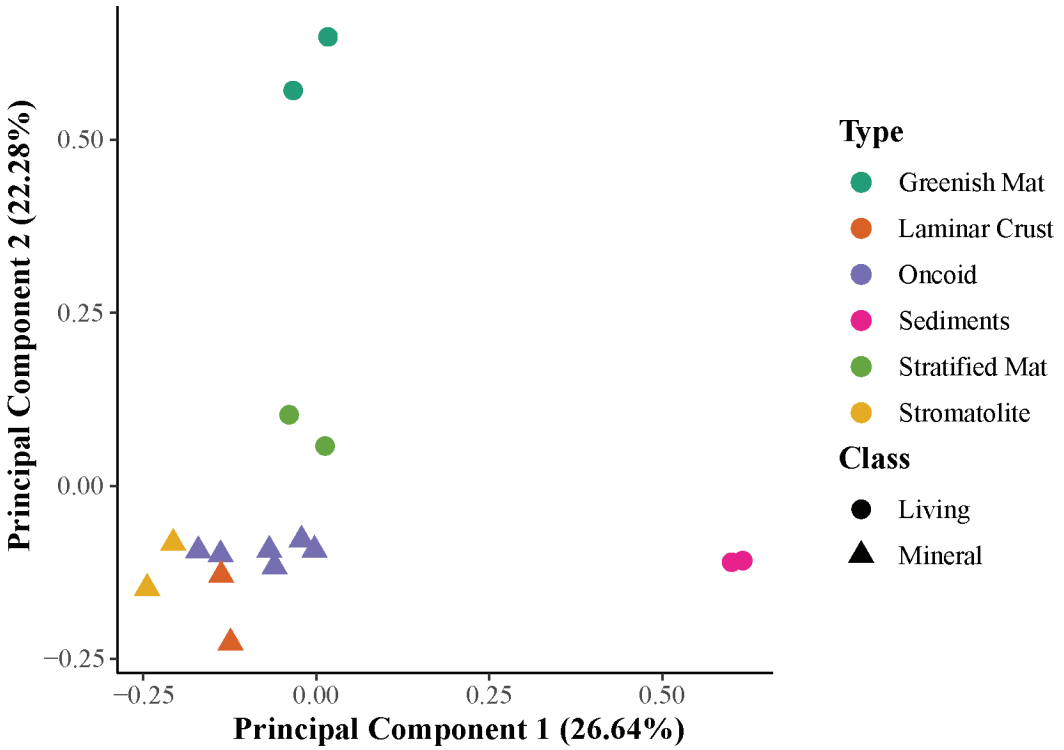

Figure 5.2: Principal component analysis of fatty acid profiles for all sample types analyzed.

acids in the samples analyzed. Branched fatty acids were also found in all samples analyzed accounting for between 6-30% of total fatty acids.

Principal component analysis indicates that fatty acid profiles varied between the different structure types with carbonate structures (i.e. oncoids, laminar crusts, and stromatolites) having more similar profiles to each other than those from microbial mats or sediments (Figure 5.2). Replicate samples of each type were also more similar to each other than other sample types. Additionally, stratified mats had fatty acid profiles more similar to carbonate structures than those from greenish mats or sediments. Fatty acids from carbonate structures and sediments had relatively higher proportions of short-chain saturated compounds compared to microbial mats and sediments. Microbial mats had relatively higher proportions of mono- and poly-unsaturated compounds compared to other structure types. Sediments had higher concentrations of long chain fatty acids compared to both carbonate structures and microbial

Table 5.7: Relative abundances (% of total) of sterols from all sample types analyzed.

			Stratified Mat	Sediment	Greenish Mat	Oncoid	Laminar Crust	Stromatolite
			n=2	n=2	n=2	n=6	n=2	n=2
Trivial Name	Name							
Cholesterol	Cholest-5en-3β-ol	$C_{27}\ \Delta^5$	11.30 ± 4.00	20.09 ± 3.06	9.30 ± 1.22	11.53 ± 2.01	11.68 ± 6.61	11.16 ± 0.49
Cholestanol	5α-Cholestan-3β-ol	$C_{27}\ \Delta^0$	13.51 ± 3.89	14.67 ± 6.69	12.42 ± 0.22	23.96 ± 7.54	24.50 ± 0.11	23.68 ± 1.53
Crinosterol	(22E)-24-Methylcholesta-5,22-dien-3β-ol	$C_{28}\ \Delta^{5,22}$	9.51 ± 2.13	6.14 ± 2.12	22.63 ± 1.74	14.51 ± 6.95	20.82 ± 3.86	17.58 ± 1.90
Campesterol	24-Methylcholest-5-en-3β-ol	$C_{28}\ \Delta^5$	19.10 ± 4.86	17.05 ± 1.17	17.54 ± 0.28	18.03 ± 6.12	17.07 ± 8.96	15.88 ± 4.61
Stigmasterol	(22E)-24-Ethylcholesta-5,22-dien-3β-ol	$C_{29}\ \Delta^{5,22}$	13.01 ± 2.75	5.01 ± 0.71	16.61 ± 4.12	8.17 ± 1.71	4.58 ± 6.48	7.19 ± 0.26
β-sitosterol	24-Ethycholest-5-en-3β-ol	$C_{29}\ \Delta^5$	11.80 ± 4.22	27.31 ± 2.05	18.00 ± 2.64	13.58 ± 7.67	11.70 ± 8.83	10.78 ± 2.50
Stigmastanol	24-Ethylcholestan-3β-ol	$C_{29}\ \Delta^0$	21.76 ± 21.85	9.73 ± 4.17	3.50 ± 4.95	10.22 ± 3.09	9.64 ± 3.76	13.73 ± 7.51

mats. Branched fatty acids comprised a higher proportion of fatty acids in carbonate structures and stratified mats relative to greenish mats and sediments.

5.4.2 Sterol Compositions

Sterol profiles for all samples analyzed (Table 5.2) were comprised of a mixture of seven stenols (unsaturated sterols) and stanols (saturated sterols). The relationship between the steroid profiles of different sample types indicated by principal component analysis were less clear compared to those for fatty acids (Figure 5.3). Replicates of greenish mats and sediments were more similar to each other than other structure types. In contrast, stratified mats and carbonates did not show clear patterns between replicates of the same sample type. Comparison of the relative proportion of C_{27}, C_{28}, and C_{29} steroids indicated that in general carbonate structure types had higher proportions of C_{27} and C_{28} compounds than microbial mats and sediments which had higher proportions of C_{29} steroids (Figure 5.4). Additionally, carbonate structures had a higher proportion of stanols (35% of total sterols on average) compared to microbial mats and sediments (25% of total sterols on average).

5.4.3 Fatty Acid Compound Specific Carbon Isotopes

The compound specific carbon isotopic composition of the major fatty acids of all sample types except for sediments are shown in Figure 5.5. Carbon isotopic compositions were

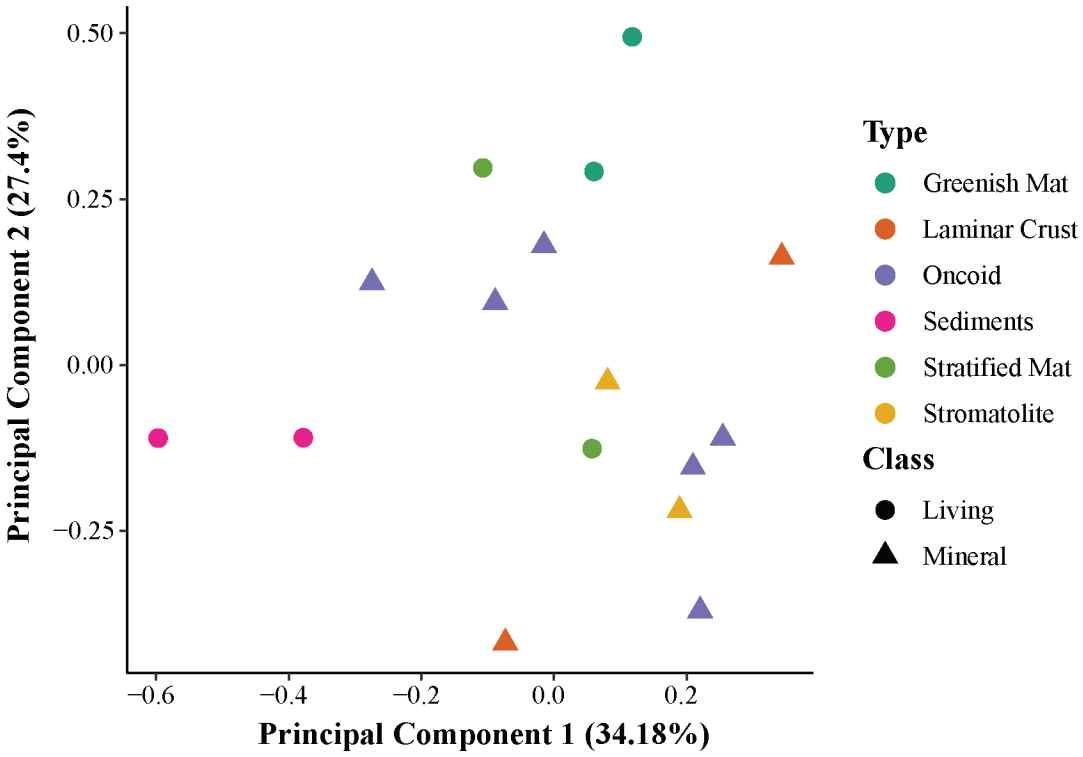

Figure 5.3: Principal component analysis of sterol profiles for all sample types analyzed.

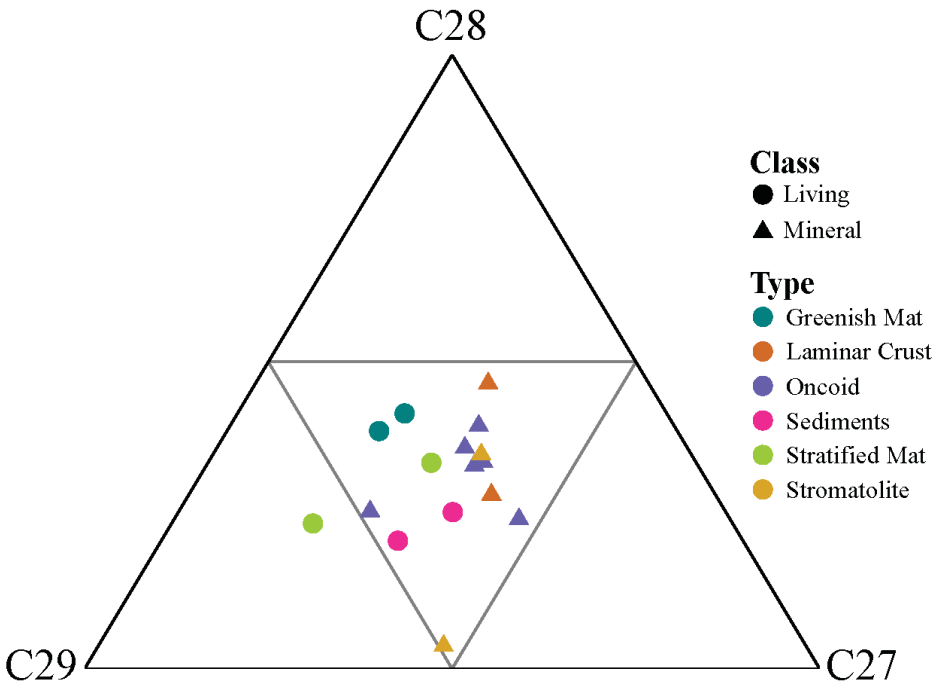

Figure 5.4: Ternary plot showing relative abundances of C_{27}, C_{28}, and C_{29} sterols for all sample types analyzed

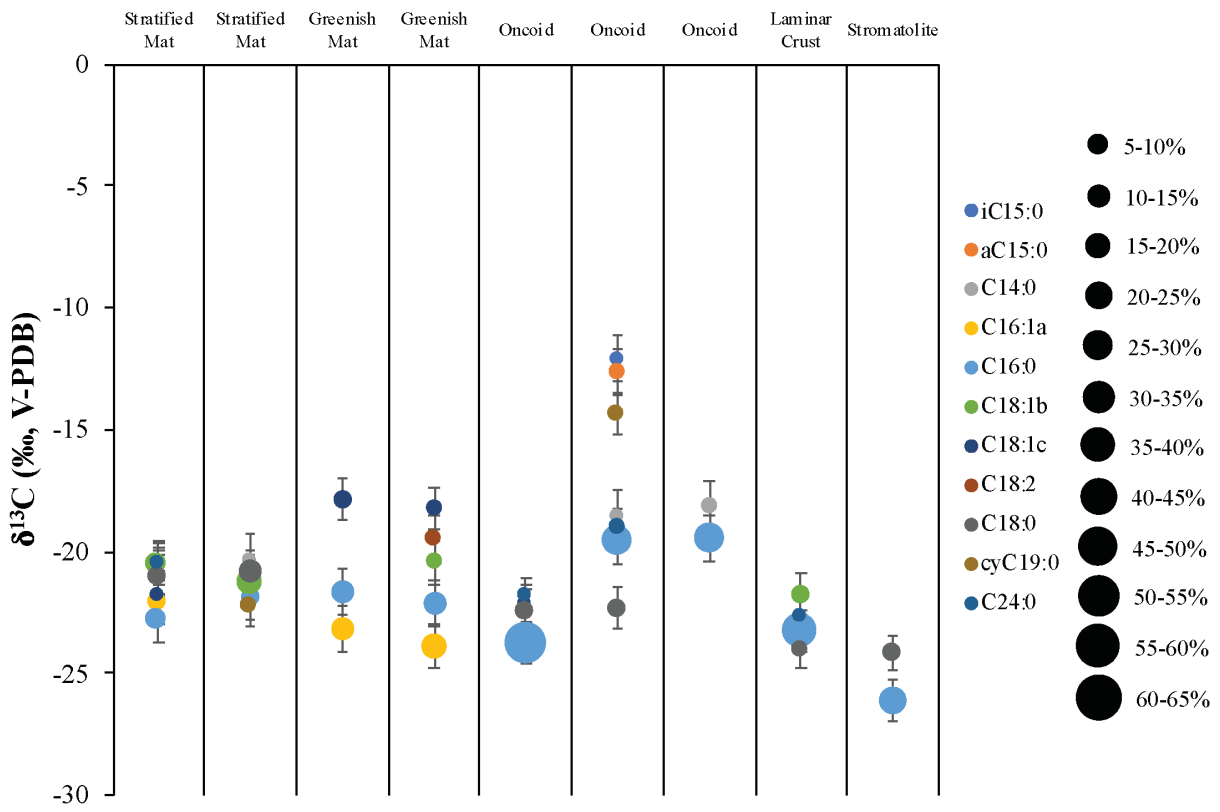

Figure 5.5: Compound specific carbon isotopic composition of the most abundant fatty acids from microbial mats and carbonates sampled in this study. Error bars are one standard deviation of propagated analytical uncertainty.

relatively similar for all compounds (ranging from -17.8 to -26.1‰) except for branched fatty acids (iC15:0, aC14:0, cyC19:0) from one oncoid which had more enriched isotopic compositions (-12.0 to -14.4‰). Variability in the isotopic composition of different fatty acids within samples analyzed was generally low (between 1.29 and 5.62‰) with the exception of the oncoid which had two distinct isotopic groups. Similarly, isotopic variability within the same fatty acids between samples analyzed was generally low (maximum difference between 1.3 and 6.6‰) with the exception of the branched compounds that had a range of ~10‰.

5.5 Discussion

5.5.1 Biomarker Compositions of Extant Microbial Communities

Previous work at Laguna Negra using microscopic analysis indicated that primary productivity in the mats is dominated by diatoms with minor contributions from cyanobacteria (Gomez et al., 2018). 16S rRNA analysis of microbial mats identified a diverse set of bacterial phyla within the mats with Deinococcus-Thermus, Verrucomicrobia, Proteobacteria, and Bacteroidetes accounting for over 50% of bacterial diversity in both stratified and greenish mats (Gomez et al., 2018). Sediments sampled in this study have not been analyzed using microscopy or genomic techniques and their microbial community structure has previously been unknown. We analyzed the fatty acid and sterol compositions of the different types of extant microbial communities (stratified mats, greenish mats, and sediments) to provide additional insight into their community structure and to enable comparison to compounds found in carbonate structures.

Fatty acid profiles in all of the extant microbial community types (stratified mats, greenish mats, and sediments) were consistent with primary productivity driven by diatoms evidenced by the abundance of saturated and monounsaturated C16 compounds, which are the dominant fatty acids found in diatoms (Volkman et al., 1998; Volkman, 2006). The polyunsaturated fatty acids C16:2 and C20:5 which are commonly found in diatoms were also present in relatively high abundances in the greenish mat (Dunstan et al., 1993). Likewise the presence and composition of sterols in the mats and sediments are consistent with diatom dominated primary productivity at Laguna Negra (Barrett et al., 1995; Rampen et al., 2010).

Minor components of the fatty acid profiles found in all sample types were consistent with the presence of a diverse bacterial community. Branched fatty acids which are interpreted as biomarkers for heterotrophic bacteria were found in all sample types accounting for between 6-

23% of total fatty acids in the samples analyzed (Kaneda, 1991) . Likewise, cyC19:0 which has been found in many other hypersaline environments and has been tentatively attributed to purple sulfur bacteria was also detected in all samples (Grimalt et al., 1992; Fourçans et al., 2004; Michelle A. Allen et al., 2010). Overall, branched fatty acids were a more common constituent of stratified mats (20.8% of total fatty acids on average) compared to greenish mats and sediments (9.2% and 11.1% of total fatty acids on average respectively) suggesting a higher relative abundance of bacteria within the microbial communities of stratified mats.

Long chain (>C20) saturated and monounsaturated fatty acids, which are typically attributed to higher plants, were also found in each sample type (Volkman, 2006). Sediments had substantially higher relative abundances (31.9% on average) of these compounds relative to stratified mats (2.9% on average) and greenish mats (5.4% on average). Some species of diatoms produce these long chain compounds in minor quantities which likely accounts for the relatively low levels within the microbial mats (Volkman et al., 1989). The increased abundance of these compounds in sediments may reflect allochthonous input of these compounds as sediments occur near the input of a seasonal snowmelt stream.

The compound specific carbon isotope compositions of fatty acids ($\delta^{13}C$) reflect the carbon fixation processes associated with their formation and may allow for more robust reconstruction of microbial ecosystem structure (Hayes, 2001). All fatty acids measured from stratified mats had relatively similar $\delta^{13}C$ compositions ranging from -20.3 to -22.8‰. Given the enriched isotopic composition of DIC ($\delta^{13}C_{DIC}$ between 0.5-15.0‰) previously measured at Laguna Negra, these values are consistent with primary productivity driven by diatoms whose biosynthetic processes at high [DIC] as is the case at Laguna Negra have maximum fractionation factors of ~30‰ (Fry, 1996; Beeler et al.,*in review*). The predominant fatty acids in greenish

mats (C16:0 and C16:1) had similar $\delta^{13}C$ compositions to fatty acids from the stratified mat ranging from -21.7 to -23.9‰ and are likely due to their origin from diatoms. Less abundant fatty acids from the greenish mats (C18:1 and C18:2) had slightly more enriched $\delta^{13}C$ compositions ranging from -17.8 to -20.5‰. These compounds are both commonly produced by cyanobacteria and the enriched values are consistent with production by cyanobacteria whose biosynthetic fractionation is slightly lower (maximum fractionation factors ~22‰ at high [DIC]) than that of diatoms (Pardue et al., 1976).

The overall biomarker compositions for all of the extant microbial community types analyzed were consistent with a microbial ecosystem dominated by diatoms. The minor constituents of the biomarker profiles in all sample types are also consistent with genomic evidence for a diverse bacterial community including cyanobacteria and heterotrophic organisms (Gomez et al. 2014). Compound specific isotopic compositions of fatty acids in greenish mats indicates a relatively higher influence of cyanobacteria compared to stratified mats. Increased abundance of long chain carbon compounds in sediments suggests the influence of allochtonously derived organic compounds likely sourced from higher plants due to seasonal stream water inputs. Collectively, the biomarker profiles of all community types are consistent with what would be expected based upon previous genomic and microscopic analyses of microbial community structure.

5.5.2 Biomarker Composition of Carbonates

In order to assess the degree to which the lipid profiles preserved in microbialites reflect the communities associated with their formation we analyzed the lipid biomarkers preserved in carbonates and compared them to those of the extant microbial communities with which they are presently associated. Overall, the fatty acid and sterol profiles were remarkably similar between

all carbonate types analyzed (Table 5.1; Figure 5.1). Interestingly, fatty acid profiles in all carbonate types were more similar to each other than to the microbial mats or sediments with which they are most commonly associated with at the lake at present (Figure 5.2). Fatty acids in carbonates tended to have higher relative proportions of saturated straight chain and branched straight chain compounds and lower relative proportions of mono- and poly- unsaturated compounds. Increased abundances of long chain fatty acids were also observed for carbonates versus microbial mats. Additionally, carbonates structures had lower relative abundances of stanols versus stenols compared to the extant microbial communities (Table 5.2).

The observed differences in the fatty acid and sterol compositions in carbonates versus extant microbial communities could represent changes in the microbial communities or lake conditions through time as preliminary U/Th dating suggests the oncoids are at least 2500 years old (Gomez et al., 2014). Changes in the microbial community structure at the lake from bacterially dominated communities in the past to more diatom dominated communities today could explain the changes in fatty acid profiles. Likewise, changes in algal populations to a more diatom rich community is consistent with the observed relative increases in C29 sterols in extant microbial communities compared to carbonates (Figure 5.3; Kodner et al., 2008) However, petrographic analysis in oncoids indicates the presence of abundant diatom microfossils within oncoids suggesting they have been the dominant primary producer at the lake throughout the period of oncoid formation (Gomez et al., 2018). Increases in salinity at the lake through time provides another potential explanation for the increased relative abundance of saturated fatty acids in carbonates as the ratio of unsaturated to saturated fatty acids produced by algae has been shown to decrease with increasing salinity (Renaud and Parry, 1994). However, oxygen isotopic compositions preserved in microbialites and regional climate records suggest an increased water

balance through time suggesting lake waters have likely become less saline with time contrasting with this interpretation (Valero-Garces et al., 1996; Grosjean et al., 1997; Buongiorno et al., 2018).

Preferential loss of more labile compounds during early diagenesis may also explain the differences in the fatty acid profiles of carbonates versus extant microbial communities. Degradation of fatty acids has been shown to follow reactivity trends following a pattern of unsaturated compounds> branched compounds > saturated compounds (Haddad et al., 1992). This pattern can explain the observed decreased in abundance of unsaturated fatty acids relative to branched and saturated fatty acids. Likewise, within the saturated fatty acid short chain compounds (<C20) were shown to be preferentially degraded relative to long chain compounds explaining the relative increase of long chain compounds in carbonates versus microbial mats.(Haddad et al., 1992). Likewise, the increased ratio of stanols to stenols in carbonates versus extant microbial communities is also consistent with degradation processes during early diagenesis (Nishimura and Koyama, 1976). Due to these lines of evidence we believe that early diagenetic transformations of lipids provides the most parsimonious explanation for the difference in lipid profiles between carbonates and their associated microbial mats.

Taken independently of the biomarker compositions of the modern microbial communities and previous observations regarding microbial community structure at Laguna Negra, the fatty acid profiles in these structures are somewhat ambiguous but are most easily interpreted as sourced from a bacterially dominated community due to the high relative proportions C16:0, C18:0, and branched compounds. The sterol profiles preserved in carbonates would suggest the presence of a eukaryotic algal community, however because sterol profiles are not independently diagnostic of any particular clade it is difficult to attribute their origin to any

particular organism (Volkman, 1986; Volkman, 2006). Likewise, fatty acid profiles lack any compounds diagnostic of specific microalgae (such as C16:2 and C20:5 for diatoms) that would allow for more robust interpretation of the sterol profiles. Compound specific carbon isotopic analysis of the major fatty acids in the carbonates generally consistent within structures and ranged -18.2 and -26.1‰ with the exception of branched structures from one oncoid which were relatively enriched ranging from -12.0 to -14.4‰. The simplest explanation for all but the enriched branched values is fractionation during primary production using the C3 carbon fixation pathway with changes in $\delta^{13}C_{DIC}$ through time driving the interstructural variability. Enriched values of the branched compounds within one of the oncoids may represent biosynthesis by an organism using an alternate carbon fixation pathway, such as a chemosynthetic pathways, with a lower fractionation factor or enrichment due to heterotrophy (Hayes, 2001).

These results indicate that early diagenetic processes may substantially alter the lipid profiles that are preserved in microbialites, which could lead to misinterpretation of their meaning. Each of the extant microbial community types had distinct initial biomarker pools arising from variability in their community structure, however the lipids that were preserved in carbonates forming in association with these different community types did not reflect these differences. Likewise, similar lipid profiles were preserved in both microbialitic morphologies (i.e oncoids and stromatolites) versus abiogenically precipitated carbonates (i.e. laminar crusts) suggesting biomarker profiles do not provide definitive evidence of the biogenicity of these structures. Overall, this work highlights the importance of the consideration of diagenetic effects when interpreting the meaning of lipids preserved in microbialites. Lipid analyses may still provide a useful tool in understanding the microbial communities associated with microbialite

formation as demonstrated in other environments, however these analyses should be used in tandem with other analytical techniques in order to better interpret their meaning.

5.5 Conclusions

Analysis of the fatty acid and sterol compositions of extant microbial communities in microbial mats and sediments at Laguna Negra were consistent with previous work indicating diatom dominated primary productivity and the presence of a diverse bacterial community (Gomez et al., 2018). Our results showed that the fatty acid and sterol profiles of carbonates at the lake did not relate to the modern microbial communities with which they are associated that have previously been linked to their formation (Gomez et al., 2018; Chapter 2). We interpret these differences to be due to preferential loss of more labile compounds during early diagenesis altering the lipid profiles preserved within the carbonates. These results indicate that the lipid biomarkers preserved in microbialites may not necessarily be indicative of the microbial communities that contribute to their formation. Importantly, without knowledge of the lipid compositions of extant microbial communities, as is the case when analyzing microbialites in the geologic record, the lipid profiles in carbonates could be incorrectly identified leading to misinterpretation of the microbial communities responsible for microbialite formation. Therefore, the presence or composition of biomarkers preserved in microbialites should not be taken independently as evidence of biogenicity or the contribution of a specific microbial community to their formation. This highlights the importance of employing a holistic approach utilizing multiple lines of evidence when interpreting the meaning of microbialites in the geologic record.

5.6 References

Allen M. A., Neilan B. A., Burns B. P., Jahnke L. L. and Summons R. E. (2010) Lipid biomarkers in Hamelin Pool microbial mats and stromatolites. *Organic Geochemistry* **41**, 1207–1218.

Allen M. A., Neilan B. A., Burns B. P., Jahnke L. L. and Summons R. E. (2010) Lipid biomarkers in Hamelin Pool microbial mats and stromatolites. *Organic Geochemistry* **41**, 1207–1218.

Barrett S. M., Volkman J. K., Dunstan G. A. and LeRoi J. -M (1995) Sterols of 14 species of marine diatoms (Bacillariophyta). *Journal of Phycology* **31**, 360–369.

Bosak T., Knoll A. H. and Petroff A. P. (2013) The Meaning of Stromatolites. *Annual Review of Earth and Planetary Sciences* **41**, 21–44.

Brady A. L., Laval B., Lim D. S. S. and Slater G. F. (2014) Autotrophic and heterotrophic associated biosignatures in modern freshwater microbialites over seasonal and spatial gradients. *Organic Geochemistry* **67**, 8–18.

Briggs D. E. G. and Summons R. E. (2014) Ancient biomolecules: Their origins, fossilization, and role in revealing the history of life. *BioEssays* **36**, 482–490.

Brocks J. J. and Pearson A. (2005) Building the biomarker tree of life. *Reviews in Mineralogy and Geochemistry* **59**, 233–258.

Buongiorno J., Gomez F. J., Fike D. A. and Kah L. C. (2018) Mineralized microbialites as archives of environmental evolution, Laguna Negra, Catamarca Province, Argentina. *Geobiology*.

Dunstan G. A., Volkman J. K., Barrett S. M., Leroi J.-M. and Jeffrey S. W. (1993) Essential polyunsaturated fatty acids from 14 species of diatom (Bacillariophyceae). *Phytochemistry*

35, 155–161.

Dupraz C., Reid R. P., Braissant O., Decho A. W., Norman R. S. and Visscher P. T. (2009) Processes of carbonate precipitation in modern microbial mats. *Earth-Science Reviews* **96**, 141–162.

Dupraz C. and Visscher P. (2005) Microbial lithification in marine stromatolites and hypersaline mats. *Trends in Microbiology* **13**, 429–438.

Fourçans A., De Oteyza T. G., Wieland A., Solé A., Diestra E., Van Bleijswijk J., Grimalt J. O., Kühl M., Esteve I., Muyzer G., Caumette P. and Duran R. (2004) Characterization of functional bacterial groups in a hypersaline microbial mat community (Salins-de-Giraud, Camargue, France). *FEMS Microbiology Ecology* **51**, 55–70.

Fry B. (1996) 13C/12C fractionation by marine diatoms. *Marine Ecology Progress Series* **134**, 283–294.

Gomez F. J., Kah L. C., Bartley J. K. and Astini R. A. (2014) Microbialites in a high-altitude Andean lake: multiple controls on carbonate precipitation and lamina accretion. *Palaios* **29**, 233–249.

Gomez F. J., Mlewski C., Boidi F. J., Farías M. E. and Gérard E. (2018) Calcium Carbonate Precipitation in Diatom-rich Microbial Mats: The Laguna Negra Hypersaline Lake, Catamarca, Argentina. *Journal of Sedimentary Research* **88**, 727–742.

Grimalt J. O., de Wit R., Teixidor P. and Albaigés J. (1992) Lipid biogeochemistry of Phormidium and Microcoleus mats. *Organic Geochemistry* **19**, 509–530.

Grosjean M., Valero-Garcés B. L., Geyh M. A., Messerli B., Schotterer U., Schreier H. and Kelts K. (1997) Mid- and late-Holocene limnogeology of Laguna del Negro Francisco, northern Chile, and its palaeoclimatic implications. *The Holocene* **7**, 151–159.

Grotzinger J. P. and Knoll A. H. (1999) Stromatolites in Precambrian carbonates: evolutionary mileposts or environmental dipsticks? *Annual Review of Earth and Planetary Sciences* **27**, 313–358.

Haddad R. I., Martens C. S. and Farrington J. W. (1992) Quantifying early diagenesis of fatty acids in a rapidly accumulating coastal marine sediment. *Organic Geochemistry* **19**, 205–216.

Hayes J. (2001) Fractionation of carbon and hydrogen isotopes in biosynthetic processes. *Reviews in Mineralogy and Geochemistry* **43**, 225–277.

Jahnke L. L., Embaye T., Hope J., Turk K. A., Van Zuilen M., Des Marais D. J., Farmer J. D. and Summons R. E. (2004) Lipid biomarker and carbon isotopic signatures for stromatolite-forming, microbial mat communities and Phormidium cultures from Yellowstone National Park. *Geobiology* **2**, 31–47.

Johnson D. B., Beddows P. A., Flynn T. M. and Osburn M. R. (2018) Microbial diversity and biomarker analysis of modern freshwater microbialites from Laguna Bacalar, Mexico. *Geobiology* **16**, 319–337.

Jungblut A. D., Allen M. A., Burns B. P. and Neilan B. A. (2009) Lipid biomarker analysis of cyanobacteria-dominated microbial mats in meltwater ponds on the McMurdo Ice Shelf, Antarctica. *Organic Geochemistry* **40**, 258–269.

Kaneda T. (1991) Iso- and anteiso-fatty acids in bacteria: biosynthesis, function, and taxonomic significance. *Microbiological reviews* **55**, 288–302.

Kodner R. B., Pearson A., Summons R. E. and Knoll A. H. (2008) Sterols in red and green algae: quantification, phylogeny, and relevance for the interpretation of geologic steranes. *Geobiology* **6**, 411–20.

Luo G., Hallmann C., Xie S., Ruan X. and Summons R. E. (2015) Comparative microbial diversity and redox environments of black shale and stromatolite facies in the Mesoproterozoic Xiamaling Formation. *Geochimica et Cosmochimica Acta* **151**, 150–167.

Mlewski E. C., Pisapia C., Gomez F., Lecourt L., Soto Rueda E., Benzerara K., Ménez B., Borensztajn S., Jamme F., Réfrégiers M. and Gérard E. (2018) Characterization of Pustular Mats and Related Rivularia-Rich Laminations in Oncoids From the Laguna Negra Lake (Argentina). *Frontiers in microbiology* **9**, 996.

Nishimura M. and Koyama T. (1976) Stenols and stanols in lake sediments and diatoms. *Chemical Geology* **17**, 229–239.

Olcott Marshall A. and Cestari N. A. (2015) Biomarker Analysis of Samples Visually Identified as Microbial in the Eocene Green River Formation: An Analogue for Mars. *Astrobiology* **15**, 770–775.

Pardue J. W., Scalan R. S., Van Baalen C. and Parker P. L. (1976) Maximum carbon isotope fractionation in photosynthesis by blue-green algae and a green alga. *Geochimica et Cosmochimica Acta* **40**, 309–312.

Peters K., Walters C. and Moldowan J. (2005) *The biomarker guide: biomarkers and isotopes in the environment and human history*.,

Peters S. E., Husson J. M. and Wilcots J. (2017) The rise and fall of stromatolites in shallow marine environments. *Geology* **45**, 487–490.

Polissar P. J. and D'Andrea W. J. (2014) Uncertainty in paleohydrologic reconstructions from molecular δD values. *Geochimica et Cosmochimica Acta* **129**, 146–156.

Rampen S. W., Abbas B. A., Schouten S. and Damsté J. S. S. (2010) A comprehensive study of sterols in marine diatoms (Bacillariophyta): Implications for their use as tracers for diatom

productivity. *Limnology and Oceanography* **55**, 91–105.

Renaud S. M. and Parry D. L. (1994) Microalgae for use in tropical aquaculture II: Effect of salinity on growth, gross chemical composition and fatty acid composition of three species of marine microalgae. *Journal of Applied Phycology* **6**, 347–356.

Riding R. (2000) Microbial carbonates: the geological record of calcified bacterial–algal mats and biofilms. *Sedimentology* **47**, 179–214.

Rodríguez-Ruiz J., Belarbi E.-H., Sánchez J. L. G. and Alonso D. L. (1998) Rapid simultaneous lipid extraction and transesterification for fatty acid analyses. *Biotechnology Techniques* **12**, 689–691.

Saito R., Kaiho K., Oba M., Fujibayashi M., Tong J. and Tian L. (2015) Predominance of archaea-derived hydrocarbons in an Early Triassic microbialite. *Organic Geochemistry* **85**, 66–75.

Schopf J. and Kudryavtsev A. (2007) Evidence of Archean life: stromatolites and microfossils. *Precambrian Research*.

Spear J. R. and Corsetti F. A. (2013) The evolution of geobiology in the context of living stromatolites. In pp. 549–565.

Summons R. E. and Lincoln S. A. (2012) Biomarkers: Informative Molecules for Studies in Geobiology. In *Fundamentals of Geobiology* John Wiley & Sons, Ltd, Chichester, UK. pp. 269–296.

Valero-Garces B., Grosjean M., Schwalb A., Geyh M., Messerli B. and Kelts K. (1996) Limnogeology of Laguna Miscanti: evidence for mid to late Holocene moisture changes in the Atacama Altiplano (Northern Chile). *Journal of Paleolimnology* **16**, 1–21.

Volkman J. K. (1986) A review of sterol markers for marine and terrigenous organic matter.

Organic Geochemistry **9**, 83–99.

Volkman J. K. (2006) Lipid markers for marine organic matter. *Handbook of Environmental Chemistry, Volume 2: Reactions and Processes* **2 N**, 27–70.

Volkman J. K., Barrett S. M., Blackburn S. I., Mansour M. P., Sikes E. L. and Gelin F. (1998) Microalgal biomarkers: A review of recent research developments. *Organic Geochemistry* **29**, 1163–1179.

Volkman J. K., Jeffrey S. W., Nichols P. D., Rogers G. I. and Garland C. D. (1989) Fatty acid and lipid composition of 10 species of microalgae used in mariculture. *Journal of Experimental Marine Biology and Ecology* **128**, 219–240.

Chapter 6: Conclusions

Microbialites constitute a vast archive of geobiological information providing an invaluable tool for furthering our understanding of how life and its environment have co-evolved over Earth's history. Likewise, because they provide geological evidence of microbial processes that can be recognized at the macro- scale, they offer an attractive target in astrobiological investigations. Yet, the potential of these structures to inform us about the history of life on Earth and possibly other planets has not been fully realized due to an incomplete understanding of the processes that control their formation, morphological characteristics, and geochemical compositions. Each of these parameters ultimately result from the combination of microbial, geochemical, and physical processes, and deconvolving their relative roles is crucial to the ability to better interpret the meaning of microbialites in the rock record. Modern environments of microbialite formation allow for the analysis of these processes alongside the mineralized structures they produce enabling a better understanding of their relative contributions to microbialite formation. However, the number of modern environments of microbialite formation that have been extensively studied is severely limited compared to the vast number of these environments preserved in the geologic record. Consequently, the applicability of lessons learned from these settings to interpreting microbialites in the rock record is uncertain. Study of additional modern settings of microbialite formation is necessary to more fully understand the processes governing the growth and characteristics to better understand their meaning in the geologic record.

The research presented in this dissertation helps to fill this information gap by assessing the processes controlling the growth and geochemical characteristics of microbialites from the

modern hypersaline lake Laguna Negra, Argentina. Chapter 2 focused on analyzing the processes controlling the spatial variability in the distribution of microbialites at the macro- to mega- scale. We found that the spatial distributions of different carbonate morphologies was related to variability in their associations with microbial mats suggesting their large scale distributions are related to microbial processes. These results differ from results in other modern environments that attribute the large scale distribution of microbialites to physical processes. Chapter 3 assessed the processes controlling the large stable carbon and oxygen isotopic enrichments preserved within the carbonate minerals comprising microbialites at Laguna Negra. We found that these enrichments were controlled by the geochemical evolution of the waters from which the carbonates precipitated due to the combined abiotic processes of evaporation, degassing, and carbonate precipitation. This suggests that similarly large fractionations should not necessarily be used as evidence for biological activity but may still provide information regarding other environmental conditions. Chapter 4 used clumped isotope thermometry to understand he controls of intrastructural variability in the stable oxygen isotopic compositions of microbialites and evaluate the potential of microbialites to serve as terrestrial paleoclimate archives. We found that the temperatures from which carbonates precipitated have remained relatively constant throughout their formation, while the oxygen isotopic composition of the waters from which they precipitated have decreased through time likely due to increased water balance at the lake. This result is consistent with regional paleoclimate records and supports the use of microbialites as paleoenvironmental archives. Chapter 5 investigated the utility of lipid biomarkers to preserve information regarding the microbial communities associated with microbialite formation. We found that early diagenetic alteration of lipids could potentially lead to misinterpretation of the

meaning of the lipid profiles preserved in microbialites indicating that lipid profiles should be used in tandem with other analyses in order to fully assess their meaning.

Collectively, the results of this research enhance our ability to accurately interpret the meaning of microbialites and their geochemical signatures in the geologic record. Each of the characteristics of microbialites analyzed in this study reflected to varying degrees the microbial, geochemical, and physical processes that drove their formation. Overall, this work highlights the need for a holistic approach for the study of microbialites that integrates multiple lines of evidence in order to fully assess the processes responsible for their formation. Utilization of this holistic approach is also necessary in order to be able to better interpret the biogenicity of possible microbialites on early Earth or other planets. Continuing work at Laguna Negra focused on assessing temporal variability in lake conditions can serve to further resolve the controls of the growth and characteristics of microbialites at the lake. Overall, microbialites provide an indispensable tool in the field of geobiology and increasing our understanding of the processes responsible for their formation and the controls of their morphological and geochemical characteristics will allow for a better understanding of the history of life on Earth and potentially other planets.

Appendix: Electron microprobe analysis of Laguna Negra microbialites

Elemental maps and spot analyses were created using electron probe microanalysis (EPMA) with a JEOL JXA 8200 electron microprobe equipped with five wavelength-dispersive spectrometers and an energy-dispersive spectrometer in the Electron Microprobe Facility at Washington University in St. Louis. Elemental maps were created for a suite of major and minor elements commonly found in carbonate rocks. Maps were generated at a 14 micron pixel size with a dwell time of 25 milliseconds. Spot analyses were performed for calcium, magnesium, manganese, iron, and strontium. Spot analyses were performed at a 50 micron spot size and compared to a standard of known elemental concentrations to generate quantitative results. Areas of interest for spot analyses were determined from elemental mapping and performed in triplicate within an area of measurement. Spot analyses data can be accessed at: https://figshare.com/s/9369b73382b37ab5ad5f

Elemental maps and backscatter electron images indicate geochemical variability across small spatial scales within individual microbialite morphologies (Figure A.1). Spot analyses performed on areas of interest determined from elemental mapping allows for quantitative comparison of elemental abundances (Figure A.2). Results are reported as mean value of the triplicate analyses with error bars of one standard deviation. These quantitative results confirm the variability observed in elemental mapping. While the observed patterns are qualitatively distinct, the maximum variability observed for any element within a single morphology is less than one weight percent. This variability is most pronounced within the laminar crust with highly variable magnesium concentrations observed between clotted and isopachous fabrics. High standard deviations for minor elements in oncoids indicates variability on spatial scales smaller than those capable of measurement by EPMA. In contrast, to the other carbonate morphologies the stromatolite is highly uniform in its minor element distribution.

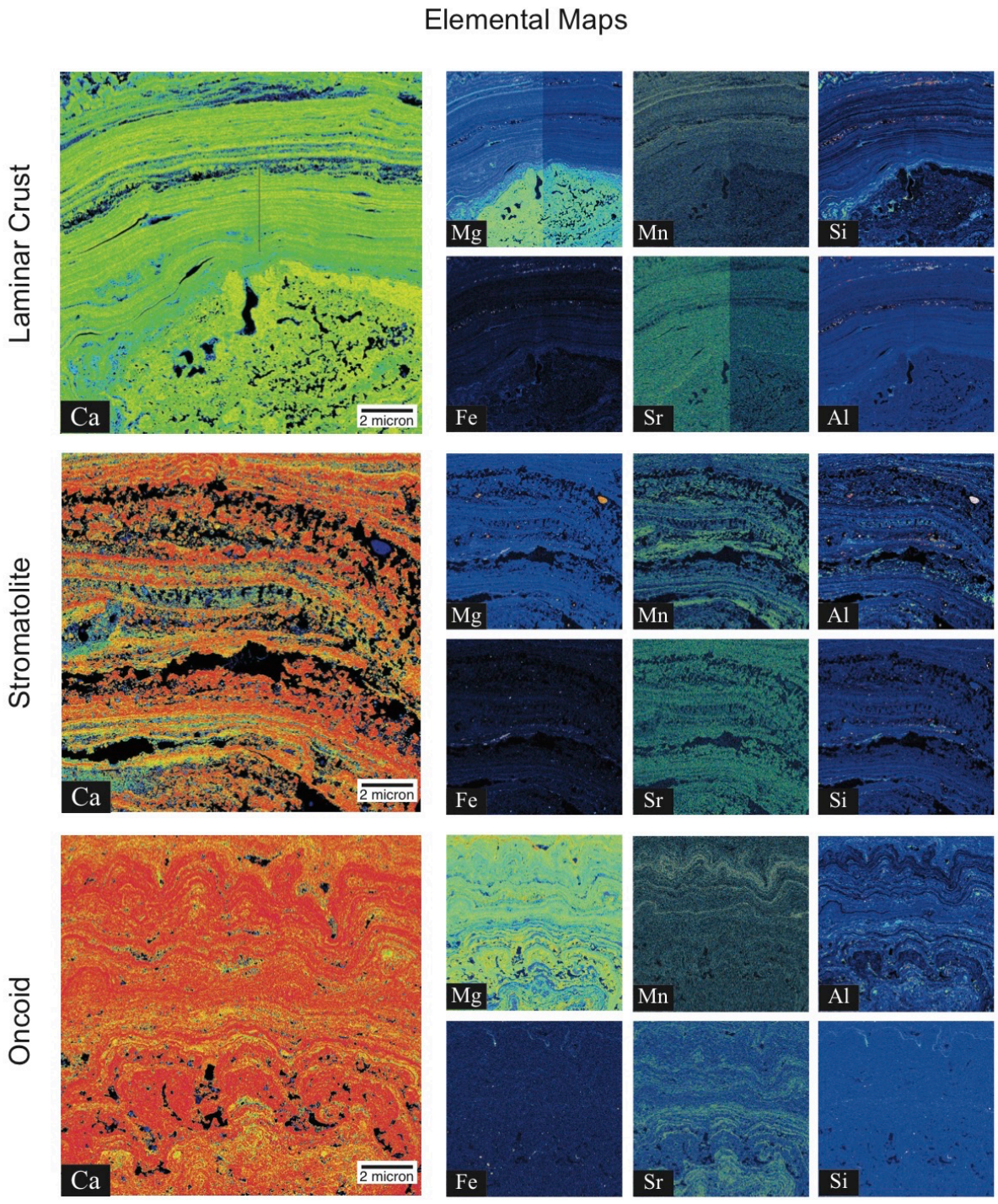

Figure A.1: Elemental maps of some major and minor elements from endmember carbonate morphologies at Laguna Negra. Brighter colors correspond to higher relative concentrations of the analyzed element.

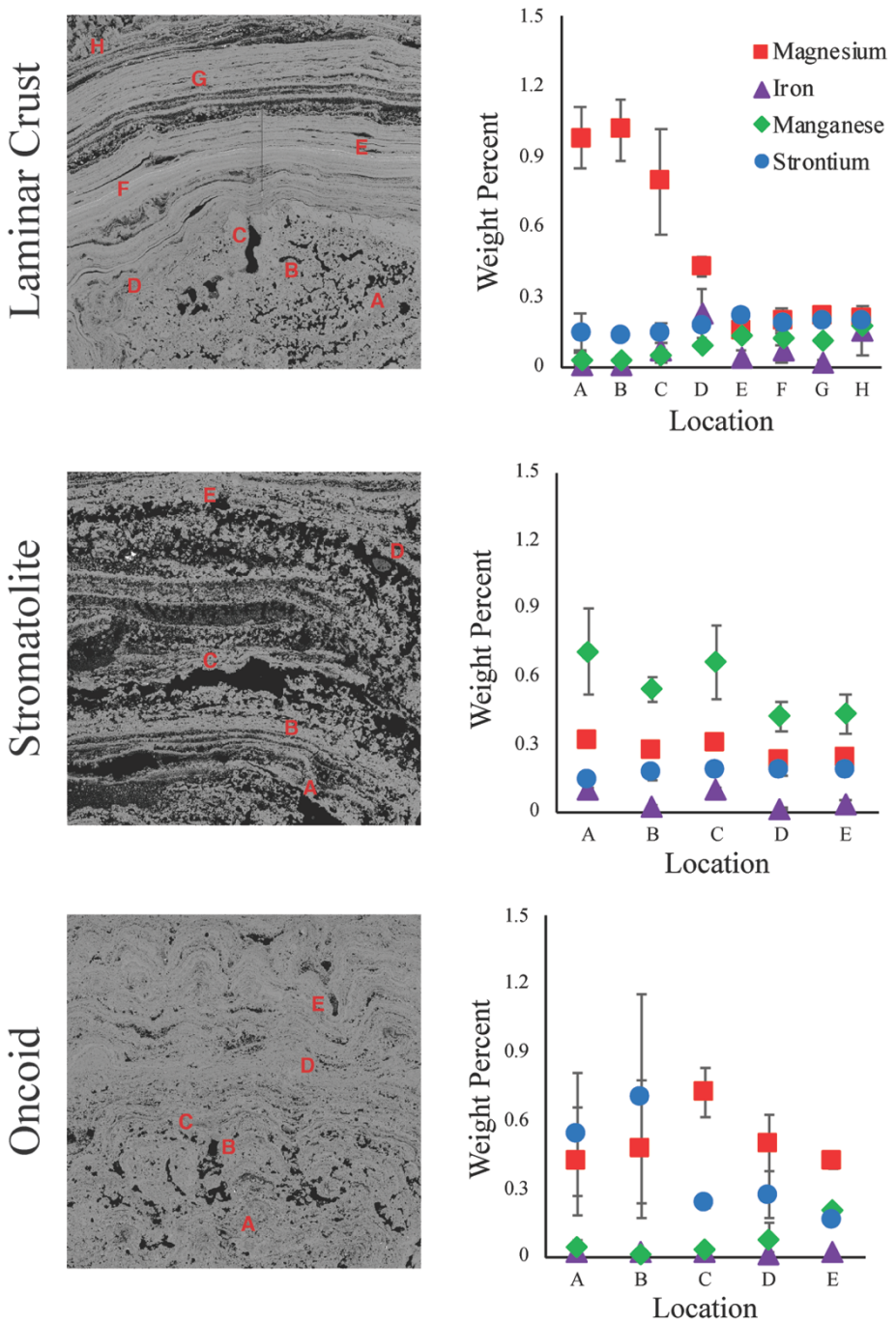

Figure A.2: Spot analyses for major and minor elements of the endmember carbonate morphologies. Mean values are reported as the mean of three analyses within a single area with error bars of one standard deviation. Locations of analyses are shown on corresponding backscatter electron maps of the samples.